IN THE NAME OF GOD, MOST GRACIOUS,

MOST MERCIFUL.

RIAD KOCACHE

M.Sc. THESIS

A STUDY OF THE BEHAVIOUR OF THE SINGLE PHASE INDUCTION TYPE ENERGY METER AND THE DESIGN OF AN INSTRUMENTATION SYSTEM FOR ITS CALIBRATION

DECEMBER, 1967

SYNOPSIS

The work investigates the problems encountered in the calibration of single phase induction type Electricity Meters. It endeavours to produce an instrumentation scheme based on a better knowledge of the behaviour of the meter. This behaviour was studied under the following modes.

1) The load behaviour of the meter.
2) The behaviour of the meter within one revolution of its disc.
3) The phase relationships between the relevant quantities in the meter.
4) The friction in the register mechanism.

Suitable instruments were developed to enable this study.

An instrumentation system was designed and a prototype constructed, with the following aims in mind.

1) Conformity with B.S. regulations.
2) Reduction of personal and systematic errors.
3) Economic factors.
   a) Reduction of the time required for calibration per meter.
   b) Aiming for simple reliable design, using a minimal of components.
   c) Ability to use the system to calibrate a range of meters having different load capacities.

Certain calibration techniques were evolved and their usefulness assessed.

ACKNOWLEDGEMENTS

I wish to thank Dr. D. Karo, Dr.ès Sc., Dr.Eng., Ph.D., B.Sc., Dipl. Eng., C.Eng., F.I.E.E., for his continued help and encouragement and for the suggestion of the research topic. The Chamberlain and Hookham Co. Ltd., for supporting the research and especially Mr. B. Stonehouse, Chief Engineer. The Electrical Engineering Department of the University of Aston, for providing the research facilities.

Also to thank Messrs. E. Roberts, F. Hunt, H. Roberts and C. Penn for their co-operation.

CONTENTS

REVIEW OF CALIBRATION METHODS AND TECHNIQUES FOR SINGLE PHASE INDUCTION TYPE ELECTRICAL ENERGY METERS

1.1 INTRODUCTION: (1,2,3,4,5,6,7,8,9,10,11)

The use of the induction type energy meter for the registration of electrical energy, has been increasing since the turn of the century. The gradual change over from direct current to alternating current, and the extensive use of electricity in the home and in industry on one hand, and the accuracy, cheapness and simplicity of construction on the other hand, are some of the main causes for this increase. New materials and improved designs have decreased the meter errors and extended its operating range well into both the lower and higher loads. Better methods for temperature, frequency and voltage compensation were evolved. The overlapping of the home and industrial loads produced a new breed of long range meters, ranges up to 600% of full load are now available. These improvements resulted also in lengthening the life time of the meter and in cheaper and simpler servicing.

In the early days of metering practice, when a large number of manufacturers and a greater number of supply authorities existed; the Electricity Inspectors, who were appointed by the supply authorities; but who were independent of them, had the power and duties of certifying the consumer's meters. The manufacturers carried out a form of calibration, however their

limits of error and methods differed greatly. In this they were guided by the Electricity Lighting Act 1899. The need for new legislation regarding the limits of error and methods of calibration, was felt for a time in the supply industry, however no such step was feasible till the meters took a more standard form and the supply industry was better organised. The incident which brought about this desired legislation was the dispute between 'Joseph' and the 'Eastham Corporation'. Later a Bill was drafted and passed as 'The Electricity Supply (Meters) Act', 1936.

(12)

1.2 THE ELECTRICITY SUPPLY (METERS) ACT:

The passing of this act brought about fundamental changes to meter testing. Whilst previously the meter was considered correct unless the consumer disputed its accuracy, the meter must now be within the specified limits of error. In addition it must be of approved design and construction. Meter Examiners who are appointed by the supply authorities have to test the meters and issue test certificates. The test equipment used must conform to the specifications issued by the Electricity Commissioners in a supplement to the Act, which prescribed also approved methods of testing.

1.3 Limits of Error: (13)

British Standard 37 pt. I and II, describes a range of tests and requirements. Fig.(1) shows the acceptable limits of error at marked voltage, standard frequency and temperature. To ensure these limits, test points at which the meter is adjusted and its errors ascertained are selected. Fig.(2) shows common test points. A flow diagram for a common procedure of adjusting the meter is shown in Fig.(3).

1.4 Presetting:

In order that the meter will be within a reasonable range of error prior to its calibration; some form of 'presetting' adjustment is done whilst the meter is still on the production line.

i) Marked voltage and full load current at 0 power factor are applied to the meter and the inductive load adjustment is set such that the rotor does not move. This is sometimes done prior to the installment of the permanent magnet.

ii) Marked voltage is applied alone and the frictional adjustment is set so as to prevent the rotor from moving whilst a creep hole is under the voltage coil.

iii) The main adjustment is set by comparing the speed of the rotor with that of a sub-standard, or by using a stroboscope.

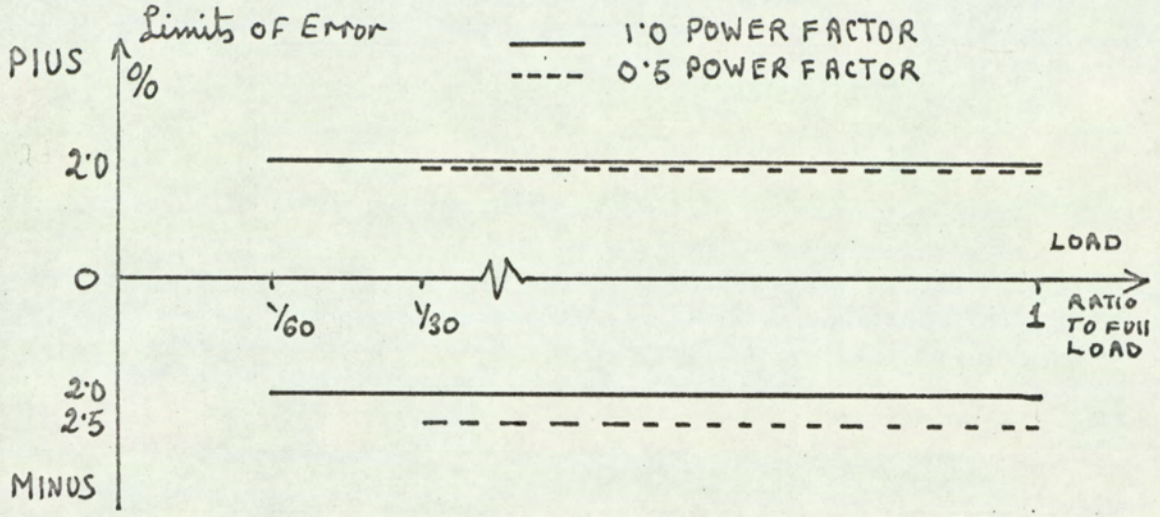

Fig.(1). Diagram showing the acceptable limits of error for single phase induction meters at marked voltage, standard frequency and temperature as given in B.S.37

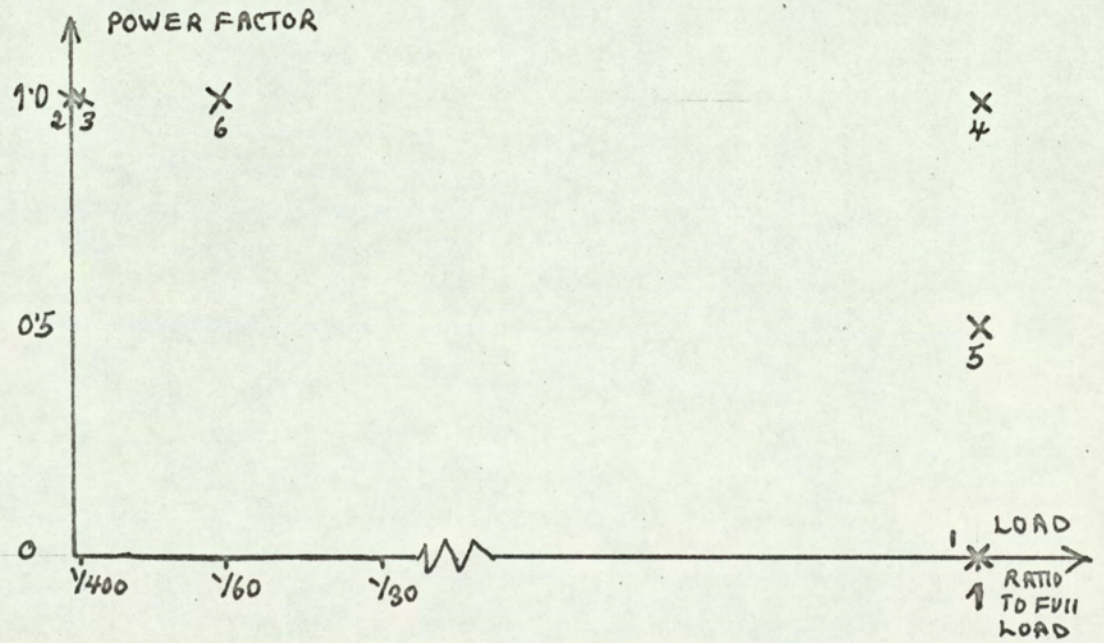

Fig.(2) Diagram showing common test points at which the errors of the meter are assessed

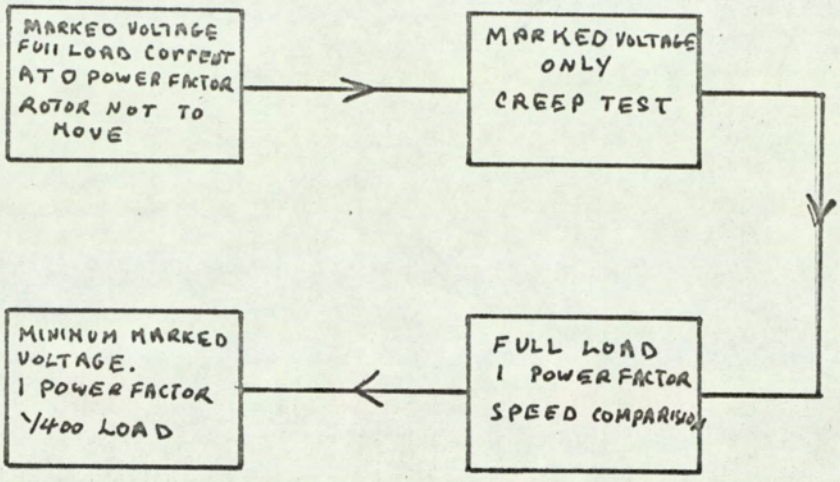

'A'

'B'

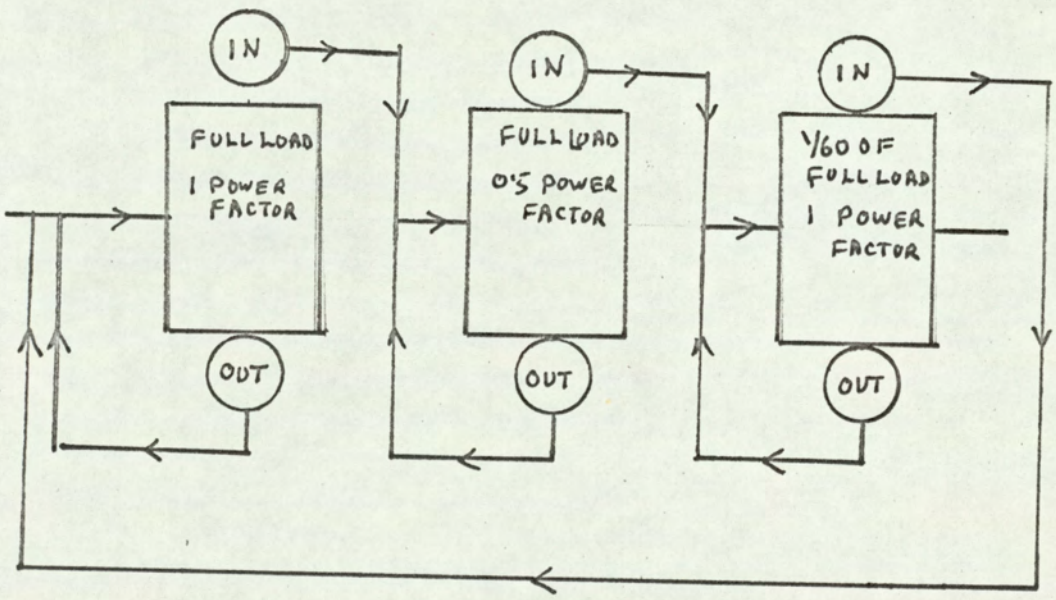

Fig.(3) A flow diagram showing one common procedure of adjusting the meter.

A) Pre-setting adjustments.
B) Final adjustment.

iv) Meters are adjusted so as they start and continue to run on starting current (1/400 of full load minimum marked voltage and unity power factor).

(14, 15, 16, 17, 18.)

1.5 Approved Methods of Testing:

Three methods are recommended in the supplement of the 1936 Meters Act, each being designed to ensure the greatest accuracy from the equipment used. A necessary condition applicable to all methods is that the pressure coils must be energised for one hour at least before calibrating the meter.

i) 'Time-Power' Method: The disc of the meter is timed for at least three complete revolutions or one hundred seconds, whichever is longer. Each of the specified loads in turn is held steady at the nominal value indicated by a sub-standard wattmeter. In addition, a dial test run at one of the specified loads is required to test the registering counter. The nominal percentage error of the meter is:-

$$\frac{T - t}{t} \times 100 \quad \ldots\ldots \quad (1)$$

where T, is the calculated time for the test load from the meter constant,

t, is the observed time.

To this is added the calibration error of the substandard wattmeter.

This method is the most accurate and is usually used by the N.P.L. to calibrate rotating sub-standards. The indicating sub-standard wattmeter has smaller errors due to self heating, waveform distortion or voltage variation, than the best rotating sub-standard. Its specified accuracy is $\pm$ 0.1% F.S.D., whilst that of the rotating sub-standard is $\pm$ 0.5% from 1 1/4 to 1/5 of rated current and $\pm$ 1% at 1/10 rated current, $\pm$ 1.5% at 1/20 of rated current, and for 0.5 lag the first two limits are doubled. The sub-standard wattmeter is usually calibrated against primary standards using a D.C. potentiometer. Transfer errors due to the inductive effects and mutual inductances[19] are small, in a well designed wattmeter. The National Bureau of Standards developed the 'Glass wattmeter' in order to minimise transfer errors, Shotter and Hawks AC/DC Comparator is another alternative. The errors of the stop-watch are comparatively small. However, there is a great amount of personal errors involved in detecting the passage of the black spot of the disc against a reference and in the response time of the operator which is of the order of 0.3 of a second. The main difficulty in this method is in keeping the nominal power constant, this is usually kept by an operator, thus an additional personal and

random error is introduced. This method checks the meter as a wattmeter, hence the necessity of a dial test to ensure accurate integration.

ii) "Comparison of Disc Revolutions with a Rotating sub-standard Meter" Method:

The disc revolutions of the meters under test are compared with that of a rotating sub-standard meter. The load on the sub-standard being not less than 25%, nor more than 125% of its full load. The number of complete revolutions of the meter under test, for any given load, is ascertained by multiplying the percentage of the marked current at the load by 2/5. The duration of the test being not less than five complete revolutions and need not be greater than twenty-five complete revolutions. A dial test at one of the prescribed loads is also necessary.

The nominal percentage error is given by:-

$$\frac{R - R'}{R'} \times 100 \quad \ldots\ldots \quad (2)$$

where R, is the set number of revolutions.

R' is the observed number of revolutions,

to this must be added the error of the sub-standard.

It is usual in mass production to use a sub-standard meter which is similar to those under test. The meters will have then about the same temperature, frequency, and

voltage change of error, if any of these parameters change during the test. There is no need, in this method, to keep the load constant. A large number of meters can be calibrated at once. Precision starting and stopping is essential (usually done by braking the pressure circuit). If this is done manually, a personal error is introduced; whence the necessity of long test runs. The errors of the sub-standard are relatively large, and if it is different from the meters under test, frequency, temperature and voltage errors differ. This method checks the meter as a wattmeter, hence the necessity of a dial test to ensure accurate integration.

iii) "Long Period Dial Tests" Method:

The advance of the register of the meter under test is observed for the passage of a given amount of energy. The energy is measured by a rotating sub-standard or by a "Time-Power" method. These tests are conducted at each of the prescribed loads. The duration of each test being of sufficient length of time to allow the last pointer of each meter under test to make at least ten revolutions.

The load on the sub-standard rotating meter must not be less than 25% or more than 125% of its full load for any test. Furthermore, the rotating sub-standard must be retested against a sub-standard wattmeter at least once per month.

The nominal percentage error is given by,

$$\frac{K - K'}{K'} \times 100 \quad \ldots\ldots \quad (3)$$

where K, is the registration of the meter in K.wh.

K', is the true K.wh. passed through the meter as indicated by a substandard.

To this must be added the errors of the sub-standard.

This method checks the meter as a K.wh. meter and the long period gives a greater opportunity of discovering any intermittent mechanical defect. A large number of meters can be tested simultaneously. The tests run consecutively and no steady load being necessary. The main disadvantage is the very long period required for the test.

(20,21,22)

1.6 Modern Techniques in Meter Calibration and Testing:

The utilisation of modern techniques for the Calibration of electricity meters aimed mainly at,

a) Elimination of the personal errors in testing;

b) Reduction of skill required in testing and simplification of operating procedure;

c) Reduction of time taken for testing and calibration;

d) Reasonable cost of equipment;

e) To aim at a uniform flow of meters from production line to testing and hence packing;

Photoelectric devices, electronics and a variety of equipment are included in modern meter testing. Claims of accuracy, speed and efficiency are made. Most of these methods can be classified into groups relating them to the approved methods discussed before, the developments being those of techniques rather than method. Due to the speed variation of the disc within one-revolution, and its relative importance at low loads, no method has yet been devised for a test for less than one complete revolution of the disc.

i) Improvements in the 'Time-Power' method:

Although this is the most accurate method of calibration, it is not very popular. This is mainly due to the difficulty in keeping the load constant and that only one meter can be calibrated at a time.

Felton[23] (N.P.L.) describes a device which records the time for any given number of revolutions (up to 99) which is selected. The revolutions of the disc being detected by a photoelectric cell and then counted. The first impulse starts a stop-watch which is stopped at the end of the pre-selected number of revolutions. The aim in using this equipment is mainly to eliminate the operator who usually times the disc with a stop-watch. The other operator is retained in order to keep a steady load.

Pegaliari [24] and others describe an Instrument console which can ,

a) Calibrate and test a meter to be used as a sub-standard by means of a precision wattmeter and crystal controled counter.

b) Calibrate and test, production meters by the wattmeter and counter.

c) Calibrate production meters by comparison with a rotating sub-standard.

d) Test production meters (error curves) by comparison with a rotating sub-standard meter on various loads, either by an operator or automatically by a pre-set programme.

The system utilises photoelectric detection and a quartz crystal time standard and a digital display of error which can be produced on a printer. One meter is tested at a time, however, five meters can be connected and tested consecutively. Resolution is 1/1000. The system is elaborate and costly.

ii) Improvements in the "Speed Comparison" Method

This seems to be the most popular method. Early attempts [25] were directed towards using photoelectric devices to start and stop the rotating sub-standard and hence to eliminate the conventional potential switch used for manual testing.

Improved accuracy resulted, due to the elimination of personal errors, and the test was speeded up due to the fewer number of revolutions necessary.

An error indicator in the form of a 'Magic Eye' is described by Bull [26]. This gives visual indication of the amount by which the meter under test is slower or faster than a rotating sub-standard. This technique requires alignment of the meter and sub-standard, and an elaborate set up, this on the other hand is compensated by the need of one-revolution testing only. Another form of continuous error display was developed by Robison and Wickham[27]. Fig.(4) shows a block diagram of the system, light impulses detected by photoelectric means and produced by serrations on both the meter tested and the sub-standard, are amplified and shaped and utilised toproduce a display on a C.R.T. The sub-standard meter controls the horizontal sweep circuit, and the meter under test controls the vertical. The trace becomes stationary when the discs of both meters are rotating at the same speed, and moves across the screen when the two speeds are different. The direction of travel determines whether the meter is slow or fast. A resolution of 0.1% is claimed. Other similar techniques are found in the literature [28]. The U.S. National Bureau of standards adopted the speed comparison method

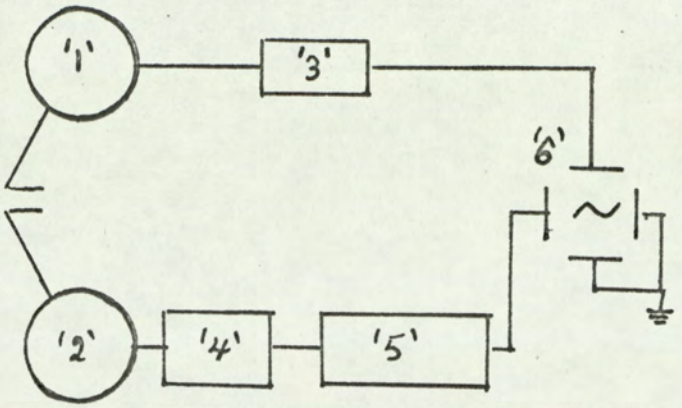

Fig.(4) Block diagram of the electronic circuit showing the control of the horizontal sweep circuit by the phototube of the standard meter and the vertical deflection produced by the phototube of the test meter.

1. Multiplier phototube on test Meter.
2. Multiplier phototube on standard meter.
3. Amplifier.
4. Impedance matching amplifier.
5. Sweep circuit, synchronizing amplifier.
6. C.R.T.

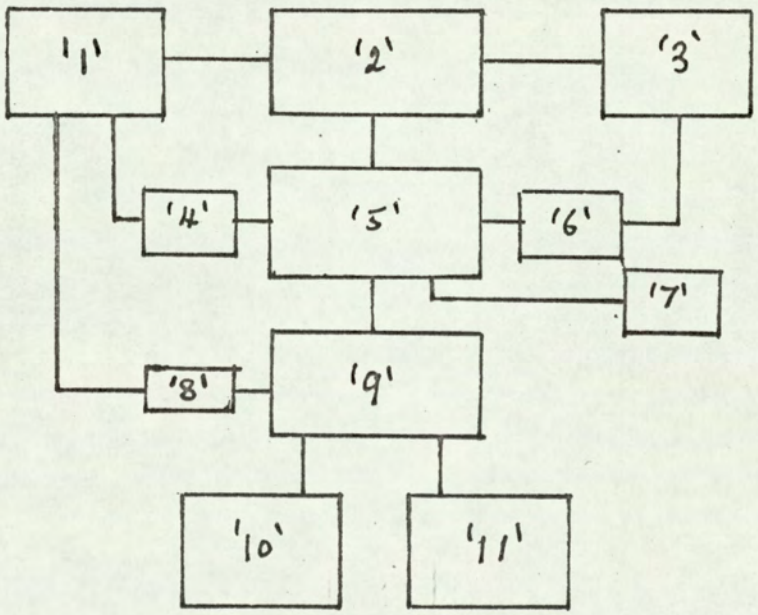

Fig.(5) Block diagram of an automatic digital read-out calibration equipment.

1. Precision rotating sub-standard.
2. Load and control.
3. Meter under test.
4. Check preamp.
5. Electronic control unit.
6. Test preamp.
7. Remote control.
8. Preamp.
9. Gated electronic counter.
10. Visual in-line read-out.
11. Automatic printer or card punch.

in 1955[29], in place of the 'Time-Power' method. The rotating sub-standards are carefully chosen (without registering mechanism) and calibrated by the 'Time-Power' method. They are placed in temperature controlled boxes. The revolutions of the sub-standard are detected photoelectrically and a pre-set number of revolutions can be selected. The way of error display consists of using the output of the photodetector which occurs at the beginning and end of each run, to trigger an electronic circuit that pulses a mercury-vapour lamp and produces a persistent spot of light on a phosphorescent band. The position of these two spots, one at the beginning and one at the end of the run, can be read to the nearest 1/1000 of a revolution on a scale, hence errors can be found.

Digital display and automatic printing are described by Antonelli.[30] Fig.(5) shows a block diagram of the [illegible] system. Standard timing pulses are derived photoelectrically from the rotating sub-standard, which has a 1000 lines around its circumference, and the percentage error in one revolution for the meter under test is displayed. Resolution of 0.1% is claimed. A very similar system is described by Rogers[31], the rotating sub-standard meter however has only 250 slots cut in its disc, their effect is doubled by passing the light beam through a grating. Baggot[32] of the London Electricity Board describes a similar system used in the Bexley Heath test station.

In an attempt to increase the accuracy of the speed Comparison method, Friedl[33] describes an arrangement which possesses means to compensate the error of the rotating sub-standard, An AC/DC transfer instrument is used, the total errors are claimed to be less than $\pm$ 0.05%.

Holz[34] reports the use of a recorder in testing meters. Electronic means are provided for converting pulses generated by rotation of the rotating sub-standard meter disc into power for driving a series of synchronous motors. Each motor drives a drum containing a raised helix, the rotational speed of which is, therefore, proportional to the speed of the sub-standard. Photo-electric detection is used on the meter under test and a one revolution gives an impulse which is used to operate a printing bar. The bar hits a portion of the raised helix on the synchronously driven drum, and prints a series of dots on a paper tape positioned above the helix, the paper being inched forword for each operation. Thus, if the test meter has the exact speed of the sub-standard, the raised helix will always present the same position to the printing bar when it operates, and the dots will appear as a vertical line up the paper tape. Any deviation in speed will cause the line of dots to appear off the vertical, the slope of which is a measure of the difference in accuracy of the test meter to the sub-standard meter.

The Sangemo Ltd. Co. in the U.S.A. [35] and the Sangemo Weston Co. [36] in this country use this method. Forty meters are calibrated at a time in half an hour. Accuracies of ± 0.2% at full load unity power factor, ± 0.4% at low loads unity power factor and ± 0.8% at full load 0.5 lagging power factor, are claimed. It is not mentioned whether this includes the errors of the sub-standard. This system is complicated and not as accurate as some of the techniques mentioned before.

The techniques described above share some common disadvantages, the most important being:

a) <u>The limits of error of the rotating sub-standard</u>:

The errors of the sub-standard must always be known, and must be added to those of the calibration. This requires frequent calibration of the sub-standard or the presence of an A.C/D.C. transfer instrument. The limits of error of the sub-standard makes it desirable that the resolution of the equipment be of the order of ± 0.1% and discourages the use of a calibrated production meter as a sub-standard because it has to be used below the 25% of its full load. Claims of equal temperature, frequency and voltage variations on both the sub-standard and meter under test are true; but one must remember that the meters are warmed up initially to about the same temperature and

that in most cases some form of voltage and frequency regulation exists.

b) Cyclic Variations: This non-uniform motion exists in the rotors of both the sub-standard and the meter under test. It has the effect of accentuating the observed errors or reducing them, at low load tests, depending on the relative positions of the rotors at starting. Also the non-uniform friction in the register mechanism add to this if it is present.

c) Economic Factors: Most systems describe testing one meter at a time, as test units have to be duplicated in quantity testing. A different sub-standard is needed for each type of meter, the alternative being the use of expensive current transformers. A form of power regulation of the order of 0.1% is still required.

d) Friction in Gear Trains: No technique has been described to assess the friction in the register mechanism and one has to assume that either this is ignored and only the gear ratio is tested, or a dial test is used, then all claims of speed and efficiency must be re-evaluated.

1.7 Stroboscopic Methods.

Despite the fact that stroboscopic methods are not listed with the approved methods, they have played and are still playing an important part in Meter Testing.

One of the earliest applications of stroboscopic testing was patented by Blathy[37] of Austria Hungary. His method required slotting the discs of the meters, and an elaborate procedure for positioning the meter under test. It had also the disadvantage of not enabling the viewer to determine if the meter was slow or fast. Nevertheless, his pioneering work led later to the many developments in stroboscopic testing.

Sparkes [38] describes a stroboscopic device, which is a watt-meter with a light vernier scale for measuring watt-seconds and giving instantaneous indication of Meter speed. This is an interesting and ingenious though elaborate technique. By its substitution of the flash lamp with light impulses the rate of which is proportional to the power, it allowed a wide range of speeds to be checked. Percentage errors are displayed by a pointer meter and a resolution of 0.3% at full load is quoted.

Moore[39] reports in 1928 that "The measurement of speed by means of stroboscopic observations has become an accepted test - capable of precision results". In his paper he reviews present day improvements in the stroboscopic techniques and its application in meter testing. Later in 1933, Maurer[40] gave a

review of stroboscopic methods, and made various suggestions for extending their usefulness.

Two main difficulties faced the workers using stroboscopic methods.

a) The definition of the image deteriorated at lower speeds.

b) The cyclic variations in the speed of the disc produced cyclic shifting in the image.

Bradshaw [41] discusses these difficulties and describes a method of viewing the disc through a 'viewing disc', this disc is driven by a varying adjustable frequency. With this method he was able to test meters to a reasonable degree of accuracy down to 1/20th of full load. A patent taken by the Aron Electricity Meter Ltd. [42] discloses another way of overcoming these difficulties. This is accomplished by the use of an artifice whereby the 1/20th load speed is temporarily increased for calibration purposes. Thus stroboscopic vision is good and cyclic variations disappear. This is achieved by using a high speed sub-standard for low load calibration and fitting the meter under test with a weak brake magnet. A normal speed sub-standard is used for the other adjustments. The average time of calibration is stated as 2.5 minutes per meter and accuracies of the order of $\pm$ 0.5% are maintained.

A combination of stroboscopic and photoelectric test system is described by Price [43]. Full load unity power factor and full load

0.5 power factor are tested stroboscopically. Light loads are tested by a photo-electric start-stop speed comparison method.

Lynch and Princi [44] describe a system where the speed of a sub-standard meter is detected photoelectrically and used to operate a synchronous motor. A slotted disc, mounted on the synchronous motor shaft, interrupts a beam of light which projects through a suitable optical system an image of the teeth on the edge of the disc onto a screen.

A system which uses revolving optical compensators to view the disc of a meter under test, and to compare its speed with that of a sub-standard meter, is used by Musson and Mell [45]. An image of the disc marks is obtained which is very similar to a stroboscopic image; but more clearly defined because there is a neglibible loss of light in the system, and it is almost immune from "flicker". This image has the advantage that cyclic variations do not prevent its use for light-load testing. Loads from 1/20th of full load are used, and accuracies of $\pm$ 0.25% are quoted.

Petch [46] gives details of a system whereby the suitably marked discs are illuminated with a flashing light, the rate of flash being derived photo-electrically from a rotating sub-standard meter. This is used to control a synchronous shutter at the focus of a small projector. In order to avoid the difficulties at low loads, the sub-standard pulses are counted for several revolutions of the meter under test, this is done by suitable synchronous motor driven counters.

The stroboscopic method is an attractive and simple one, and a great number of ingenious devices have been developed to overcome the difficulties encountered at low loads, nevertheless it is still not capable of tests below the $1/20^{th}$ of full load. This necessitates a hybrid system and the provision of two sets of equipment. With the advent of digital display and the modern techniques described earlier this method proves useful if used only in presetting the meters.

THE SPEED-LOAD CHARACTERISTICS OF THE SINGLE PHASE INDUCTION TYPE ENERGY METER

2.1 Introduction:

It is usual to display the characteristics of a single phase induction type energy meter in what is commonly termed the load curve of the meter. This is a plot of percentage error against load. An alternative way of presenting the behaviour of the meter, would be to plot the speed of the disc against the load. This curve will display the characteristics of the meter as a watt-meter; however, as most calibration methods depend on this property, an investigation is essential, especially at the lower loads.

2.2 The timing of the disc for one revolution:

The method used to find the speed of the disc was to time it for one complete revolution to a high degree of accuracy. This was done by photo-electric detection and electronic means. Fig.6 shows a block diagram of the system used. A light source is focussed on the edge of the disc, the sharp image displayed is that of the filament of the lamp and has a thickness of the order of one millimeter. This light is detected by a detector and a pulse is produced every time the light is interrupted by the black spot on the edge of the disc. The pulse is amplified and shaped and used to drive a binary element which in turn starts and stops a precision electronic timer/counter. A digital display of the time taken for

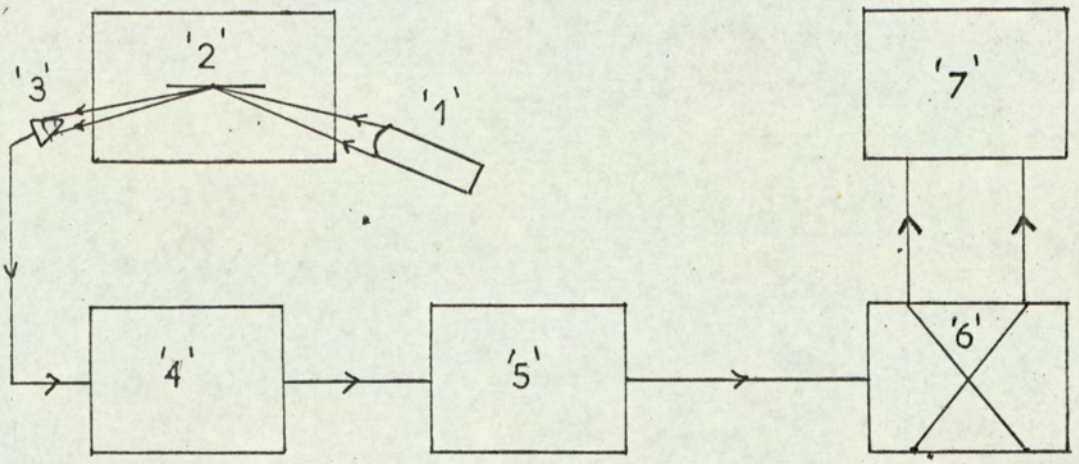

Fig. 6 - Block diagram showing the one revolution timer system

1. Light Source.
2. ENERGY METER.
3. Light Detector.
4. Amplifier.
5. Shaping circuit.
6. Binary element.
7. Electronic counter.

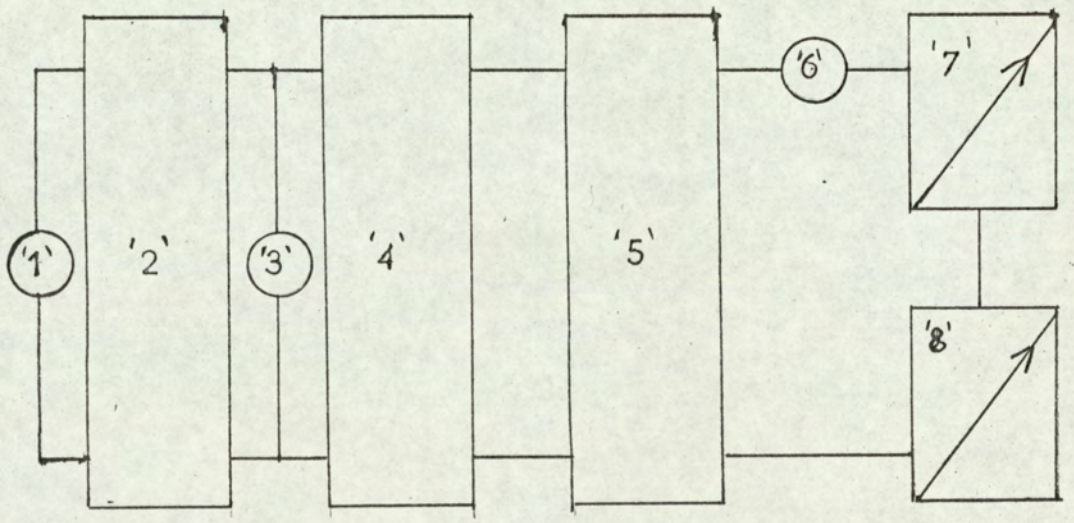

Fig. 7 - Block diagram showing the test loading arrangement

1. Mains supply.
2. Voltage regulator.
3. Monitoring Voltmeter.
4. ENERGY METER.
5. Wattmeter.
6. Monitoring Ammeter.
7. Coarse load.
8. Fine load.

one revolution of the disc is thus obtained. The load indicated by a sub-standard watt-meter is held steady during the test.

2.3 Design of the Electronic System:

Many methods of detecting 'one revolution' of the disc are found in the literature, yet most of them relied on the creep holes or on a mirror placed on the spindle to provide adequate light for detection. Those which used the black spot, relied on modulated light to avoid background interference. This last method was chosen, as it interferes the least with the meter, and to attempt to avoid light modulation. This proved possible by the use of a high intensity light beam. The light source must be driven by D.C. The main parts of the system are,

a) The detector and amplifier: Fig.8 shows the circuit diagram of the arrangement. The photo-transistor was used as a diode to improve the response time and the signal to noise ratio. A two stage amplifier was used to amplify the pulse. The time response of the system for a step input of light was,

fall time : 50 μ S.

Rise time : 10 μ S. This was for an output voltage swing of the order of 10 volts.

b) The shaping circuit: As a wide range of disc speed was anticipated, the rising edge of the detected pulse will always be dependant on the speed with which the

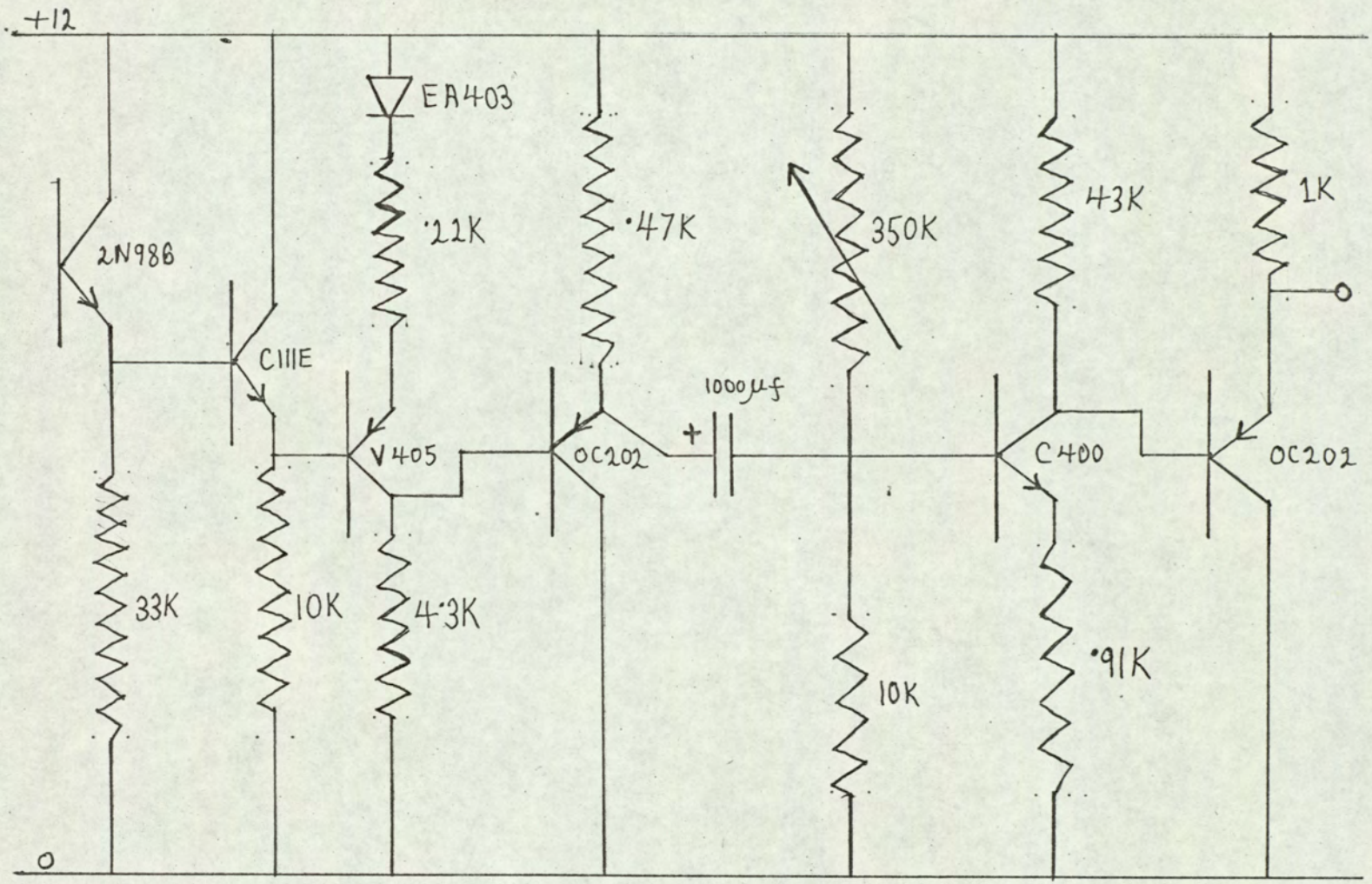

Fig. 8 - Circuit diagram of light detector and amplifier.

mark cuts the light. In order to provide a pulse of standard shape and independent of the speed of the disc a shaping circuit was used. Fig.9, shows the circuit. This produces a fast rising edge, less than 2 μ S, and of an amplitude of the order of five volts. This is always triggered when the input waveform reaches a certain voltage level, hence the start and stop commands are initiated at the same position relative to the disc, producing thus a precise one revolution detector.

c) The binary element: The shaped pulse triggers a bistable element. Fig.10 shows the circuit. This in turn provides the start and stop orders to the counter. The signal has an amplitude of five volts and a rise time of the order of 10 μ S. No logical arrangement was necessary as the counter can be started and stopped by either a positive or a negative going pulse.

d) Consideration of accuracy: The main factors affecting the accuracy of the speed measurement, assuming constant voltage, temperature, and frequency, are the accuracy of the counter* and a change in the response time of the system, both of which are estimated to be less than one in ten thousand.

* Details of the instruments and equipment used are given under General Information.

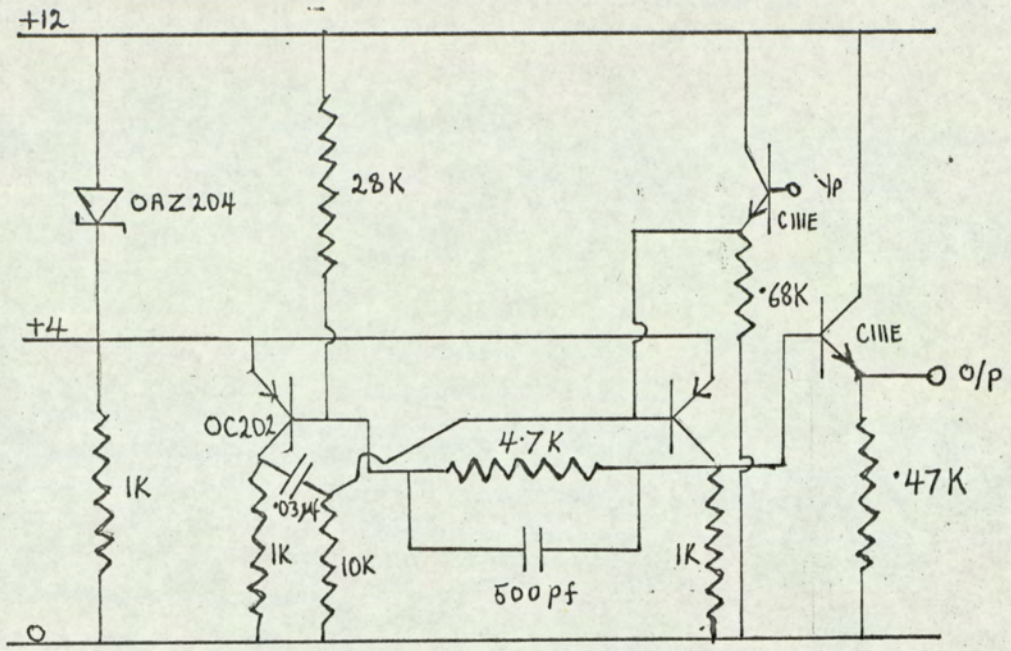

Fig. 9 - Circuit diagram of pulse shaper

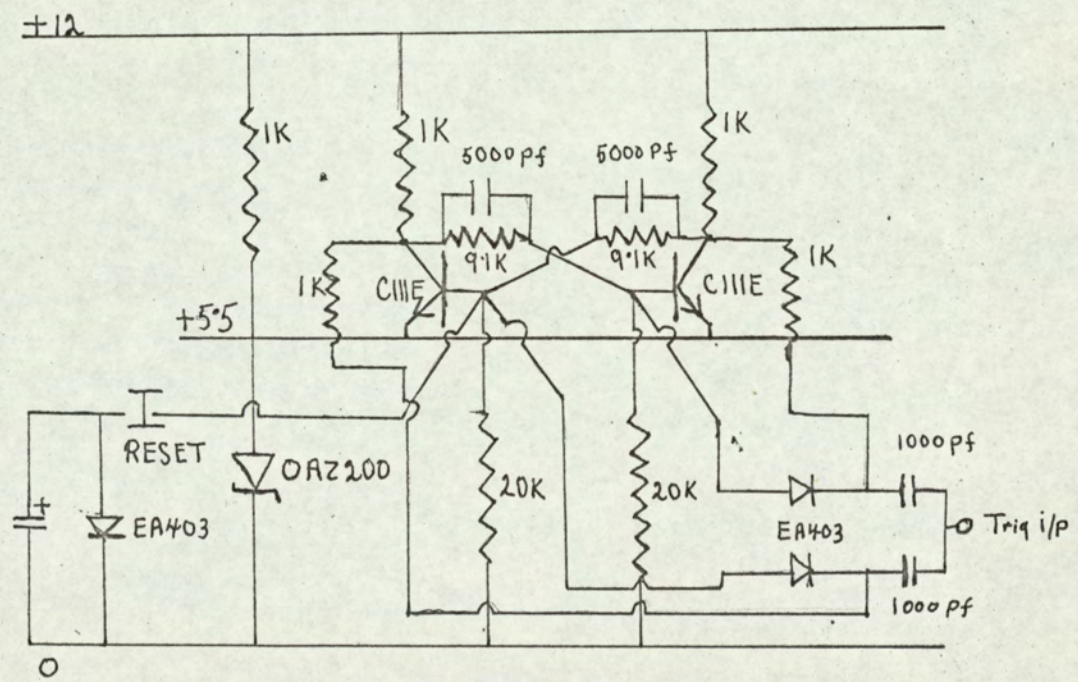

Fig. 10 - Circuit diagram of Binary element.

2.4 The supply and load arrangement:

A stable supply was necessary in this method of testing. Fig.7 shows a block diagram of the load arrangement. A constant voltage transformer 'voltstat' was used to drive a servo regulator. This produced a relatively stable supply. Precision, calibrated instruments were used to monitor power, voltage and current. A real load at unity power factor was used, this load could be altered in steps, each having suitable fine adjustment.

2.5 The test procedure and results:

The load was maintained constant at the nominal value indicated by the watt meter and the time taken for one revolution was noted. An average of several readings was used.

a) The effect of the frictional adjustment on the speed-load characteristics of the meter: This adjustment is intended for the compensation of constant torques produced by friction or other causes. Fig.11, shows its effect on the speed-load characteristics of the meter. The curves appear to be shifted by a constant value, the slope being unaltered. To ensure this observation, the differences in speed between a reference curve and that of a faster and a slower setting, were plotted against load. Fig.12(a), shows the resulting graph in the load range 1/10 - 1/100 of full load. Fig.12(b), shows it for the load range, 1/1 - 1/10 of full load. Both confirm a constant

* Details of the instrument and equipment used are given under General Information.

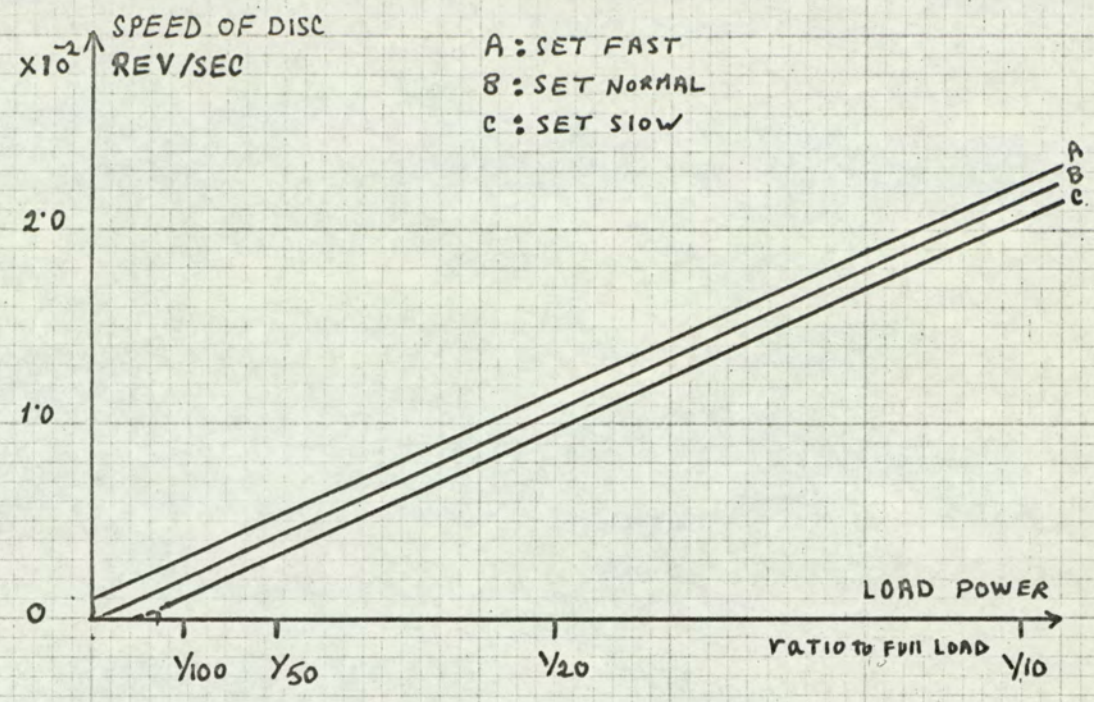

Fig. 11 - Graph showing the effect of Frictional adjustment setting on the speed-load characteristic of the meter.

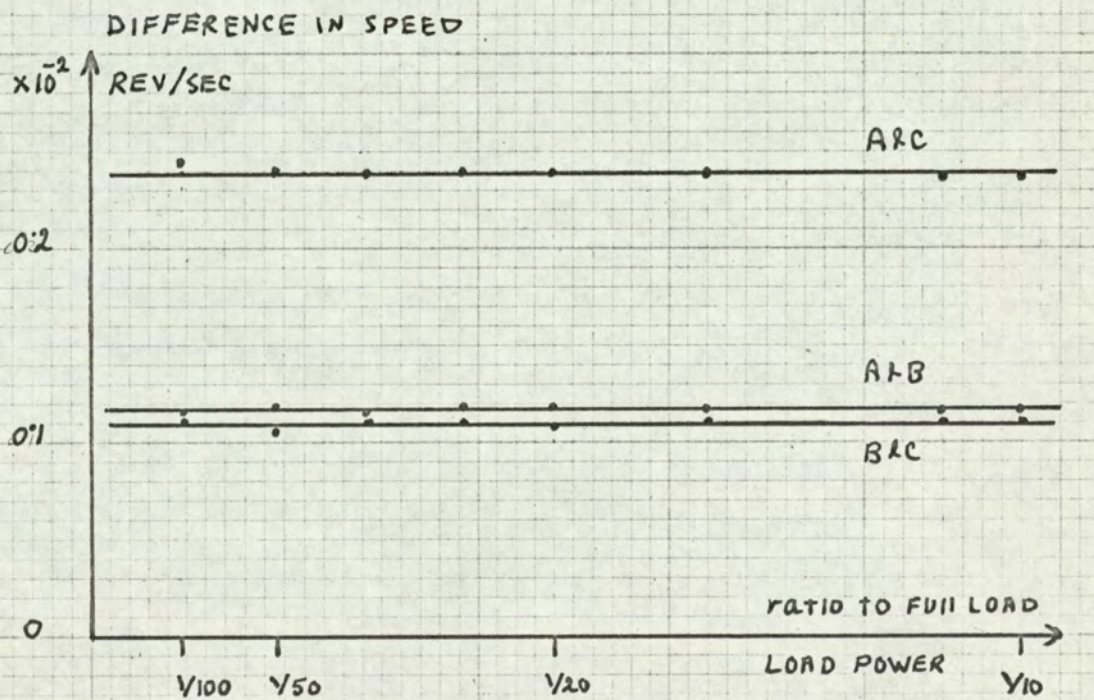

Fig. 12 (a) Graph showing the difference of speeds at a given load between different settings of the frictional adjustment, up to 1/10 of full load.

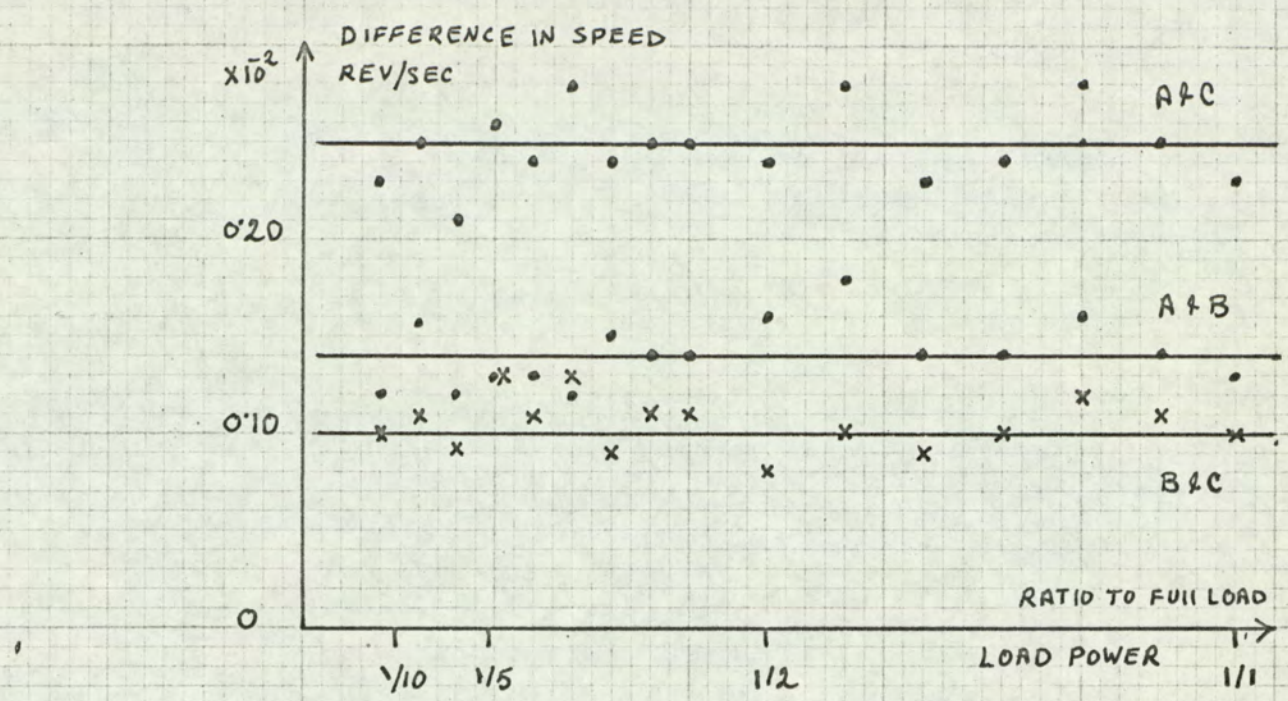

Fig. 12 (b) Graph showing the difference of speeds at a given load between different settings of the frictional adjustment up to full load

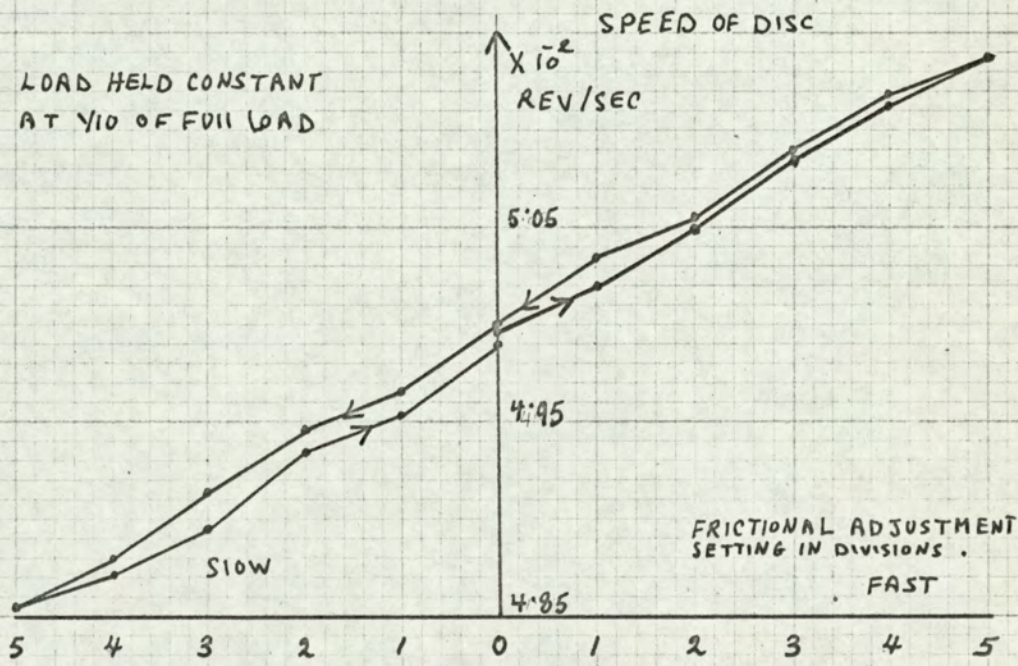

Fig. 13 - Graph showing the variation of the speed of the disc at constant load with the frictional adjustment setting

shift throughout the load range of the meter, hence the frictional compensation arrangement produces a constant torque independent of the loads. As the adjustment is produced by mechanical means, it was interesting to find out the slope and the amount of backlash. This is shown in Fig.13.

b) The effect of the main adjustment on the speed-load characteristics of the meter: This adjustment changes the amount of damping due to the brake magnet. Fig.14, shows its general effect. This appears to be a change of the slope of the curve. Fig.15, shows the slope of the adjustment and the effect of backlash.

2.6 The linearity of the speed-load characteristics of the Meter:

Tests, in the load region 1/10 - 1/100 of full load, on several meters produced characteristics which appeared to be linear. However, before they can be ruled out as straight lines an estimate of their trueness must be made. The following simple procedure was adopted. The general equation of a straight line is of the form,

$S = aW + b$ where S and W are the variables, a and b the constants. For our case,

S, will be the speed of the disc in rev./sec.

W, the load power in watts.

a, the slope of the line in rev.per second / watt.

b, the point of intersection with the speed axis.

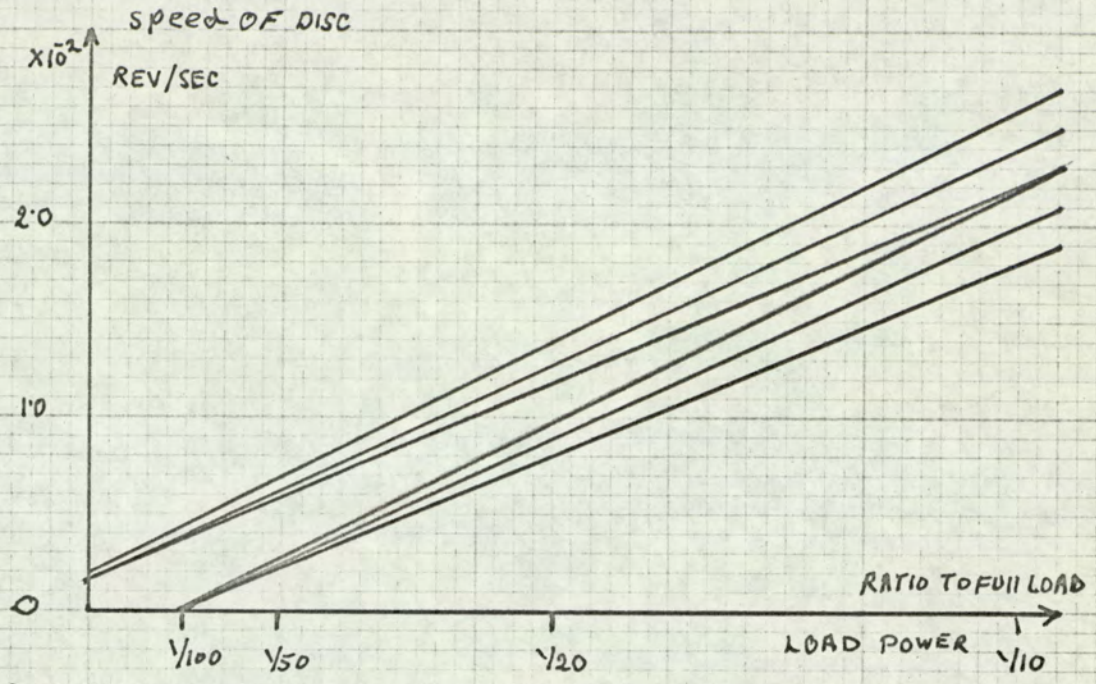

Fig. 14 - Graphs showing the effect of the main adjustment setting on the speed-load characteristics of the meter for different frictional adjustment settings

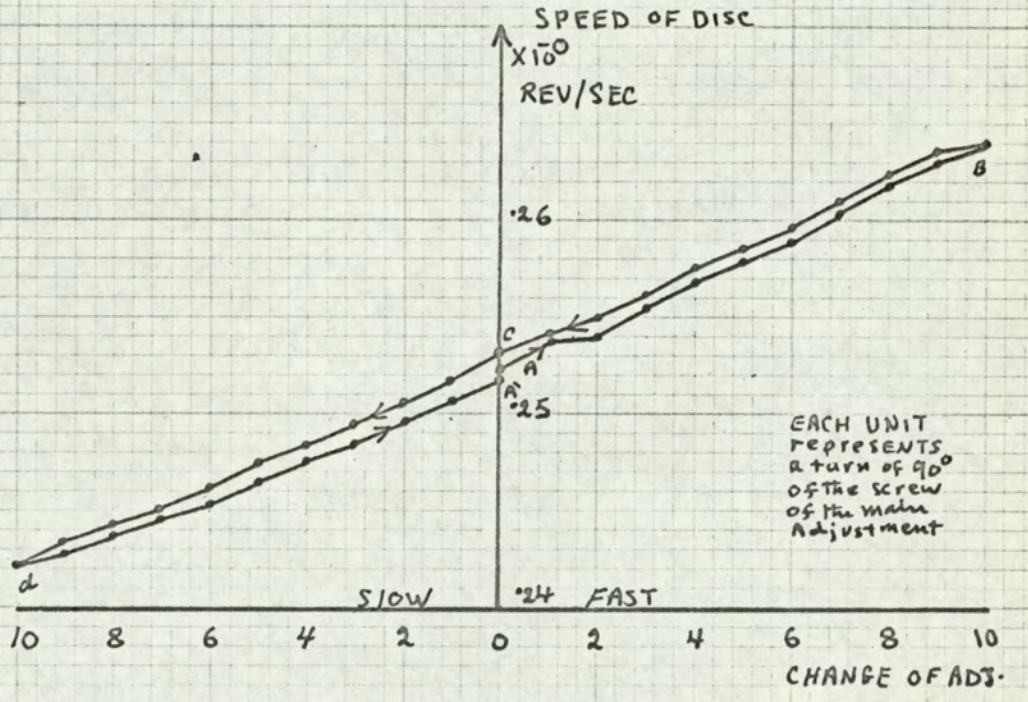

Fig.15 - Graph showing the variation of the speed of the disc at constant load with the main adjustment setting

Now, from the experimental observations two points can be chosen (S_1, W_1) and (S_2, W_2). The points chosen were those at the 1/10 and 1/100 of full load.

Using these points a straight line,

$$S = a_1 W + b_1 \quad \ldots\ldots \quad (4)$$

can be found. By substituting for W in (4) any value of power at which an observation has been made; a value S = Sc, the calculated speed, can be found. From the observed results a value S = Sp is available. Hence the relative difference $\frac{Sp - Sc}{Sc}$ given as a percentage can give a good estimate of the trueness of the lines. Figs. 16 and 17, show this for two types of meters, both of which were tested with and without registering mechanisms. Nearly all the points are found in a band of $\pm$ 0.2%.

2.7 Qualitative discussion of the factors affecting the linearity of the speed-load characteristics of the Meter:[47, 48]

Ideally the speed of the disc of an induction type energy meter should be directly proportional to the load power. However, several factors may affect this linearity, these factors will be examined briefly.

a) Friction in Bearings: This can be considered as equivalent to a constant torque and can be compensated.

b) Friction in Gear trains: This is considered later in greater detail. However, it can be considered constant for a good counter and can be compensated.

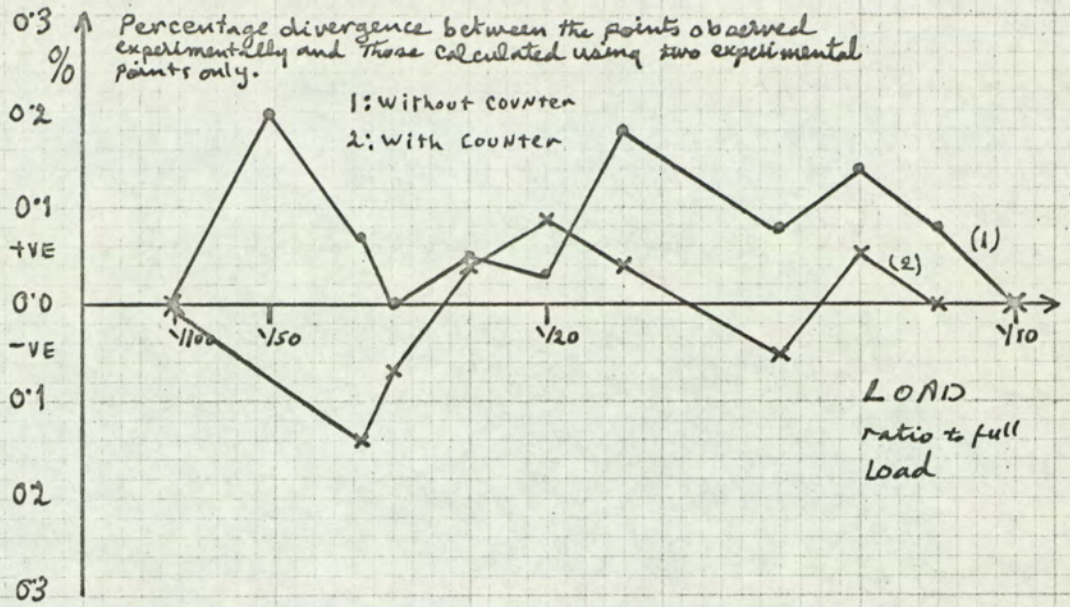

Fig. 16 - Graph showing estimates of the linearity of the speed-load characteristics for the V.L.R. meter in the region $\frac{1}{10} - \frac{1}{100}$ of full load

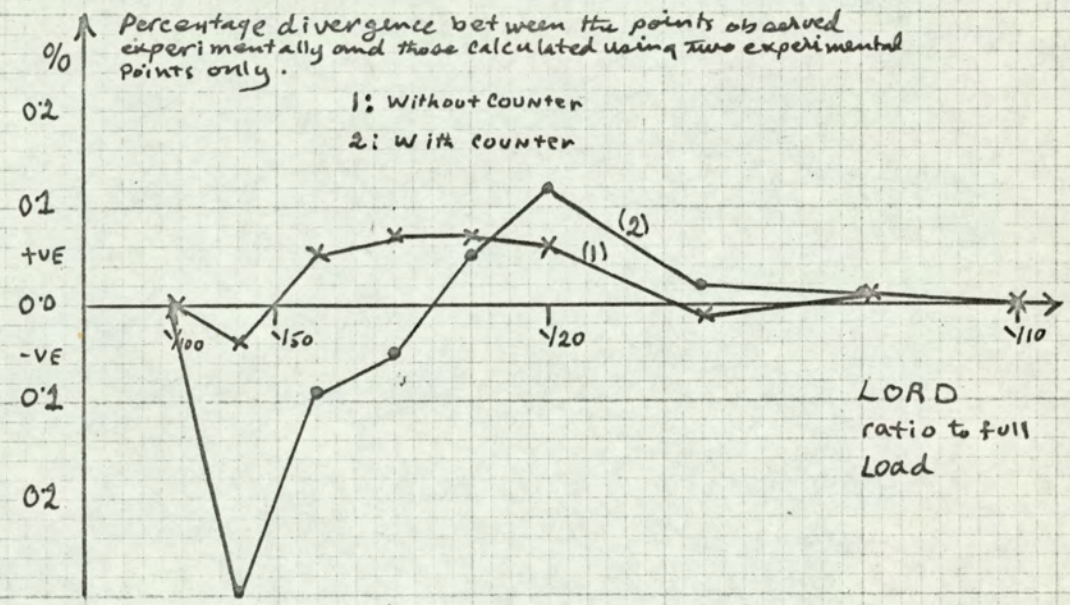

Fig. 17 - Graph showing estimates of the linearity of the speed-load characteristics for the L.R. Meter in the region $\frac{1}{10} - \frac{1}{100}$ of full load.

c) Permeability of iron in the current electromagnet:

The magnetisation curve of iron is not linear, so the torque developed in the meter and mainly at low loads will be dependent on the properties of the iron used in the current electro magnet. There is also some effects due to the quality of the material used in the magnetic shunt. These effects cannot be compensated, however, the presence of an air gap in the path of the flux of the current electro-magnet, and the use of better quality iron, all help to make the magnetisation curve more linear.

d) Possible lack of symmetry in the current electro magnet:

There is always some lack of symmetry between the current electro-magnet, with reference to the pressure electro-magnet; or the current electro-magnet may be tilted resulting in a tapered air gap between it and the disc. These torques being due to a mechanical disposition, could add or subtract a constant amount from the main torque, and can be compensated.

e) Current damping: This is proportional to the square of the current flux and the speed of rotation. The meter is usually designed with this in mind and its effect is usually conspicuous at high loads only.

It is clear from this survey that the only serious effect that cannot be compensated, is the permeability of the iron. So as the tests have shown a good degree of linearity one may conclude that these effects were small in the meters tested.

2.8 Considerations of the consistancy of the results with the simple theory of the induction meter:

Let us consider the simple theory of the induction meter,* let

W = V. I. cos ϕ, be the load power.

S be the speed of the disc in rev./sec.

Φ_i be the flux due to the current coil.

Φ_v be the flux due to the pressure coil.

Φ_m be the flux due to the permanent magnet.

K_1, K_2, K_3 and K_4, be constants at constant temperature, Voltage and frequency.

F_c to be the torque due to the frictional compensation.

F_f to be the equivalent frictional torque in the meter.

Equating the driving and damping torques,

$$S(K_1 \Phi_i^2 + K_2 \Phi_v^2 + K_3 \Phi_m^2) = K_4 VI \cos \phi + F_c - F_f \quad \ldots\ldots \quad (5)$$

As loads below 1/10 of full load are considered only, we can assume $K_1 \Phi_i^2$ to be small compared with the other damping torques. The damping torque due to the pressure coil is constant at constant pressure, so let $K_2 \Phi_v^2 = K_{11}$ and let $K_3 \Phi_m^2 = K_{22}$ (M), which is a function of the main adjustment setting 'M'. And let $F_c - F_f = K_{33}(f)$ a function of the frictional adjustment setting 'f'

* A brief review of the theories of action of the induction meter is given in Appendix I.

This leads to,

$$S = \frac{K_4}{K_{11} + K_{22}} W + \frac{K_{33}}{K_{11} + K_{22}} \quad \ldots\ldots \quad (6)$$

This is in the form of the equation of a straight line. Now, if the main adjustment is kept constant and the frictional adjustment is varied, K_{33} is the only variable in (6), hence the line will shift parallel to its old position, this is in agreement with the experimental observations. For a fixed frictional adjustment and a varying main adjustment, K_{22} is the only variable, so this will alter the slope of the line, which is again in agreement with the experimental observations.

2.9 The shape of the error curve of the meter:

From equation (6) the adjustment of the meter can be defined, for the speed observation methods, as those operations which make the part $\frac{K_{33}}{K_{11} + K_{22}} = b$, tend to zero.

And $\frac{K_4}{K_{11} + K_{22}} = a$, tend to a value in concurrence with the meter constant.

a) The effect of a wrong frictional adjustment: The relative error due to a wrong frictional adjustment is

$$\frac{b}{aW} = \frac{r_1}{W} \quad \ldots\ldots \quad (7)$$

r_1 being a constant. This is inversely proportional to the load, hence its effect is made pronounced at the lower loads.

b) The effect of a wrong Main adjustment: The relative error due to a wrong main adjustment is given by,

$$\frac{\delta a}{a} = r_2 \quad \ldots\ldots \quad (8)$$

r_2 being a constant. This is independent of the load. An expression for the relative errors, considered up to now, of the meter can be proposed,

$$r = \frac{r_1}{W} + r_2 \quad \ldots\ldots \quad (9)$$

These are relative errors at a given load. The actual registration errors of the meter when operating is a function of these inherent errors and the time spent by the meter at a given load. This aspect of the mean error of the meter is investigated by Stubbings [49].

2.10 A suggested Technique for the low load calibration:

The observed results considered before indicated a straight line characteristic for loads in the region 1/10 - 1/100 of full load. This suggests that, to try and get the line to go through the point of origin, assuming that the slope of the line is set up by a full load test, two points anywhere in that region will be necessary to ensure this condition. These points can be taken at the higher end of the load, say at 1/10 and 1/20 of full load. So, if the test equipment has the right resolution and accuracy, the usual low load test point at 1/60 full load, should be on the straight line extra polated from these two points.

2.11 The required accuracies:

Let us assume a test done for the nominal power of 1/10 of full load = W_1 and the speed was S_1, and that another test was done for the nominal power of 1/20 of full load = W_2 and the speed was S_2. Near calibrated conditions, the term 'b' will tend to zero, so the equation of the line will be,

$$S = a\,W \qquad \ldots\ldots \qquad (10)$$

taking the logarithmic differential we have the relative error given by,

$$\frac{\delta S}{S} = \frac{\delta a}{a} + \frac{\delta W}{W} \qquad \ldots\ldots \qquad (11)$$

$\frac{\delta W}{W} = 0$, as this is a specified point.

Now $$a = \frac{S_1 - S_2}{W_1 - W_2} \qquad \ldots\ldots \qquad (12)$$

Taking the logarithmic differential, the relative error is given by,

$$\frac{\delta a}{a} = \frac{S_1}{(S_1 - S_2)}\,\frac{\delta S_1}{S_1} - \frac{S_2}{(S_1 - S_2)}\,\frac{\delta S_2}{S_2} - \frac{W_1}{(W_1 - W_2)}\,\frac{\delta W_1}{W_1} + \frac{W_2}{(W_1 - W_2)}\,\frac{\delta W_2}{W_2} \qquad \ldots\ldots \qquad (13)$$

for the maximum possible error, the signs must be changed to positive.

As,

S_1 is approximately equal to $2\ S_2$

W_1 is approximately equal to $2\ W_2$,

we have,

$$\frac{\delta a}{a} = 2\,\frac{\delta S_1}{S_1} + \frac{\delta S_2}{S_2} + 2\,\frac{\delta W_1}{W_1} + \frac{\delta W_2}{W_2} \quad \ldots\ldots \qquad (14)$$

This can be changed to percentage error. So assuming the percentage error in speed is equal to α_1 and in power be α_2. So in order to obtain, 0.1% calibration accuracy. $\alpha_1 + \alpha_2$ = 0.033%, and a proper choice of α_1 and α_2 can be made.

Tests to ascertain the usefulness of this technique were conducted.

a) In the Laboratory: Where setting the two points to a resolution of 0.1% the 1/60 of full load point was found to be within $\pm$ 0.2%.

b) Using an Industrial speed-comparison method: The equipment used was similar to those described in 1.6 (ii), 25 meters were tested and adjusted, all being taken directly from the production line. The equipment displayed the percentage error digitally. With this type of equipment the points must be set so that they both have the same percentage error, this is done to allow for any main adjustment errors. The resolution of the equipment was 0.1% at high loads and about 0.3%

at low loads. It was possible to get the meters to be within $\pm$ 0.5% at 1/60 of full load by adjusting them at 1/10 and 1/20 of full load.

THE NON UNIFORM SPEED OF THE DISC OF THE INDUCTION METER WITHIN ONE REVOLUTION

3.1 Introduction:

The speed of the disc of an induction meter suffers cyclic variations. This has been reported in the literature, and has posed great difficulties to workers in the stroboscopic field of calibration. At low loads the effect is visible to the naked eye. Several factors could contribute to such behaviour;

a) Anti-creep holes;

b) Eccentric or bent discs;

c) Inequalities in the metal of which the disc is made;

d) Variation of friction in the rotor bearing;

e) Variation of friction in the counter.

Despite the importance of this effect; the only published work found, dealing with this aspect, was that of Havekin[50]. His investigations had led him to the following main conclusions;

i) The large positive errors at low loads are due to the creep holes.

ii) The speed fluctuations within one revolution are due mainly to the creep holes.

The errors of the meter at low loads are mainly a function of the frictional adjustment setting. The meter, during one revolution, gives an average speed which is constant at a given load. Experimental results showed that the meter curve can be flattened out at the lower

loads down to about 1/200 of full load. So there is no justification for (i). The experimental data given by Havekin did not provide conclusive evidence to justify the acceptance of (ii). It was thought that an investigation would be necessary to clear up the matter.

3.2 Monitoring the speed of the disc within one revolution:

The disc of the meter is divided by black lines round its circumference into a number of equal divisions. This is usually provided by the manufacturers to facilitate stroboscopic testing. It was thought that a photoelectric method of finding the time taken by the disc to travel the distance between two lines, would provide a suitable means for the intended study. Fig.18 shows a block diagram of the system. A light source focused on the face of the disc and detected by a photo electric detector provides a waveform which is amplified and shaped, and after suitable matching used to drive an Ultra* violet recorder. This system can be used to observe the transient behaviour of the meter under sudden changes in the load. Some work has been done in that field e.g. Faucett and others (51) used a stroboscopic camera for such a study.

3.3 The design of the system

The light source and detector used are the same as those described in 2.3, however, the pulse amplifier was modified slightly, the circuit is shown in Fig.20. A schmitt trigger was used to shape the

* Details of the equipment used is given under General Information.

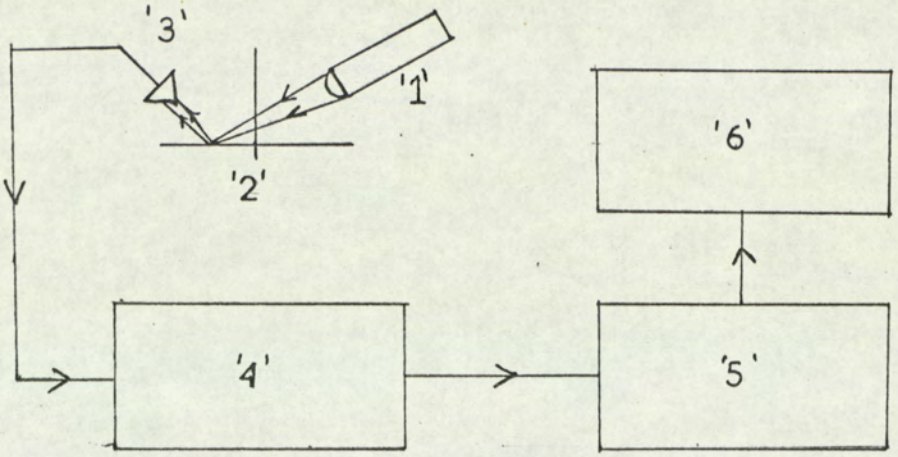

Fig. 18 - Block diagram showing the system for detecting the speed of the disc within one revolution

1. Light Source.
2. Meter Disc.
3. Phototransistor.
4. Amplifier.
5. Shaping and Matching circuits.
6. Ultraviolet recorder.

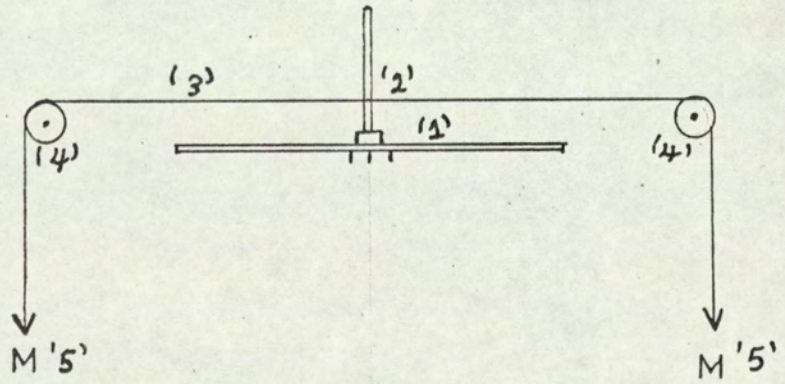

Fig. 19 - Diagram showing the constant torque drive arrangement

1. Meter disc.
2. Diametric hole in spindle.
3. Silk Thread.
4. Polished bar.
5. Driving weight.

waveform, the circuit is shown in Fig.21. This had a narrow width, of the order of 0.1 volts. In order to provide a relatively stable trigger point, the output of the schmitt was integrated and fed back to the input. Figs. 22 and 23 show oscillograms of the relevant waveforms at different positions in the system. A plate showing the equipment and general arrangement of the system is shown in Fig.24. The load arrangement was the same as that described previously.

3.4 The waveform produced:

The marks round the disc were spaced at intervals, the width of which was equal to those of the marks. Had the light beam a width equal to those of the marks, the detected waveform would have been ideally a saw tooth. The slope of which was proportional to the speed of the disc. The beam was however, of finer width than the marks, this produced a waveform having a flat top and bottom, corresponding to the total overlap when the light intensity detected was not changing. This is shown clearly in Fig. 22.A. The waveform was affected further by the relative blackness of a mark and whiteness of an interval. This produced two effects;

a) The amplitude of the waveform slightly differed.

b) The flat parts of the waveform were not perfectly flat.

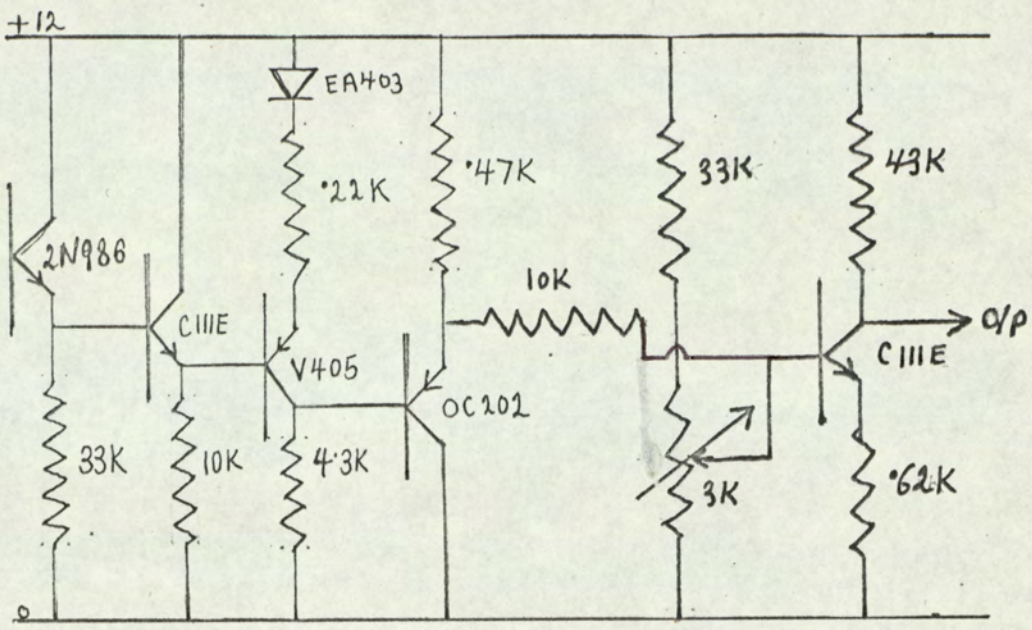

Fig. 20 - Circuit diagram showing the phototransistor and Amplifier

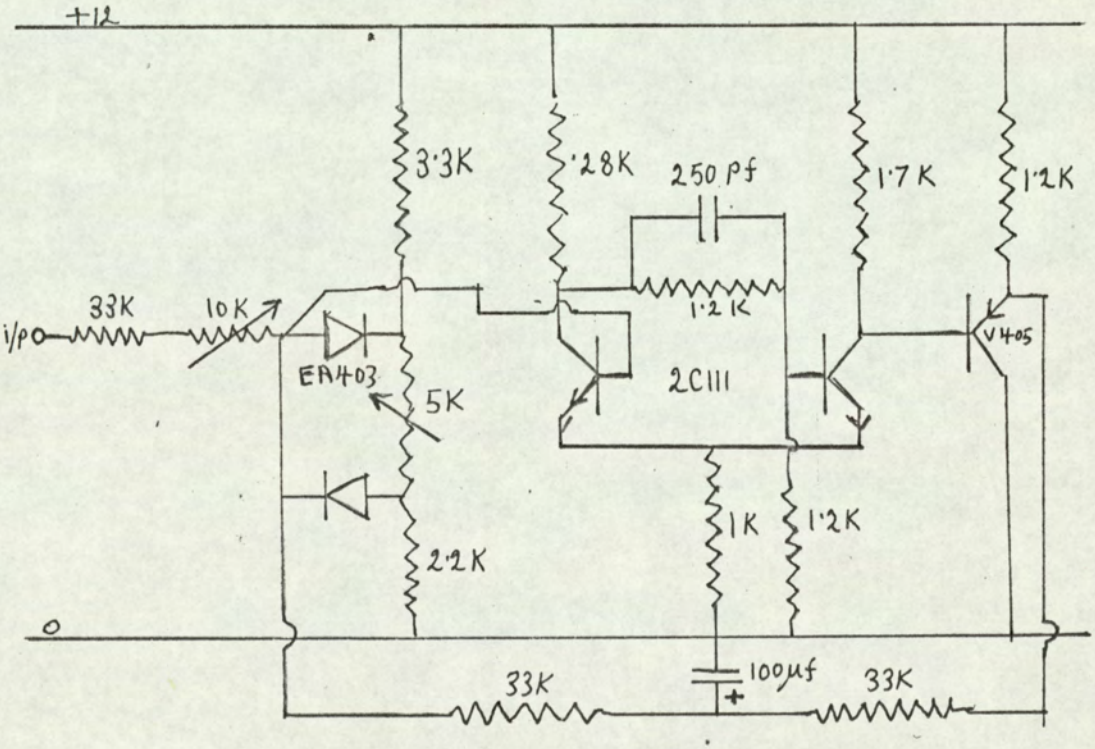

Fig. 21 - Circuit diagram showing the schmitt trigger used for shaping

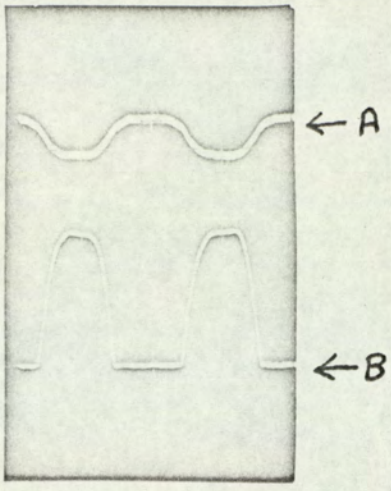

Fig. 22 - Oscillogram showing the detected waveform

A) after the first stage amplifier.

B) after the second stage amplifier.

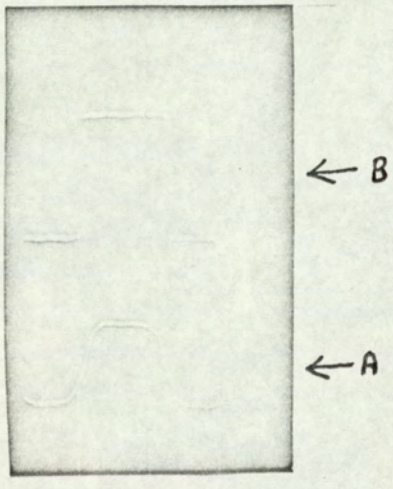

Fig. 23 - Oscillogram showing the detected waveform

A) At the input to the schmitt trigger.

B) At the output of the schmitt trigger.

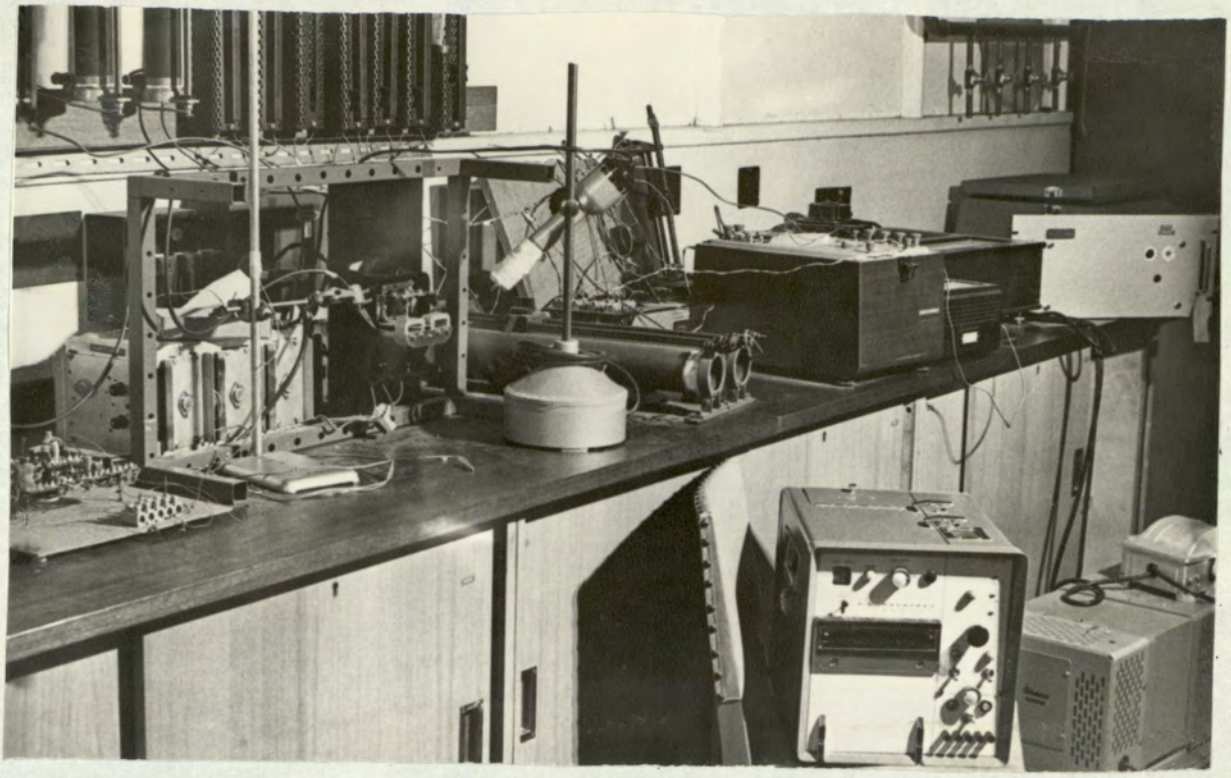

Fig.24 - Plate showing the equipment and general arrangement of the system

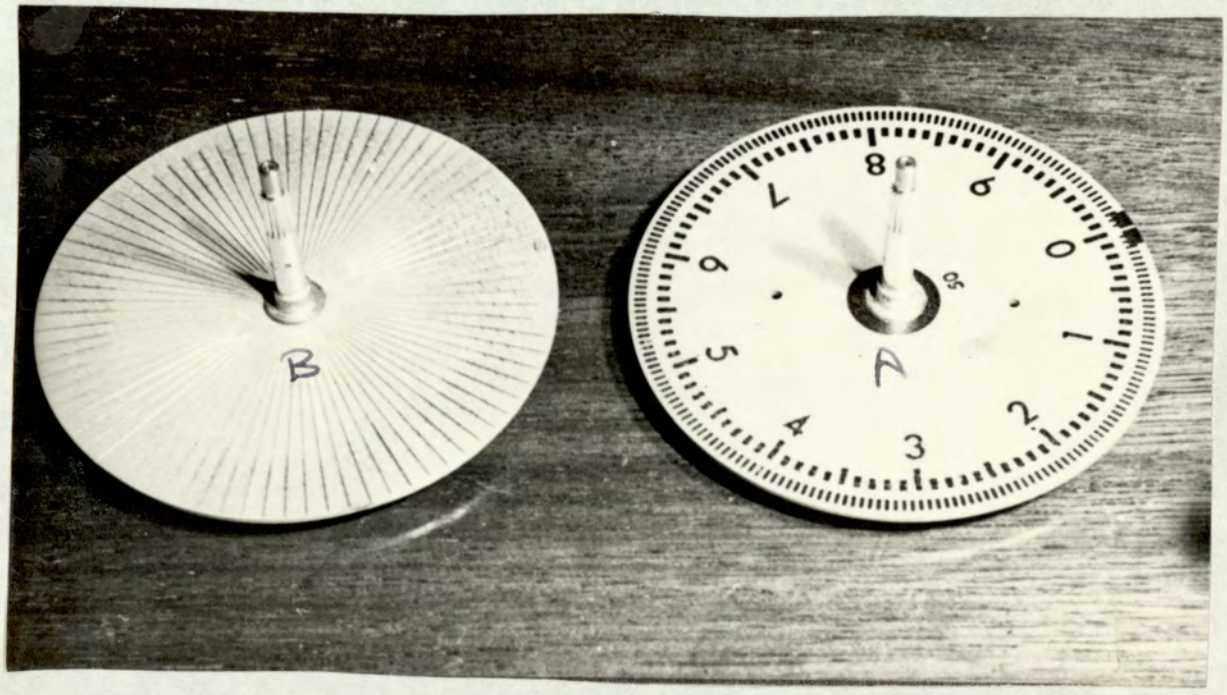

Fig. 25 - Plate showing the disc of the meter.
A : Normal disc with creep holes.
B : Disc without creep holes, suitably divided.

3.5 Factors affecting the waveform:

The major factors affecting the waveform and hence the accuracy of the detector are;

a) Non uniform spacing of the marks. Measurements with a travelling microscope showed those to be within $\pm$ 1%

b) The intensity of the light beam.

c) Factors discussed in 3.4.

d) The speed of the disc, which alters the slope of the sides of the detected waveform.

3.6 Test Procedure:

For a given load which was kept constant, the record produced by the U.V. recorder was analysed. A reference point was taken on the meter, and from the record, the time taken by the disc to travel a certain distance was found. The speed of the meter at a given region round its circumference was then calculated.

3.7 Considerations of accuracy.

The possible sources of error are;

a) The supply and indicating watt meter.

b) The uniformity of the divisions on the disc.

c) The detector and electronic equipments.

d) The fluctuations in the speed of the recorder.

e) The accuracy of the length measurement taken on the record.

A maximum possible error of the order of $\pm$ 4% was estimated.

3.8 Analysis of the results:

The speed distribution pattern, relative to a reference point, repeated itself regularly each revolution. This is shown in Fig.26. Tests on a load range of 1/250 - 1/12.5 of full load are shown in Fig. 27, a, b, c, d and e. The pattern is not symmetrical. It repeats its general shape at all the loads; however the amplitude of the pattern at a given position, depends on the load. Tests conducted on a different type of meter produced a similar pattern. This is shown in Fig. 28 a and b. Two observations can be made from comparing the two tests;

a) The shape of the pattern is nearly the same.

b) The peaks and dips occur at nearly the same positions.

The speed-load characteristics, for some positions round the circumference of the disc, were plotted. These were derived from the previous graphs, and are shown in Fig.29 a and b. The characteristics were linear and parallel to one another. They can be described by a series of straight line equations all having the same slope, but with different values for the intersection with the speed axis. This intersection is a function of position $b = f(\theta)$. θ being the position of the disc relative to a chosen reference point. So the family of lines can be represented by the straight line equation;

$$S_1 = a W + f(\theta) \quad \ldots\ldots \quad (15)$$

The average speed-load characteristic considering one complete revolution will then be described by;

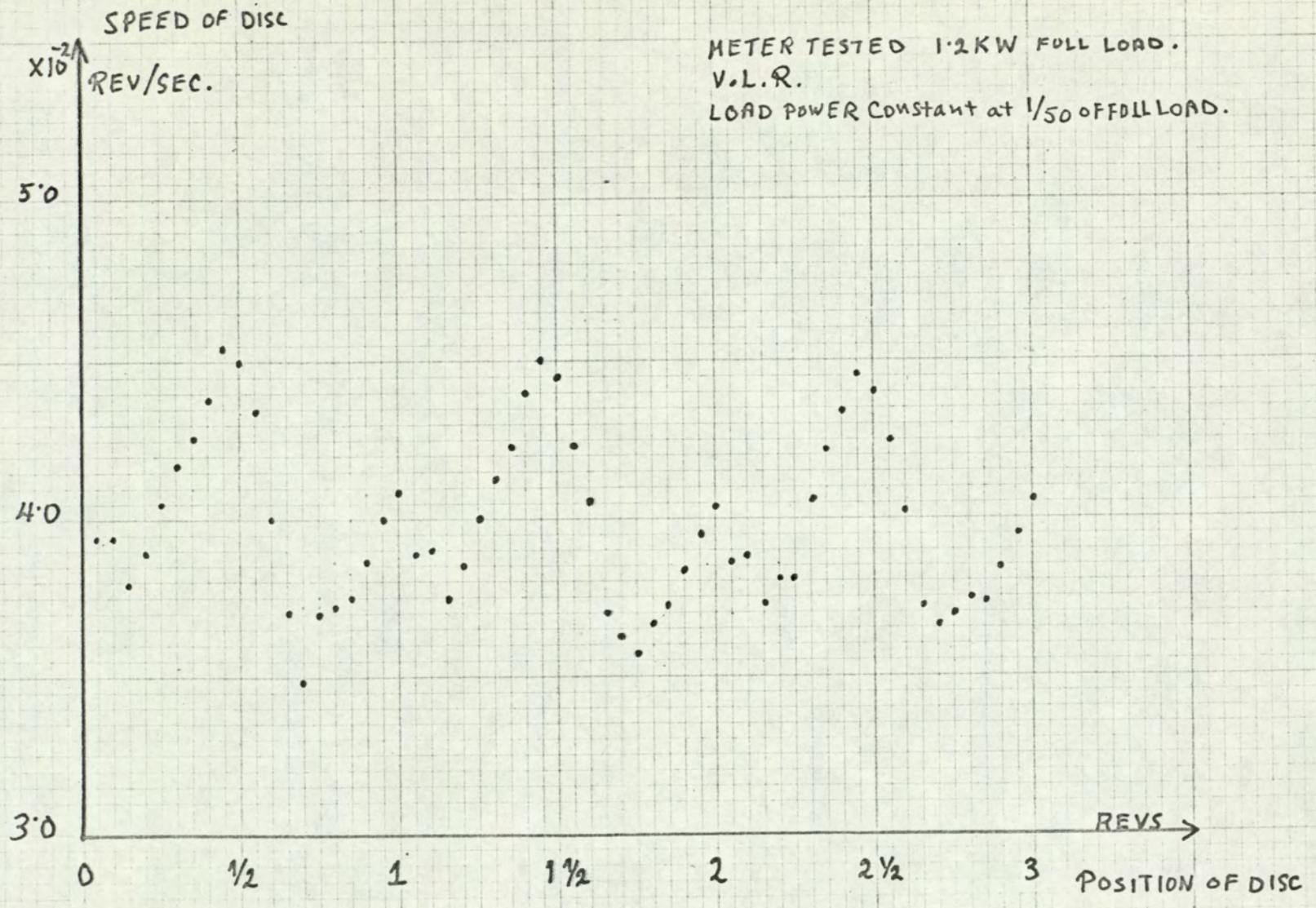

Fig. 26 - Graph showing the speed of the disc at different positions round its periphery during three consecutive revolutions

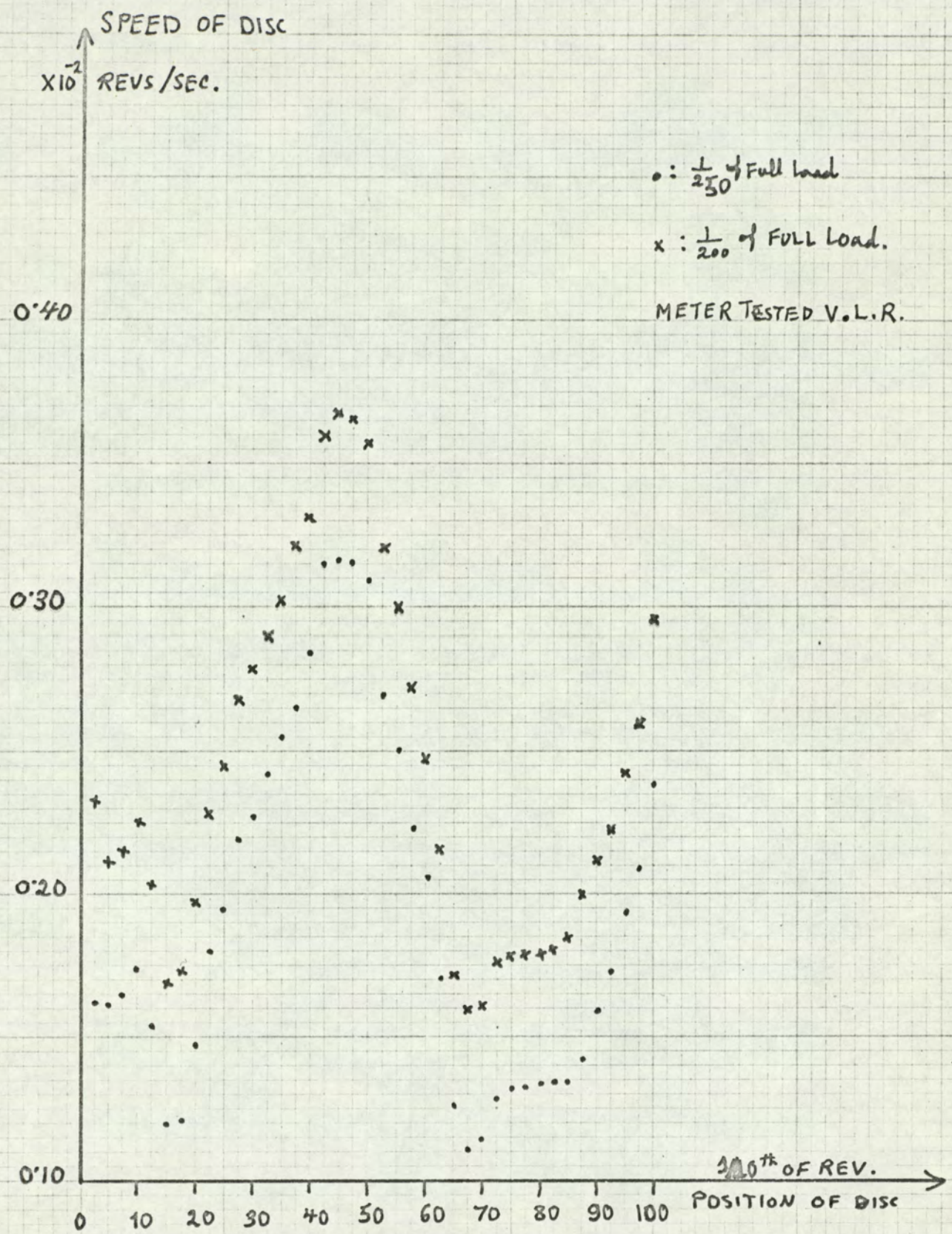

Fig.27 (a) Graphs showing the speed variation of the disc within one revolution at two different loads for a V.L.R. Meter

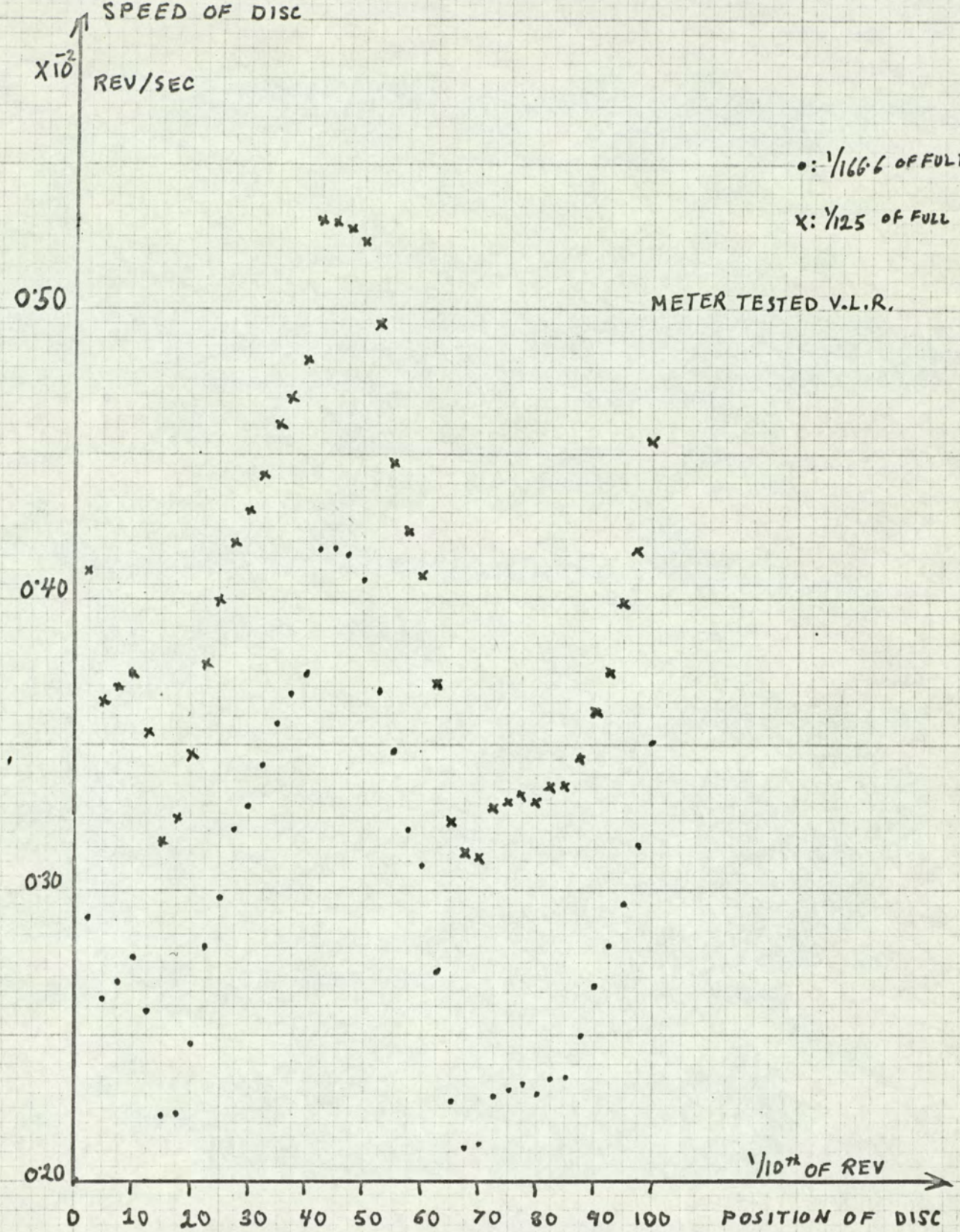

Fig. 27 (b) Graphs showing the speed variation of the disc within one revolution at two different loads for a V.L.R. Meter

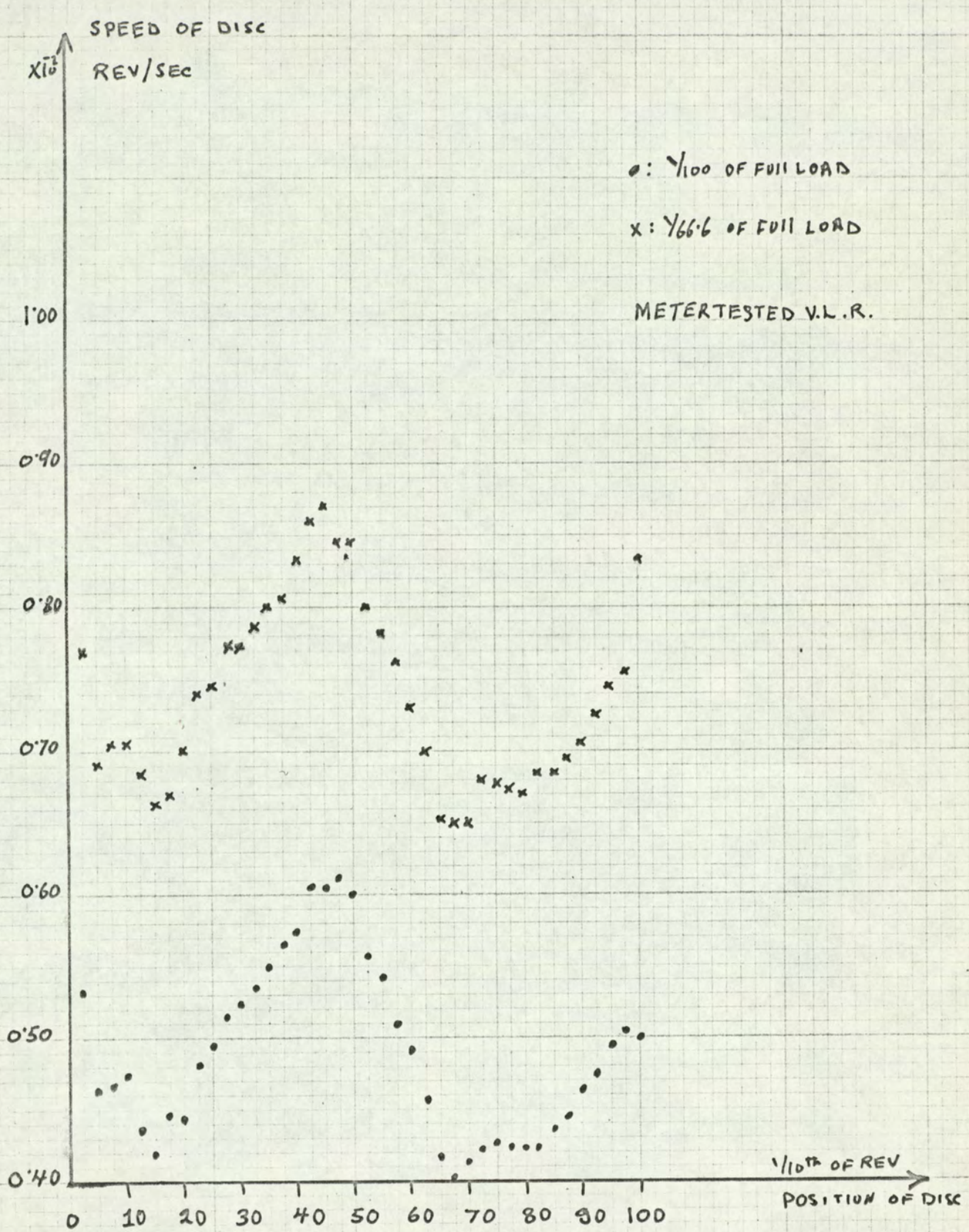

Fig. 27 (c) Graphs showing the speed variation of the disc within one revolution at two different loads for a V.L.R. Meter

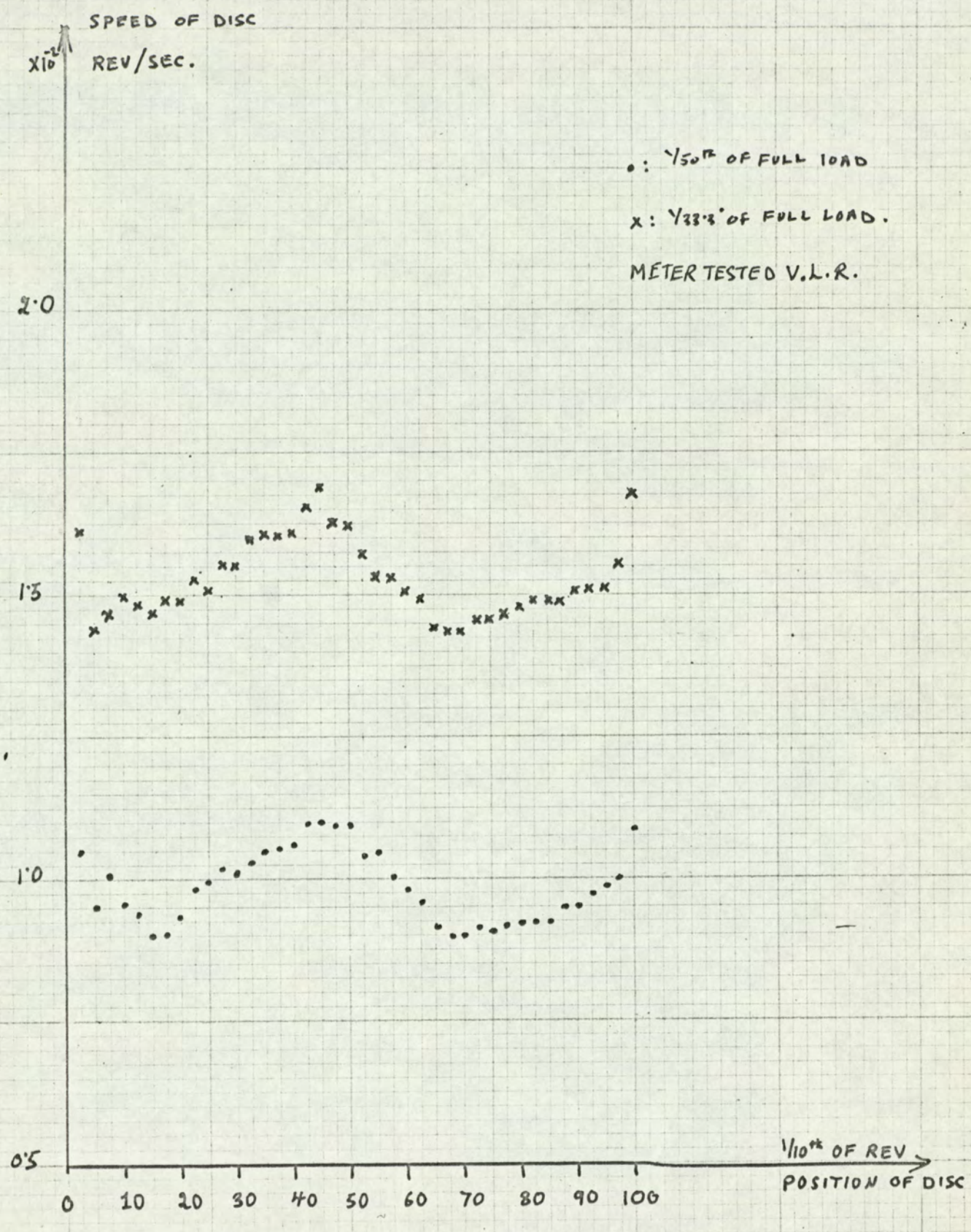

Fig. 27 (d) Graphs showing the speed variation of the disc within one revolution at two different loads for a V.L.R. Meter

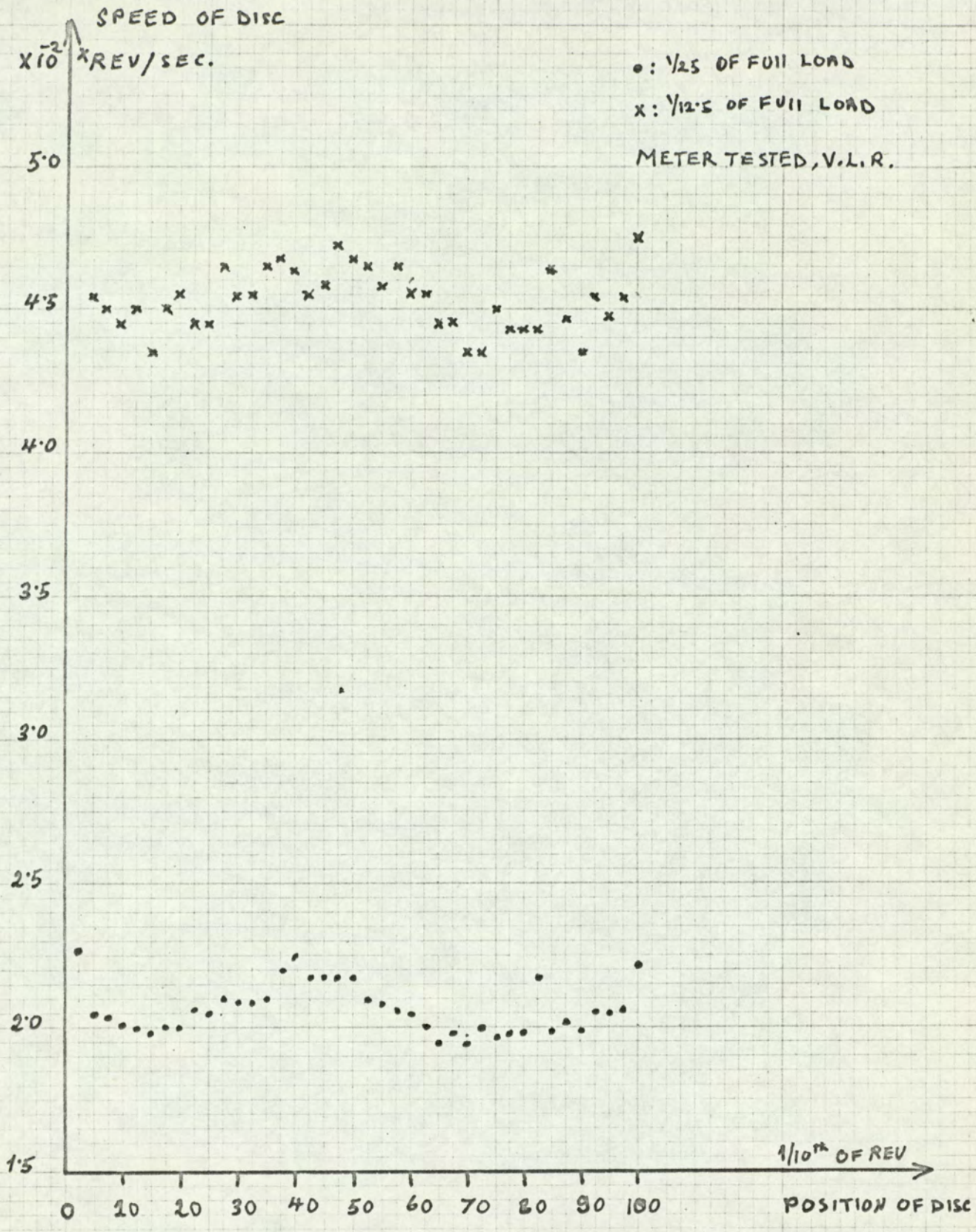

Fig. 27(e), Graph showing the speed variation of the disc within one revolution at two different loads for a V.L.R. Meter

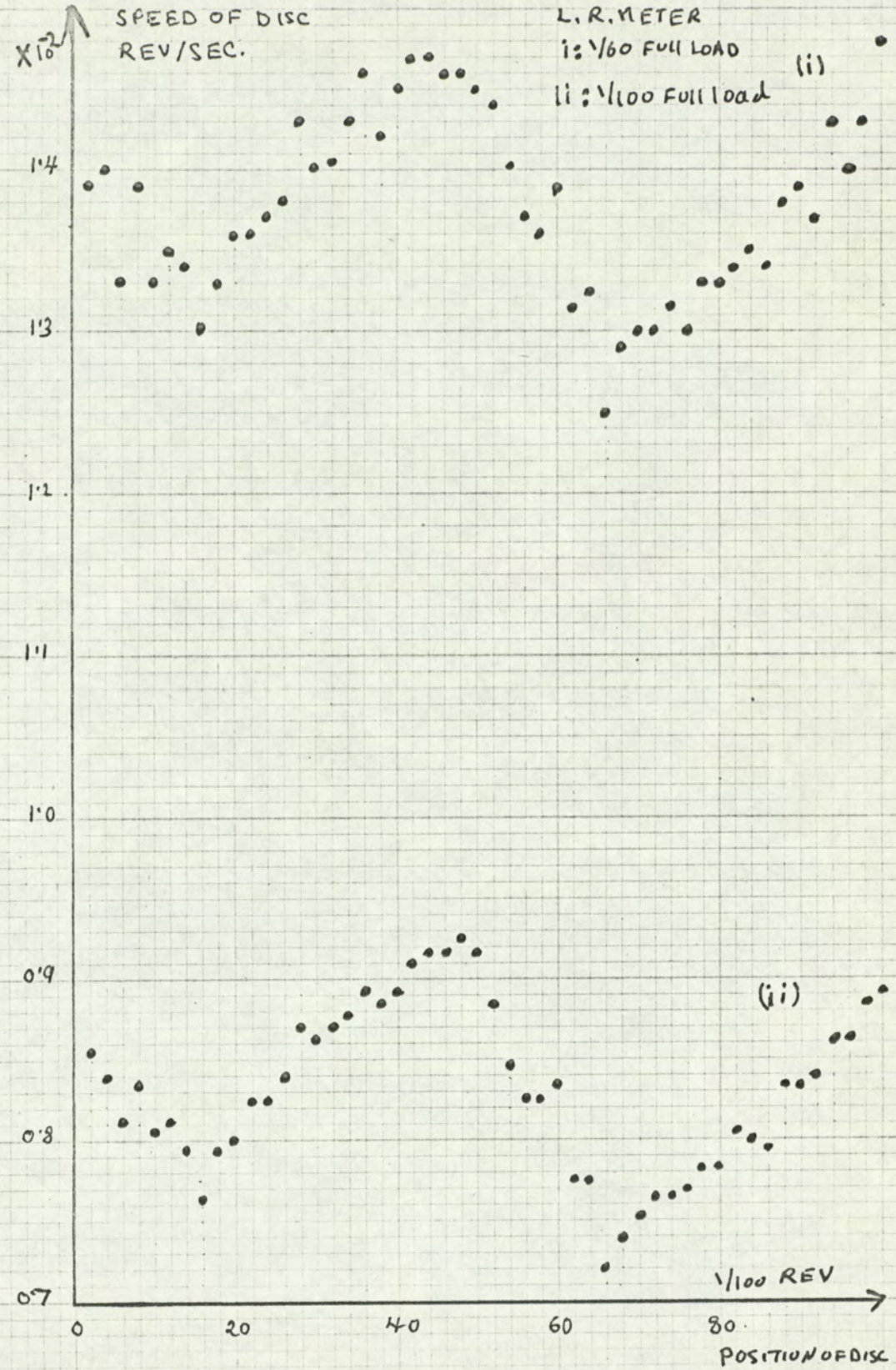

Fig. 28 (a). Graphs showing the non-uniform speed within one revolution at different loads for an L.R. Meter.

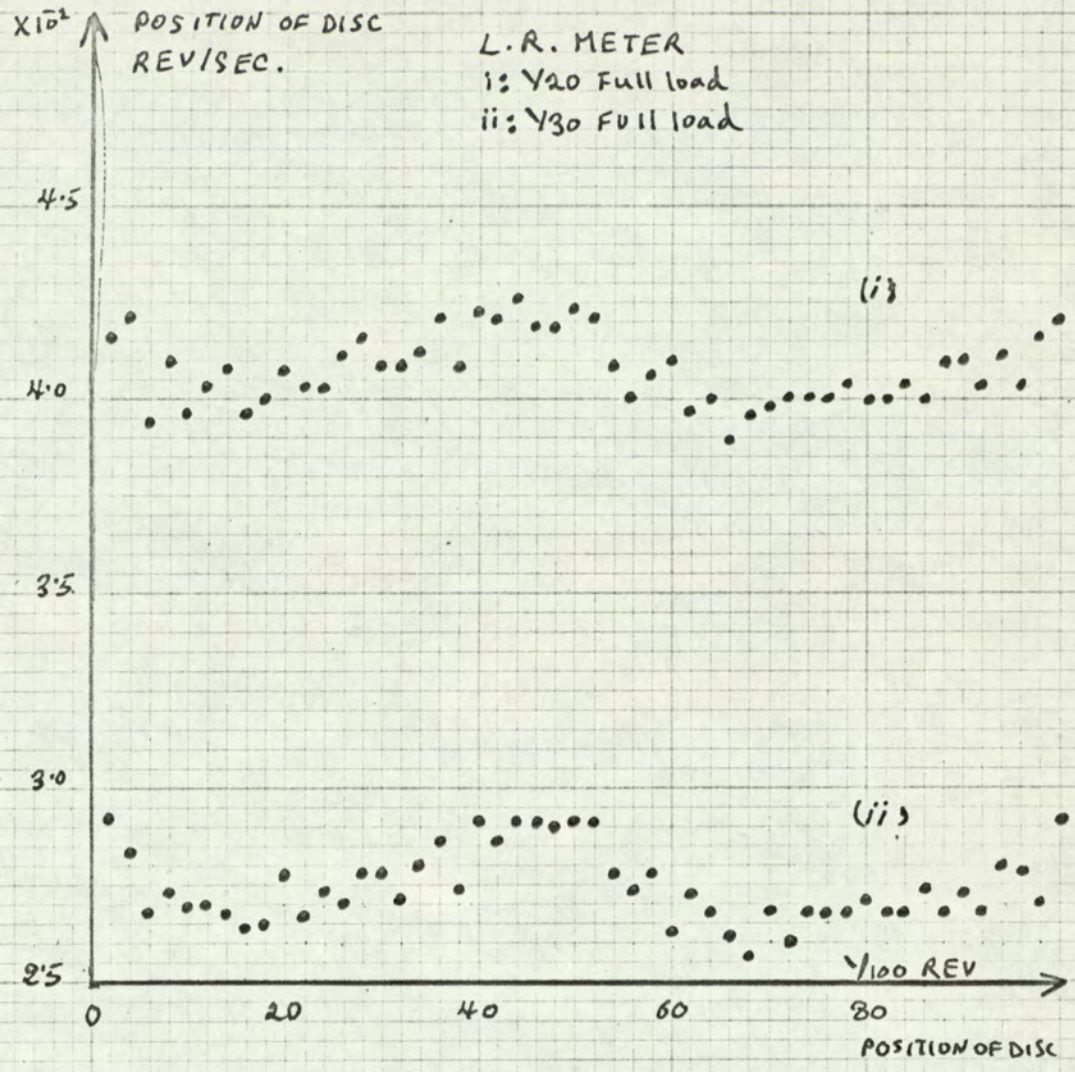

Fig. 28 (b). Graphs showing the non-uniform speed within one revolution at different loads for an L.R. Meter.

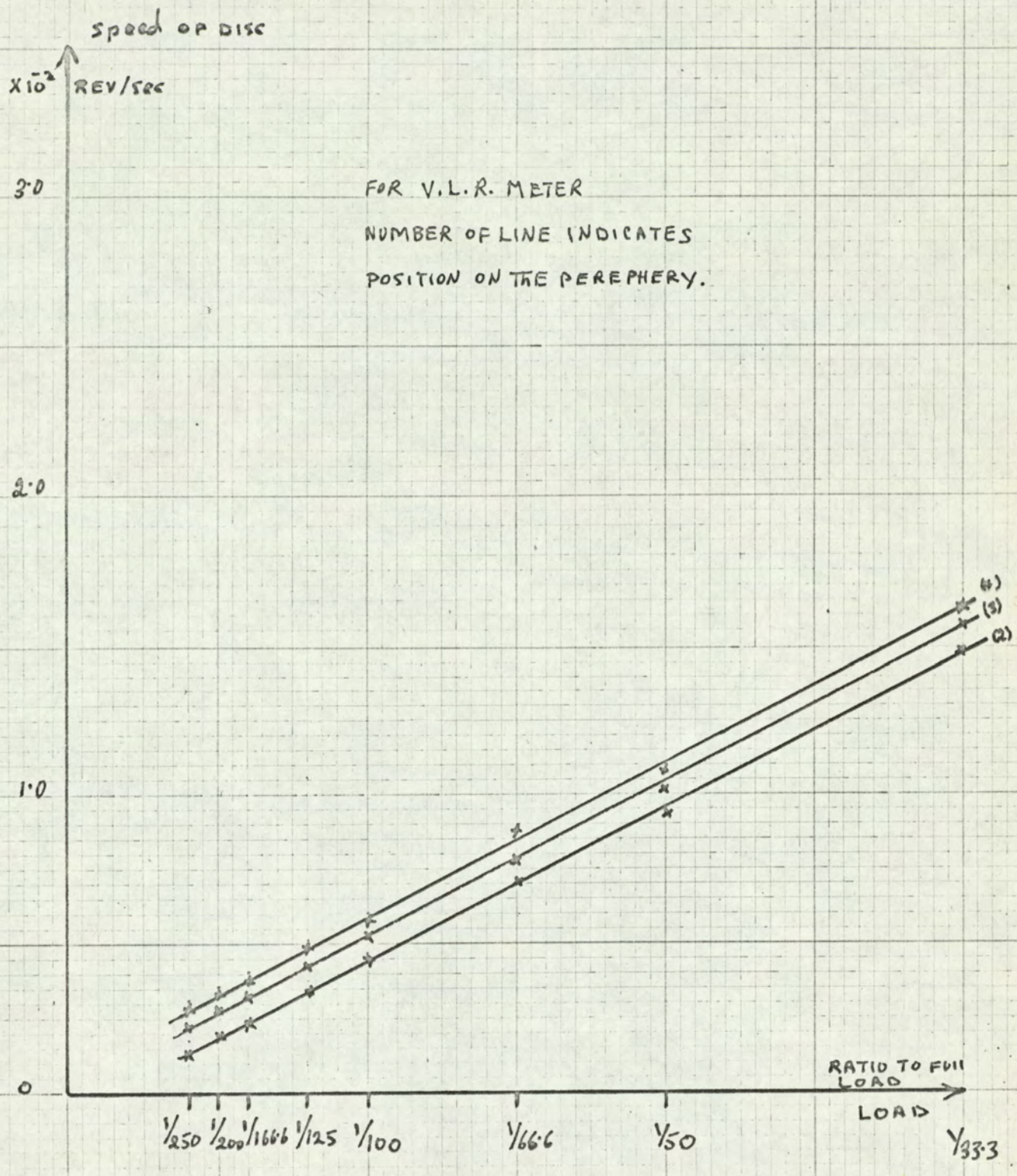

Fig. 29, A, Graph showing the relationship between the speed of the disc for three different given positions on the disc and various loads.

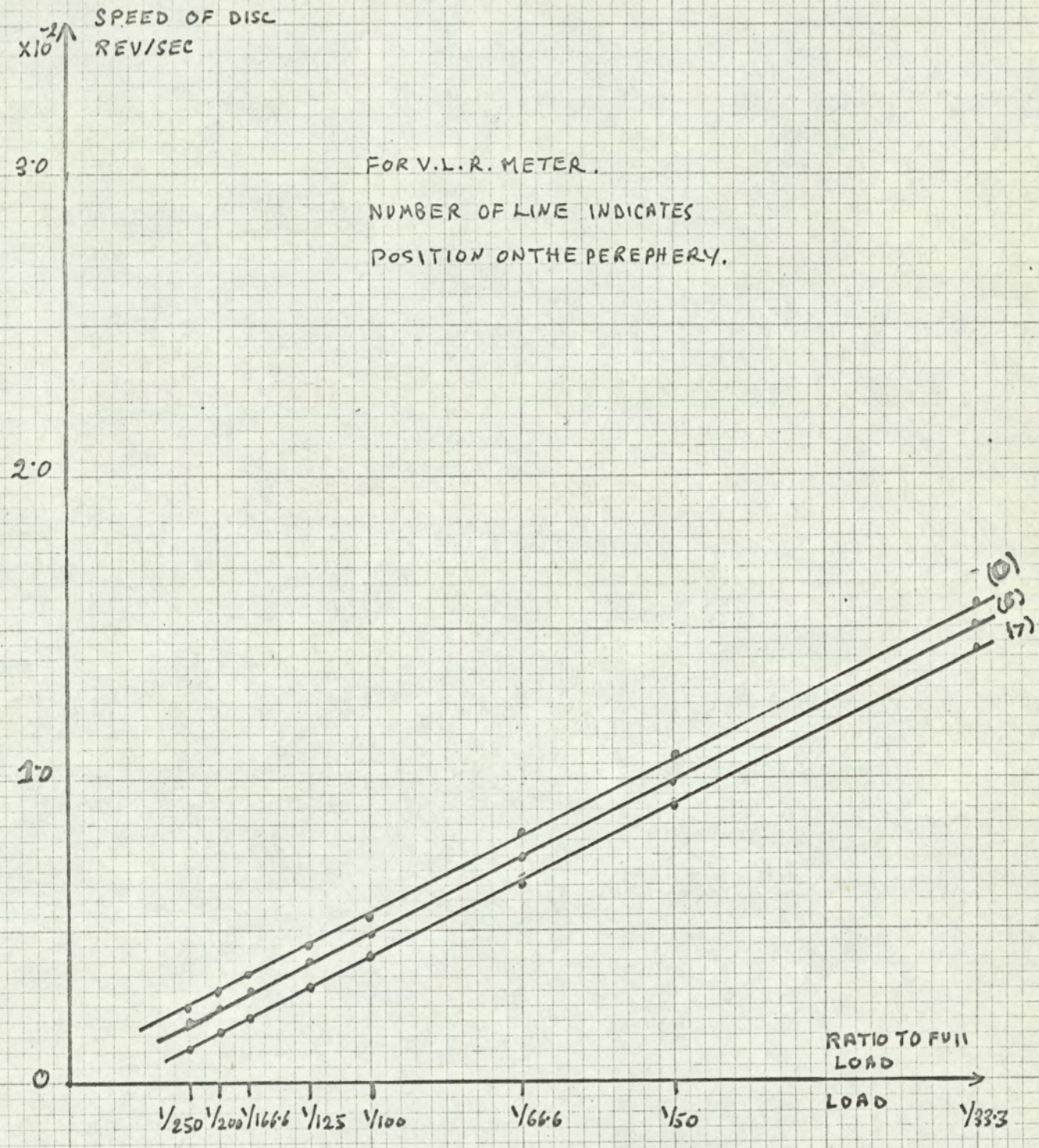

Fig. 29, B, Graphs showing the relationship between the speed of the disc for three different given positions on the disc and various loads

$$S = a W + \frac{1}{N \delta \theta} \sum_{1}^{N} f(\theta) \ \delta \theta \qquad \ldots\ldots \qquad (16)$$

Where, N is the number of divisions round the disc,

$\delta \theta$ is the width of a division.

or as expressed in the previous chapter;

$$S = a W + b \qquad \ldots\ldots \qquad \ldots\ldots \qquad (17)$$

The relative divergence of the speed at a given position is given by;

$$\frac{\text{Difference of speed from average value}}{\text{Average value}} = \frac{G(\theta)}{a W + b} \qquad \ldots\ldots \qquad (18)$$

where, $G(\theta)$ is constant for a given position.

Fig.30 shows a graph of the maximum percentage deviation of the speed of the disc from the mean speed at different loads. The shape of the graph is in agreement with (18).

It is clear, from the results considered up to now, that a constant torque whose magnitude is a function of position is present in the meter.

3.9 The separation of the effects of the active torques in the meter on the non uniform motion.

The main active torques in the meter are those;

a) the driving torque,

b) the damping torque due to the permanent magnet,

c) the damping torque due to the pressure coil,

d) the damping torque due to the series coil.

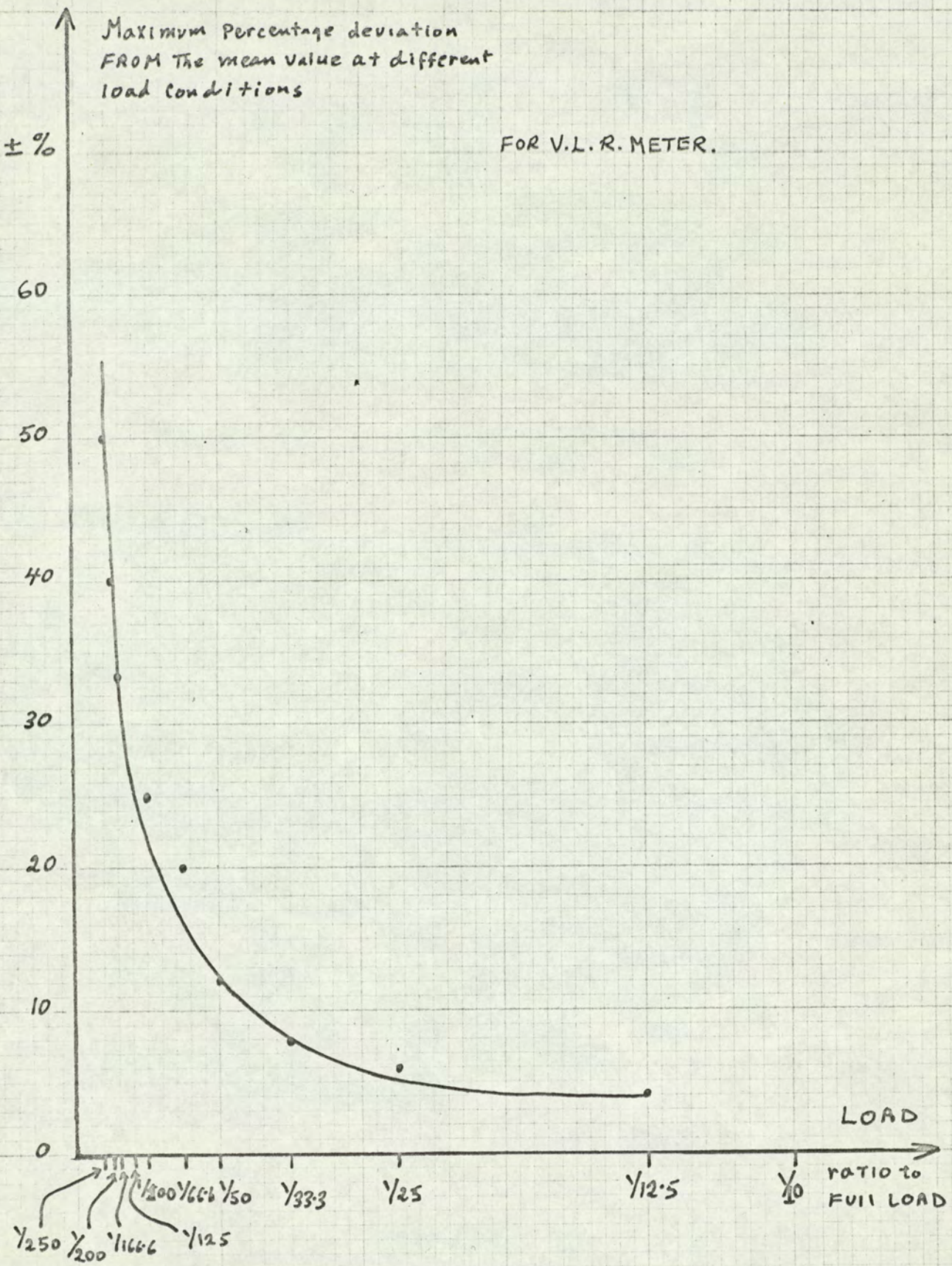

Fig.30 - Graph showing the maximum percentage deviation of the speed of the disc from the mean speed at different loads

A study of the effect of each of these torques acting alone on the disc is possible, except for (a). The method consisted of driving the disc by a relatively constant torque, produced by a couple acting on the spindle of the meters and using one of the above mentioned torques to damp the meter. Fig.19 shows the constant torque drive arrangement. Two weights 'M' are placed at the end of a silk thread, which passes through a hole in the spindle of the disc and over polished bars. Correct positioning is essential. By turning the disc, the thread is wound round the spindle, and when released the falling weights drive the disc.

3.10 Analysis of the results:

The effect of the permanent magnet was investigated first. Fig.31, shows the result, and it is clear that the permanent magnet has no effect on the speed variations, this also indicates that there is no frictional variations of any relevant magnitude, in the bearings of the meter. The tests were conducted without a counter. The added effect of the series coil damping is shown in Fig.32, the small fluctuations are mainly produced by varying friction between the silk thread and the polished bar. A big change occurs when the damping of the shunt coil is introduced, this is shown in Fig.33. This leaves no doubt that the flux responsible for the cyclic variations is the shunt flux. This is also in agreement with the conclusion drawn at the end of 3.8 as the value of this flux is constant.

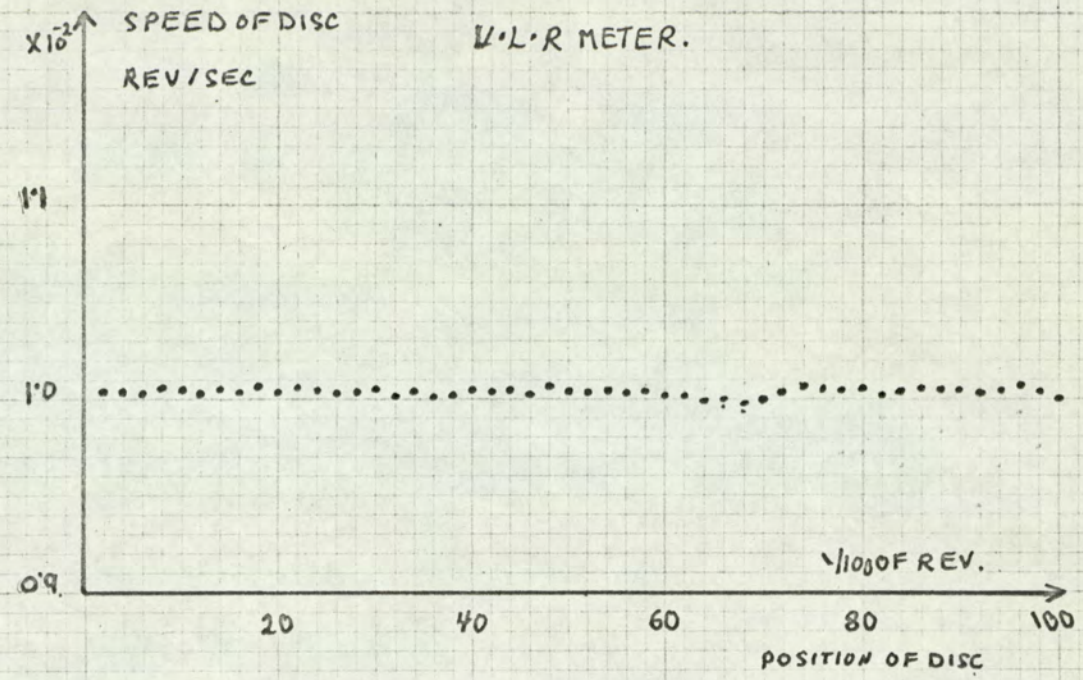

Fig. 31 - Graph showing the speed of the disc at different positions within one revolution, the disc being driven by constant torque and damped by the permanent magnet only.

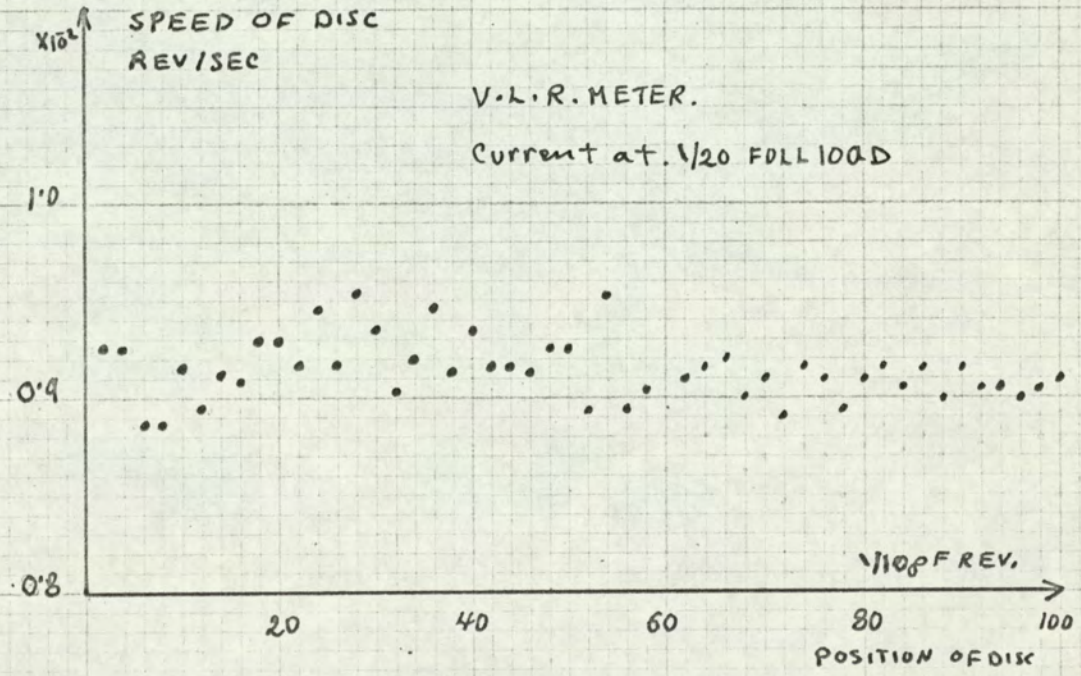

Fig. 32 - Graph showing the speed of the disc at different positions within one revolution, the disc being driven by constant torque and damped by the permanent magnet and current in series coil only.

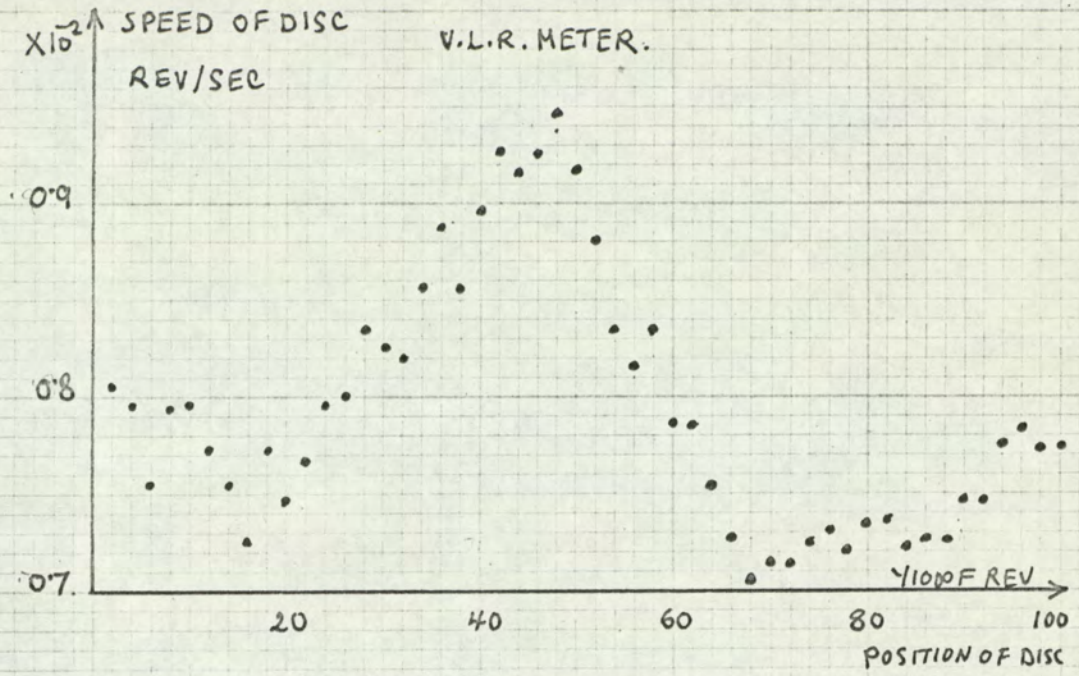

Fig. 33 - Graph showing the speed of the disc at different positions within one revolution, the disc being driven by constant torque and damped by the permanent magnet and the Shunt coil only

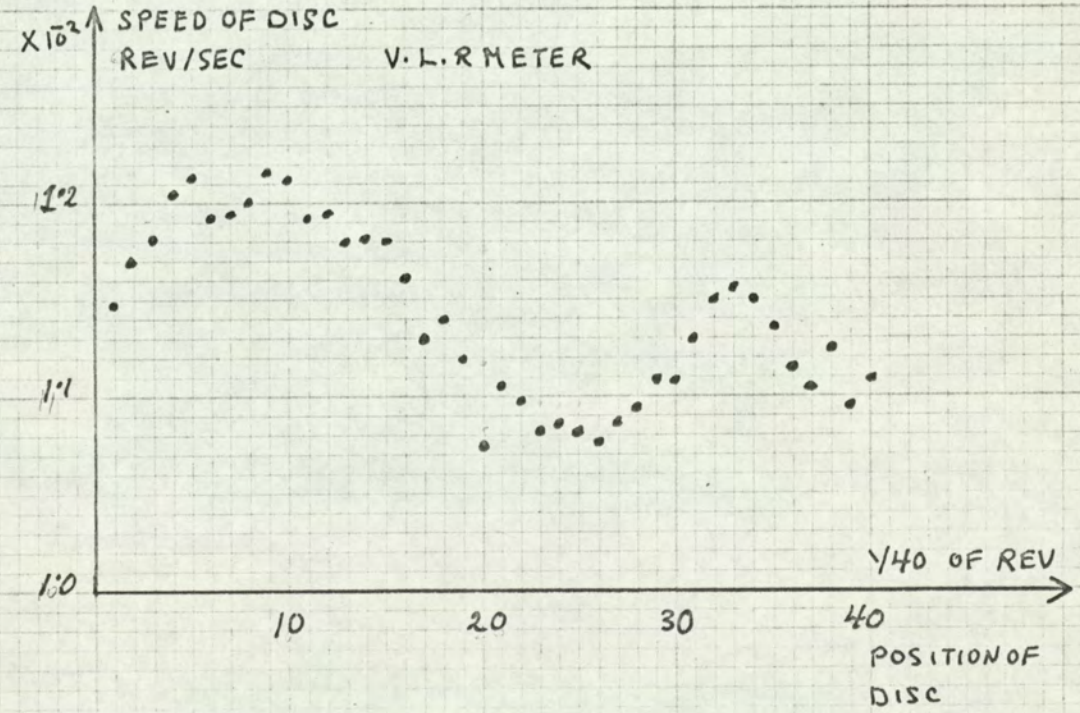

Fig. 34 - Graph showing the speed of a disc with one creep hole only, at different positions within one revolution, the disc being driven by constant torque and damped by the Shunt Coil only

In order to establish the effect of the creep holes, discs without creep holes were provided. Each disc was divided into 80 sections using a scribe and a dividing head. The disc is shown in Fig. 25,b. A test was done using a disc with one creep hole, then two, the constant torque being damped by the shunt coil only. These are shown in Figs. 34 and 35. No appreciable change occured due to the addition of the creep hole. Tests using discs without creep holes were conducted on meters under normal working conditions, Figs. 36 a and b, and 37, show tests at 1/60 of full load. All these tests show that the cyclic variations exist when the creep holes are not present, thus the cause of these variations must be the inherent mechanical structure of the disc itself, this includes eccentricity and the axis of the spindle not being at right angles to the plane of the disc. These mechanical defects could be produced during production, hence all the discs will suffer from the same defects, producing thus similar cyclic variations. Observations of the position of the disc relative to a position parallel to the plane of the disc showed fluctuations in the position producing;

i) Tapered air gap effects;

ii) A varying separation between the disc and the fixed element.

3.11 Sources of non uniform torques in the meter:

When two fluxes, having a phase difference, act on the disc a torque is produced, this torque has a value proportional to the

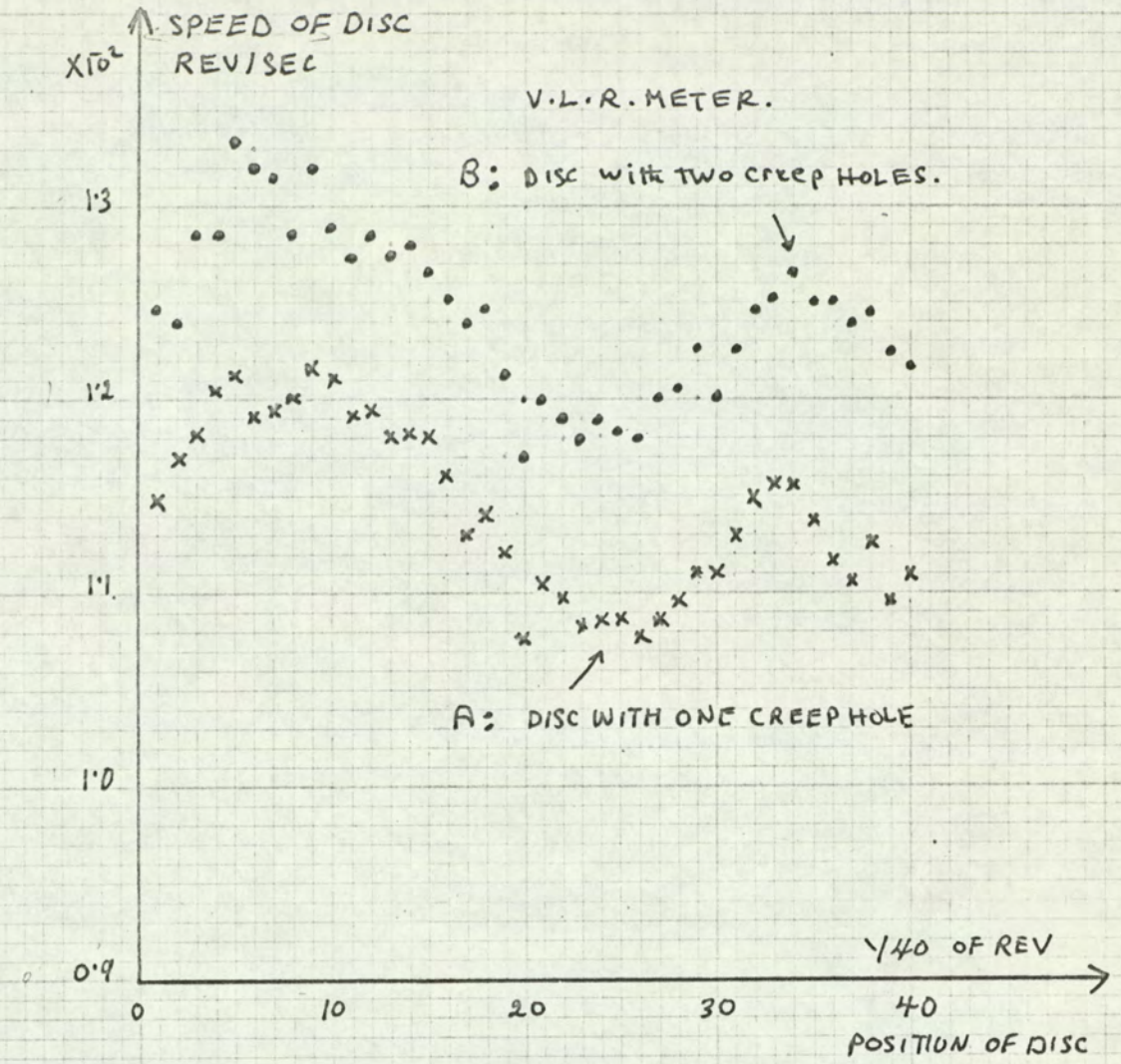

Fig. 35 - Graphs showing the speed of the disc at different positions within one revolution, the disc being driven by constant torque and damped by the Shunt coil only.

A. The disc with one creep hole.
B. The same disc with two creep holes diametrically opposite.

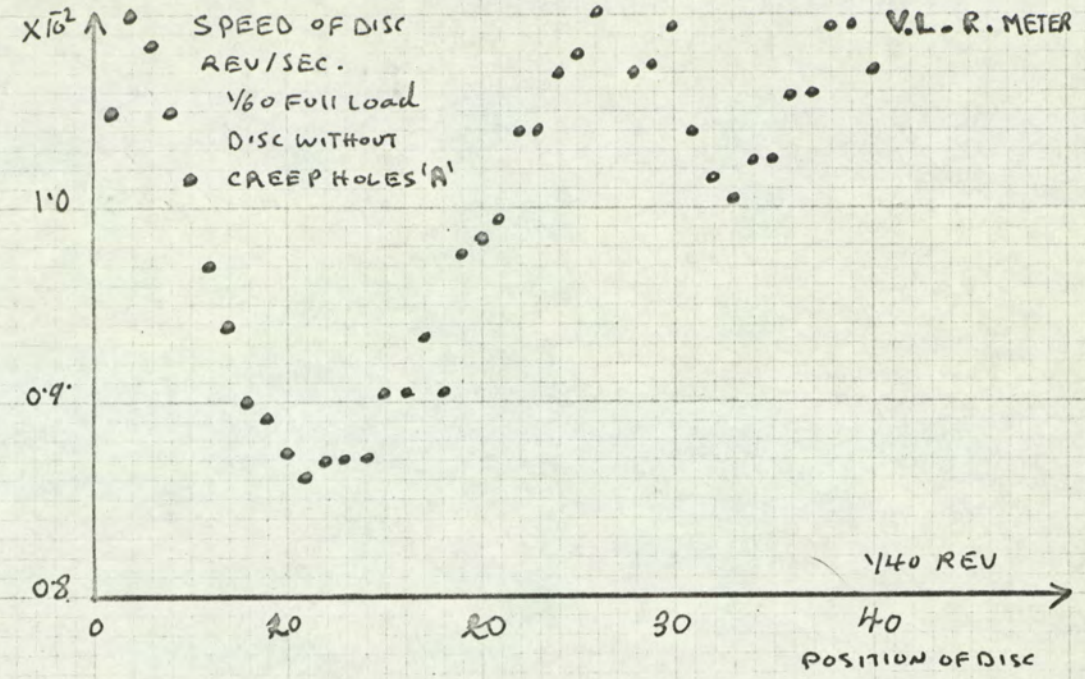

Fig. 36 a; Graph showing the non-uniform speed within one revolution using a disc 'A' without creep holes and a V.L.R. Meter.

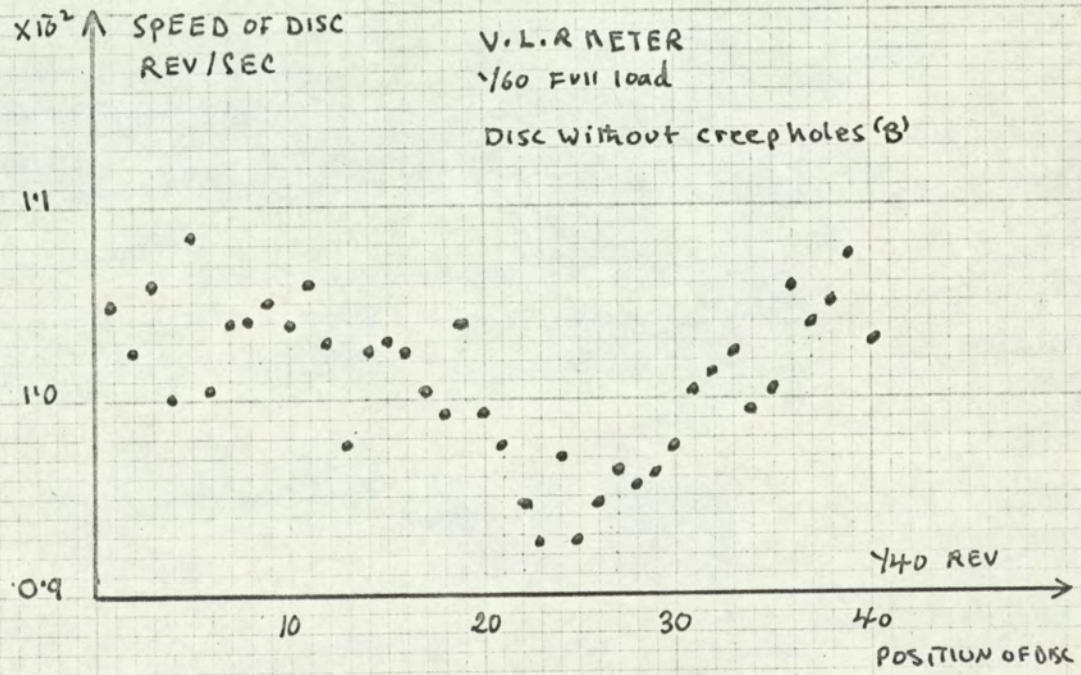

Fig. 36 b; Graph showing the non-uniform speed within one revolution using a disc 'B' without creep holes and a V.L.R. Meter.

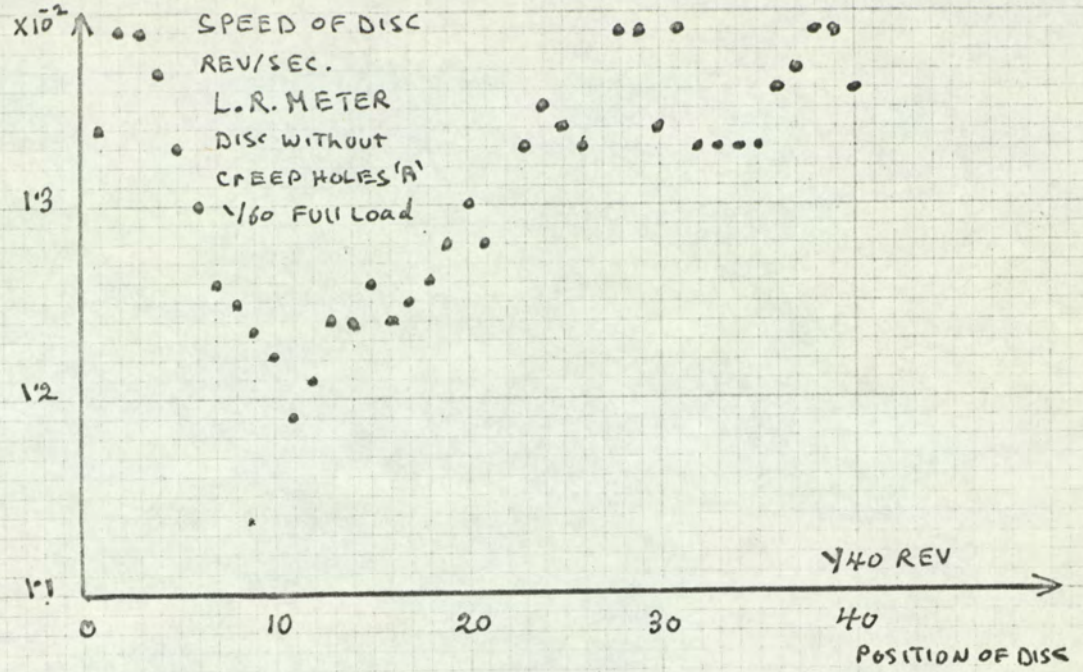

Fig.37 - Graph showing the non-uniform speed within one revolution using a disc 'A' with no creep holes and an L.R. Meter.

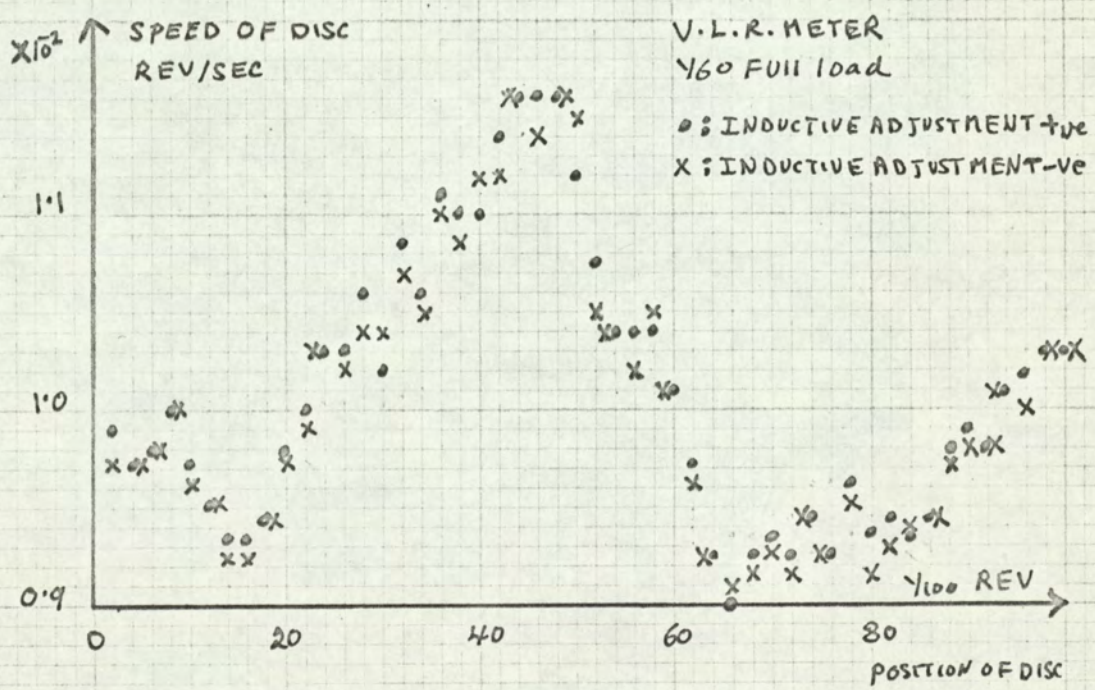

Fig.38-Graphs showing the effect of the Inductive adjustment setting on the non-uniform speed of the disc within one revolution

product of the two fluxes and the sine of the angle between them. The direction of the force being from the leading to the lagging flux. The experimental results have shown that the main flux contributing to the non uniform torques was that produced by the shunt coil. A plan view of the disc with the relevant elements projected on it is shown in Fig.39. The pole face of the shunt coil projects a given area on the disc. Now, if this area is in a plane parallel to that of the pole face, the instantaneous values of the flux, ignoring fringing, along that plane will all be in phase, hence no torque can be produced; however, if we assume the disc slightly tilted, producing a tapered air gap, this is shown in Fig.40.A, here due to the spatial displacement of the disc from á to b, the instantaneous values of the flux at a and b will be out of phase, hence a torque is produced. The greater the distance á b the greater torque. This torque is by no means small as the area involved is the projection of the shunt coil pole face on the disc.

A similar effect occurs when a creep hole is under the influence of the shunt coil. This is shown in fig.40.B, the flux in the hole leads that in the disc and a torque is produced; this passes through these stages;

i) As the hole begins to enter the shunt flux region the torque is directed towards the area under the pole,

ii) As it starts to get out, the torque is again in a direction pulling it under the pole.

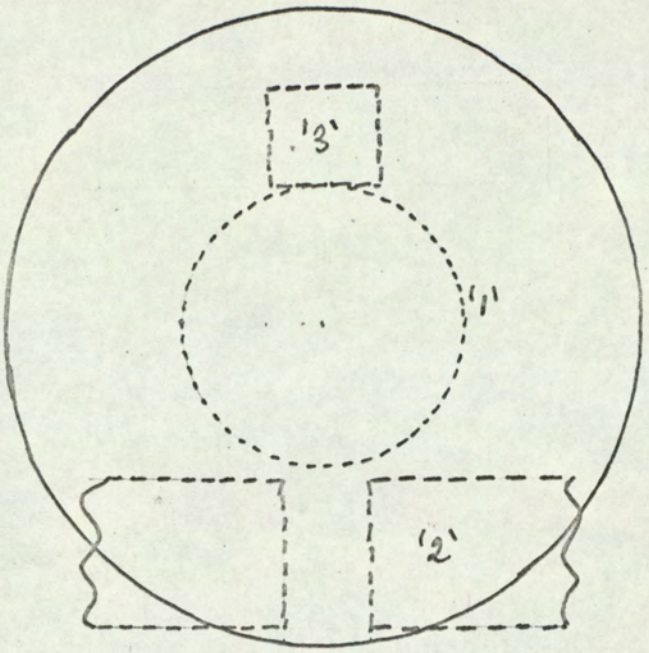

Fig.39 - A plan view of the disc, with projections of the relevant meter parts.

(1) Atrajectory of the creep holes. (2) The permanent magnet.
(3) The shunt coil pole face

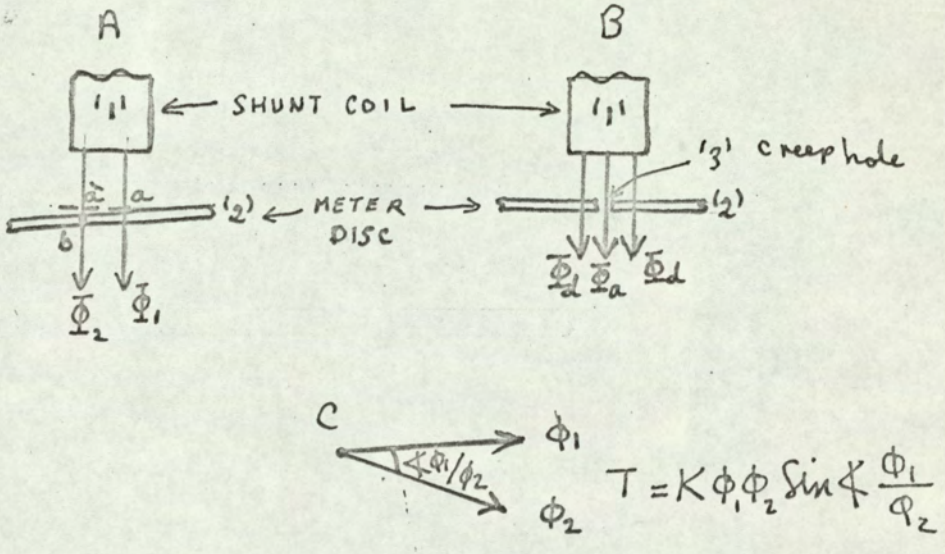

Fig.40 - Sources of non uniform torques.

A : The effect of a tapered air gap. B : The effect of a creep hole.
C : Vector diagram showing two fluxes which can act on the disc producing a torque.

iii) At a point in between two equal torques exist acting on opposite directions.

The magnitude of these torques is proportional to the area of the hole, as this is usually quite small, the torques must be small also.

3.12 The effect of the Meter adjustments on the non-uniform speed of the meter.

The inductive adjustment has a very small effect, this is shown in Fig.38. Where at a load of 1/60 of full load, the variations of the speed of the disc within one revolution are plotted for two extreme settings of the inductive load adjustment. The effect is hardly apparent. This is due to the fact that the load was at unity power factor.

The effect of the frictional adjustment is to produce a shift of the average value, this is shown in Fig.41.

3.13 The effect of the counter on the non-uniform speed of the meter.

This is shown in fig.42. The presence of a normal good counter shifts the characteristics to a slower average value retaining the same general shape. A sticky bad counter reduced the average value further and changes the general shape at some points.

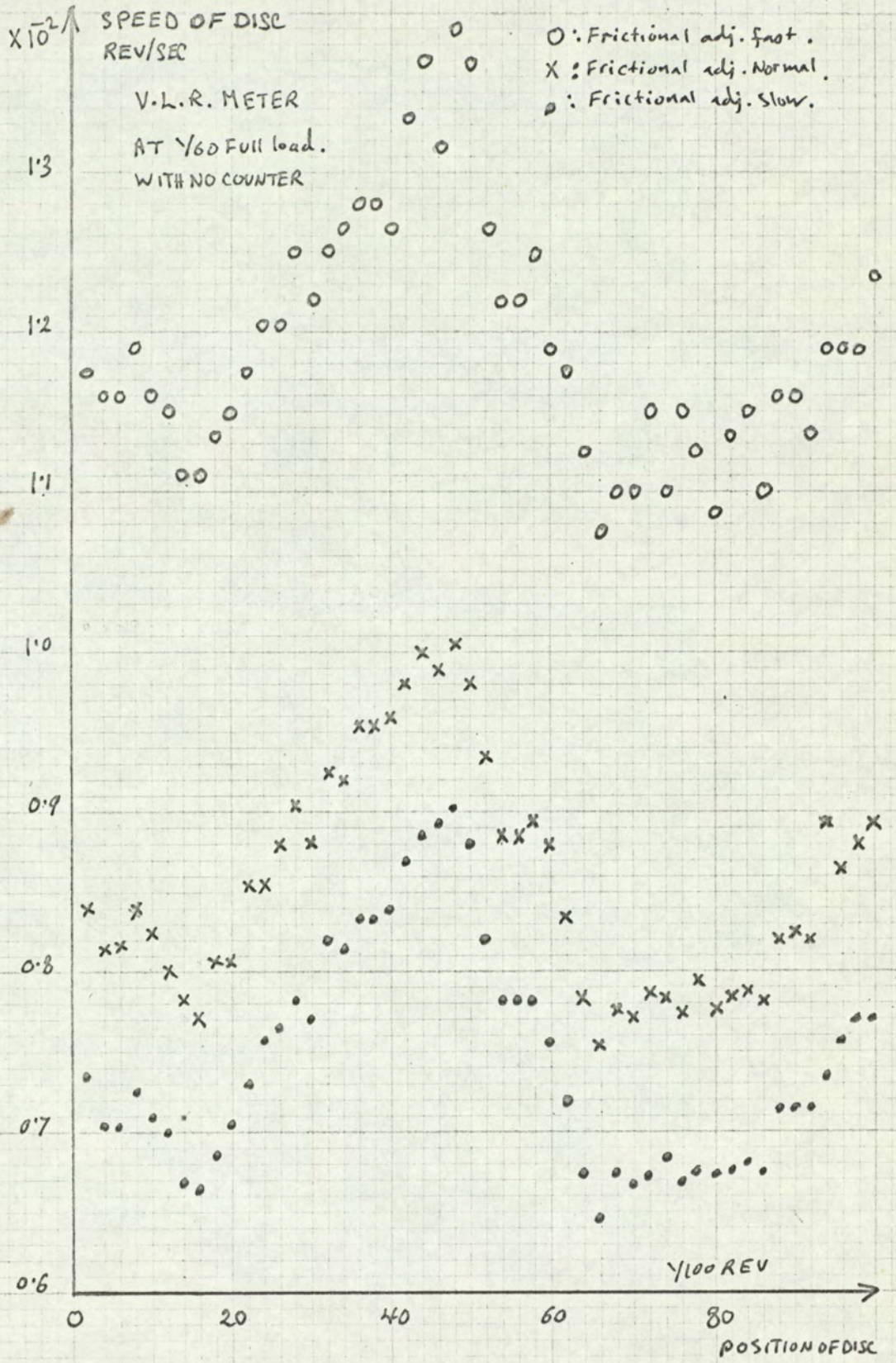

Fig.41 - Graphs showing the effect of the frictional adjustment setting on the non uniform speed of the disc within one revolution.

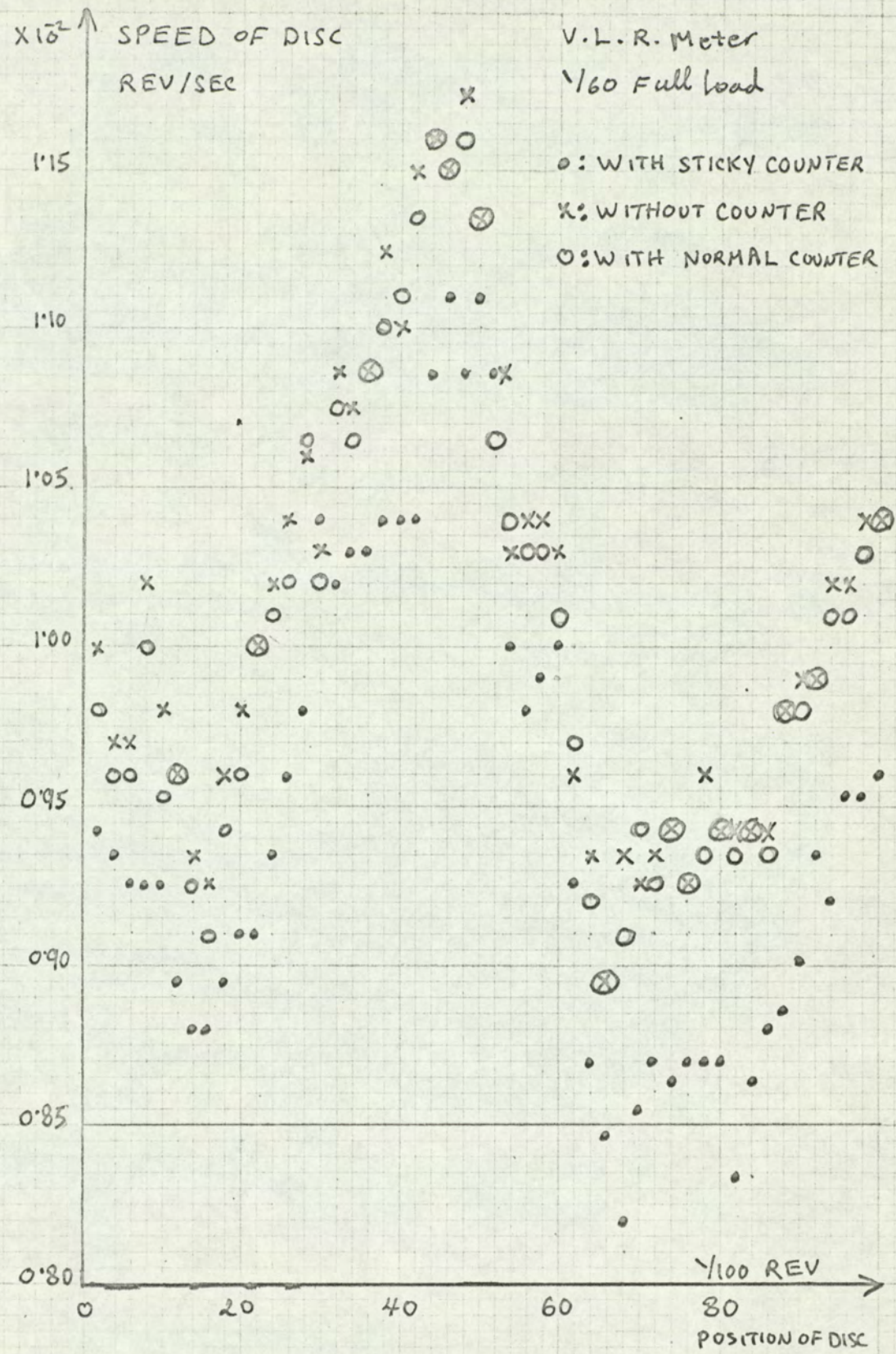

Fig. 42 - Graphs showing the effect of the Register mechanism on the variation of the speed of the disc at 1/60 Full load.

THE PHASE RELATIONSHIPS IN THE SINGLE PHASE INDUCTION METER

4.1 Introduction

The induction meter should register correctly for resistive, and reactive loads as well. This can be ensured by producing a torque in the meter, which is proportional to the load power at any power factor. The phase angle between the interacting fluxes acting on the disc, must then bare a certain relationship to the load phase angle. Due to tolerances of production, this relationship cannot be produced by simple mechanical and geometrical settings. So, an adjustment, "the inductive load adjustment" is usually provided; its effect is to shift the phase angle of the pressure flux within a certain band.

Two operations, which have been mentioned earlier, are made to produce the desired relationship;

i) Pre-setting whilst on the production line;

ii) Calibration at full load 0.5 power factor.

Both of these operations are made by observing the behaviour of the meter; no actual phase measurements are done.

4.2 The vector quantities involved and their phase inter-relationships. (52, 53).

A detailed vector diagram for a single phase induction meter is shown in fig.43. The e.m.f., E applied to the pressur coil produces a current i_v which lags E by σ_1, this angle is less than

Fig.43 A vector diagram for a single phase Induction meter showing the relevant phase relationships.

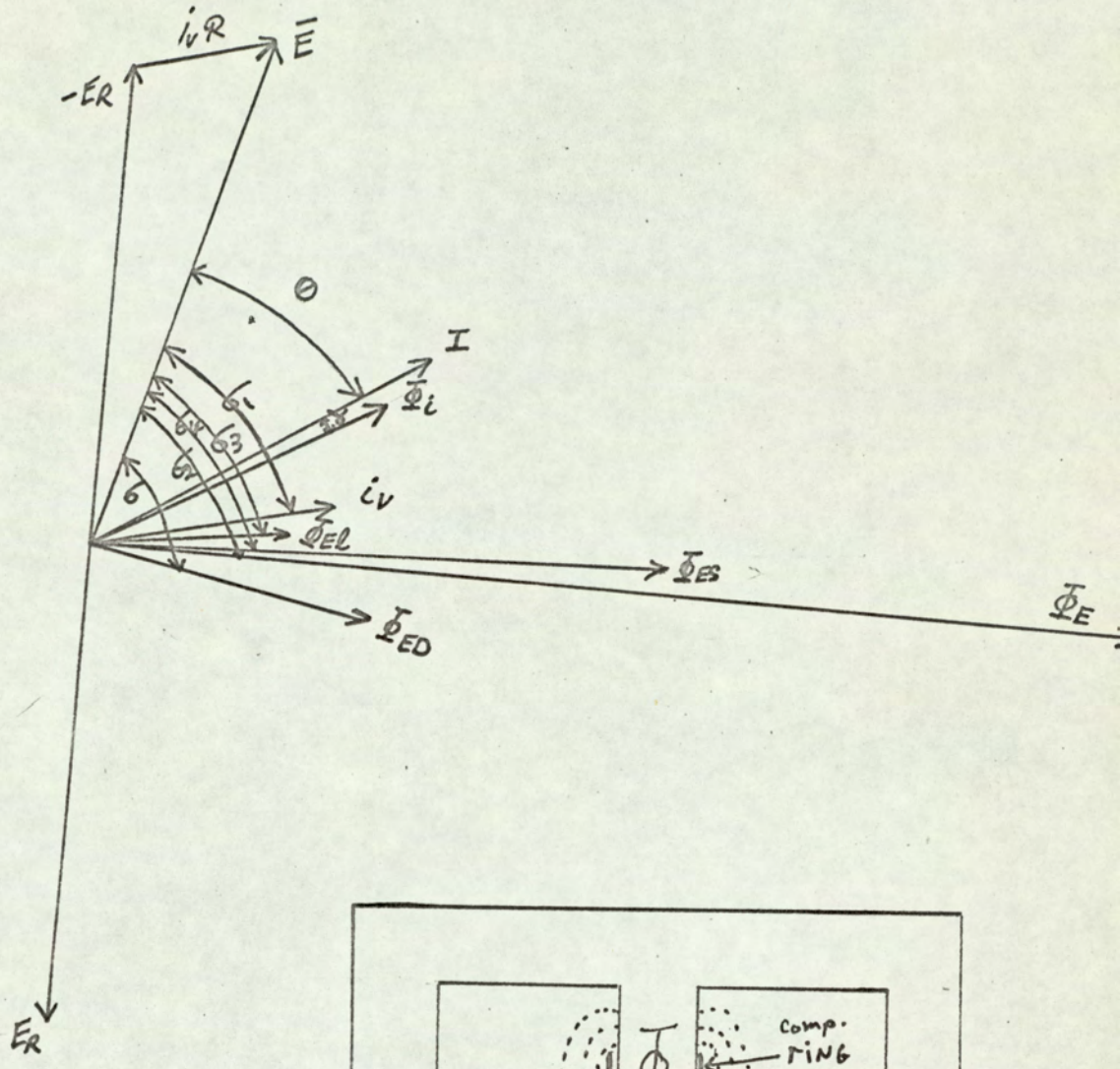

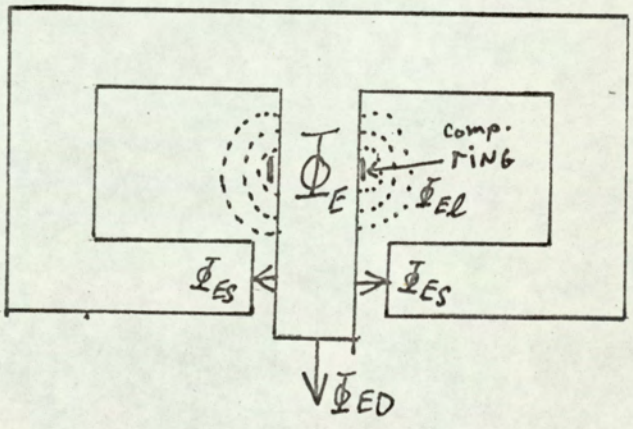

Fig.44 Diagram of the shunt coil showing the paths of the flux

90 degrees, this is due to the resistive drop $i_v R$, R being the ohmic resistance of the coil. This current produces in turn a flux Φ_E, which is proportional to E and lags it by an angle σ_2; σ_2 is greater than σ_1. This flux has three main components;

i) a leakage flux Φ_{E1}, which has a path mainly in air, it lags E by an angle σ_3.

ii) a shunt flux Φ_{ES}, this lags E by an angle σ_4; it has a short air path.

iii) a driving flux Φ_{ED} which reacts with the flux produced by the series coil, producing thus the driving torque. This lags E by an angle σ.

The load current I lags E by an angle θ. This current produces a flux which is proportional to it and lags behind it by an angle γ.

For true power the torque developed should be,

$$\text{Torque} = K\, E\, I \cos\theta \quad \ldots\ldots \quad (19)$$

The torque actually produced in the meter is,

$$= K' \Phi_i \Phi_{ED} \sin(\sigma - \gamma - \theta) \quad \ldots\ldots \quad (20)$$

K' and K, being constants at constant e.m.f, frequency and temperature.

The necessary condition for correct operation is then,

$$\cos\theta = \sin(\sigma - \gamma - \theta)$$

or

$$\underline{\sigma - \gamma = 90 \text{ degrees}} \quad \ldots\ldots \quad (21)$$

For a constant e.m.f., frequency and temperature σ is a constant. The angle γ, however, will depend on the value of the load current. This is a small angle, and can be compensated, for one value of the load current only.

4.3 Some methods of phase compensation.

A diagram of the shunt coil showing the paths of the flux is shown in fig.44.

Two main methods of phase compensation are used generally.

i) Loading the main flux. This is achieved by either a movement of a ring round the centre limb of the shunt coil, the movement can increase or decrease the flux threading the ring, or by the use of an additional fixed winding connected to an external variable resistance, the value of which controls the current in the additional winding. Both ways change σ, providing thus a certain band of phase angle which the driving flux can have.

ii) Utilising a shunt flux. The action of this flux, as can be seen from the vector diagram, is to increase the lag of the driving flux. It requires, however, a large value to produce a reasonable shift, so it is usual for this flux to have a value about 8 to 10 times that of the driving flux.

The resistance of the shunt coil must have a small value; but as this makes the coil heavy and bigger, most manufacturers in this country prefer a small coil and a shunt compensation.

A method which is used sometimes, utilises the current coil, and by loading the current flux by similar methods to (i) produces the desired compensation.

4.4 The errors due to incorrect inductive load setting.

The desired compensation (21) is not always realisable in practice. So, a small phase angle error δ is present in the meter. The relative error due to this is given by,

$$\left(\frac{\text{Sin } (90 - \theta + \delta)}{\text{Sin } (90 - \theta)} - 1 \right)$$

or, $= \text{Cos } \delta + \tan \theta \sin \delta - 1$ as δ is small,

$\cos \delta \neq 1$ hence, the relative error $= \tan \theta \sin \delta$ ..... (22)

This shows that the error is greater at low power factors.

δ is a function of the load current, however as the current is proportional to the power at a constant applied e.m.f., we can write,

$\text{Sin } \delta = \text{Sin } K'' W$. K'' being a constant, and W load power.

The relative error due to phase errors can be written then as

$$= r_3 \tan \theta \text{ Sin } K'' W \quad \ldots\ldots \quad (23)$$

Thus the total error of the meter, due to incorrect adjustments will be from (9) and (23)

$$r = r_1 + \frac{r_2}{W} + r_3 \tan \theta \text{ Sin } K'' W \quad \ldots\ldots \quad (24)$$

4.5 The design of a system for the Measurement of the Phase Angle between the applied e.m.f. and i) the flux under the central limb of the shunt coil, ii) the current in the shunt coil.

Suitable methods for the required study fall into three main groups:

i) Classical methods. Such methods require a number of observations and calculations and are not conveniently adaptable to production lines.

Direct reading phase meters lack the required accuracy.

ii) Oscilloscopic Methods. These usually require computations. Some modifications which give a direct reading exist [54,55] they lack however the desired accuracy.

iii) Electronic Methods. A variety of methods exist [56,57,58] e.g. variable delay line, zero crossing and multiplying methods.

The most suitable method was the zero crossing technique; it is simple and capable of a high degree of accuracy and a digital readout is possible. The system is shown in Fig.45. An isolated mains supply provides an e.m.f. which is applied to the shunt coil of the meter. An attenuated portion of this e.m.f. is fed to a comparator which detects the zero crossing of the waveform a square wave is thus produced, this, by suitable switching, is used to start and stop an electronic timer/counter, which displayed the

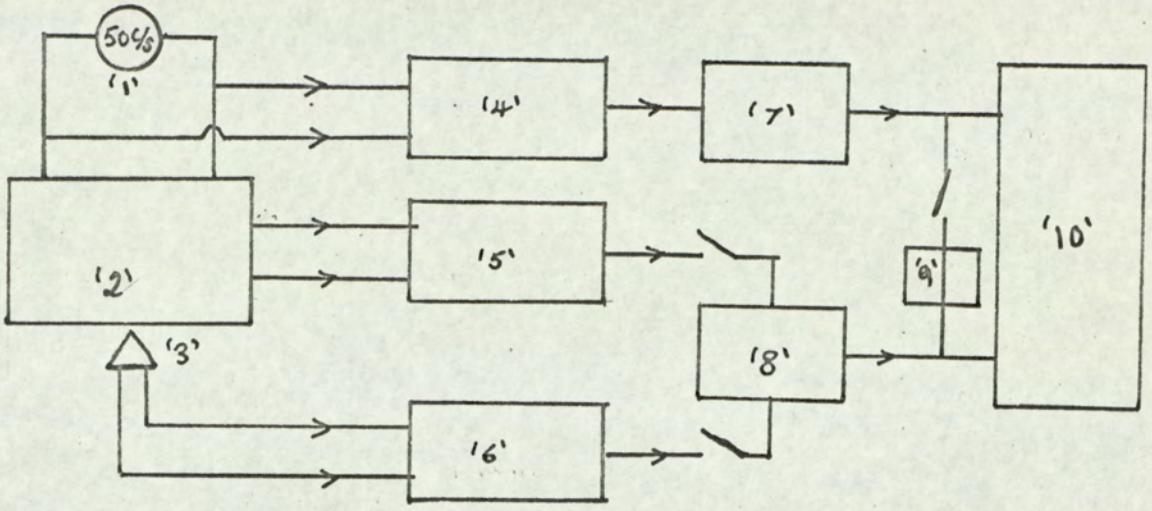

Fig. 45 - Block diagram showing the system used for measuring the phase angle between the e.m.f. applied to the pressure coil and i) The flux under the central limb. ii) The current in the coil.

1) Mains supply through an isolating transformer.
2) Energy Meter.
3) Flux Detecting Coil.
4) Voltage Amplifier.
5) Current Amplifier.
6) Flux Amplifier.
7) Comparator A.
8) Comparator B.
9) Shaping circuit.
10) Electronic Counter

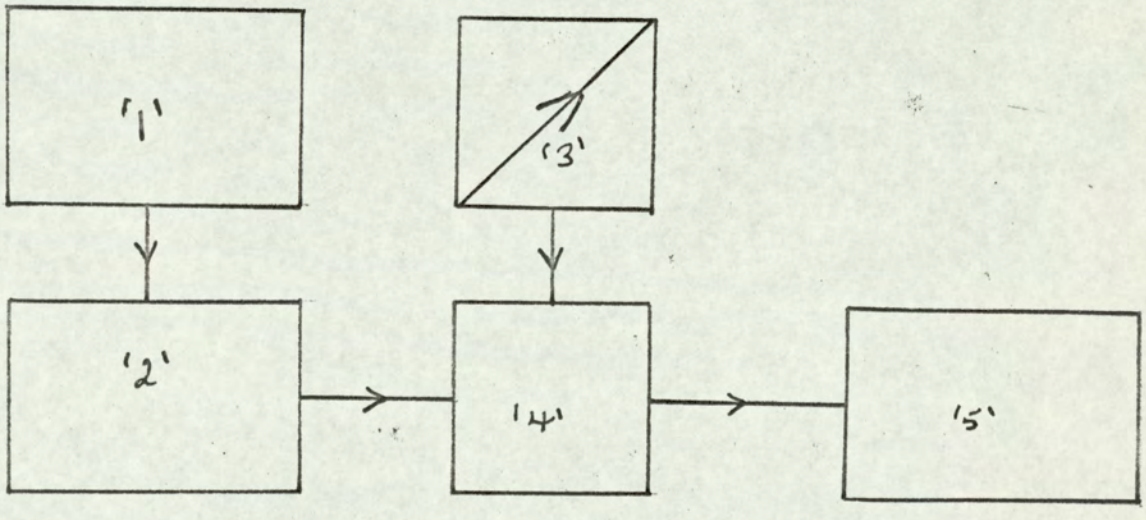

Fig. 46 - Block diagram showing the modified phase meter for on line tests.

1) Stable frequency voltage supply.
2) Energy Meter, voltage and current amplifiers and comparator.
3) Variable pulse oscillator.
4) Gates.
5) Digital display.

period of the e.m.f. waveform corresponding to 360 degrees. The circuit diagram of the voltage amplifier is shown in Fig.47.

A voltage which is proportional and in phase with the current in the shunt coil is derived by placing a small resistance in series with the shunt coil. This voltage is fed to an amplifier, this is shown in fig.48. It consists of an integrated circuit linear amplifier, (Fairchild μ702C) and a buffer stage. The output waveform is fed through a selector switch to a comparator for zero crossing detection. The circuit of the comparator is shown in Fig.49. This was again an integrated circuit (Fairchild μ 710 differential comparator), with a switching transistor and a buffer stage. In order to maintain a constant voltage level at the input integral action was used; the output was fed to the input after suitable integration. Thus a square waveform whose rising and falling edges indicate the zero crossing points of the current waveform is produced. By using the rising edge of the voltage waveform to start the counter, and that of the current waveform to stop it a time display of the phase difference between them can be produced.

A suitable coil was placed under the central limb of the shunt coil provided the means for detecting the driving flux. The flux induces an e.m.f. which is at 180 degrees behind it. This was

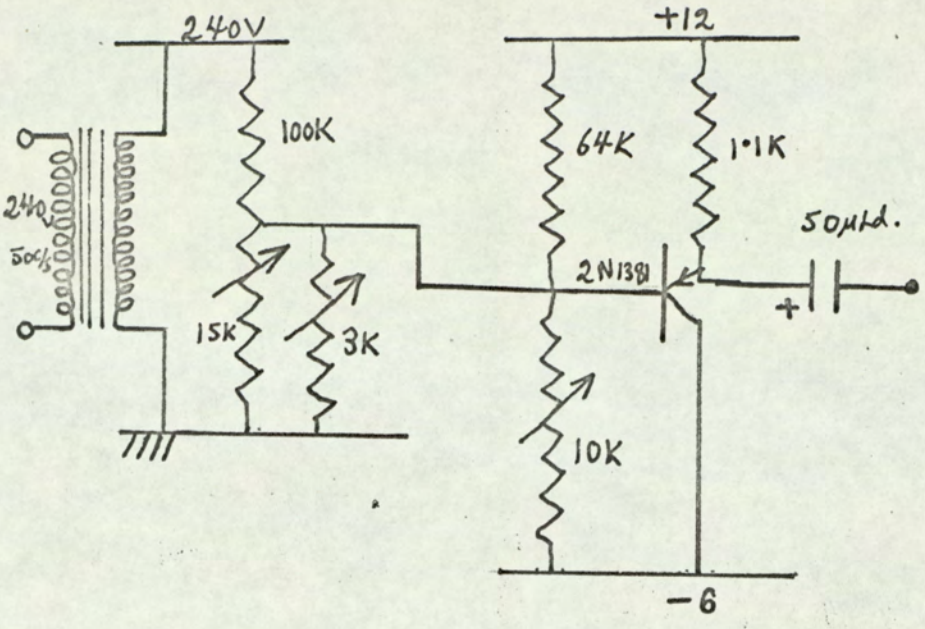

Fig.47 - Circuit diagram of voltage amplifier.

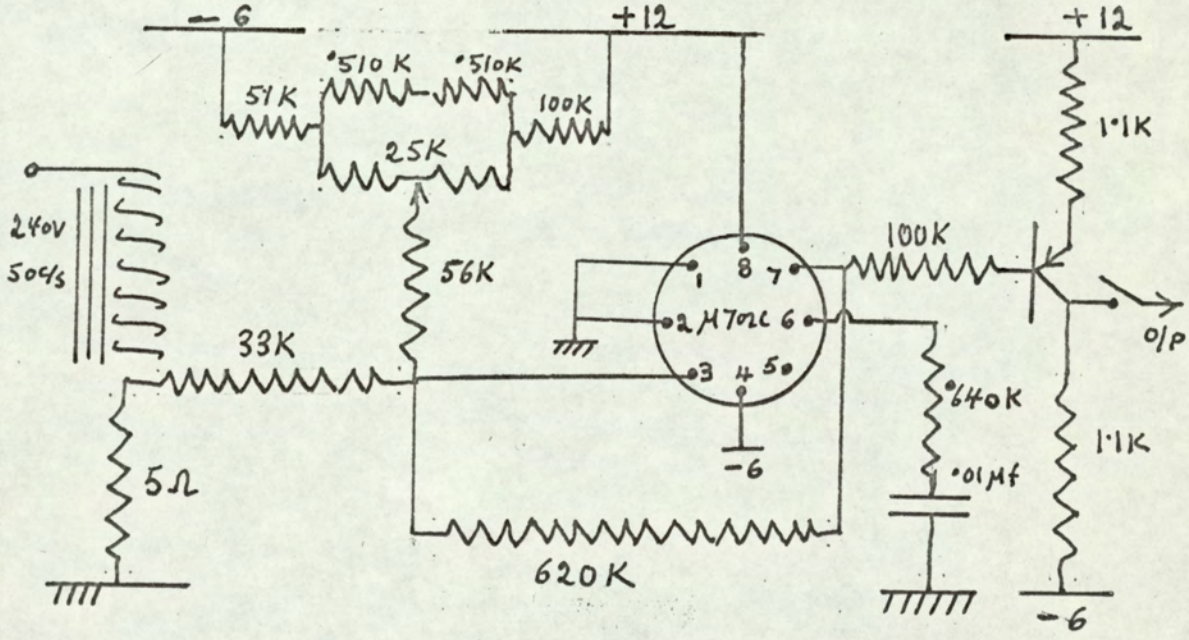

Fig.48 - Circuit diagram of current amplifier.

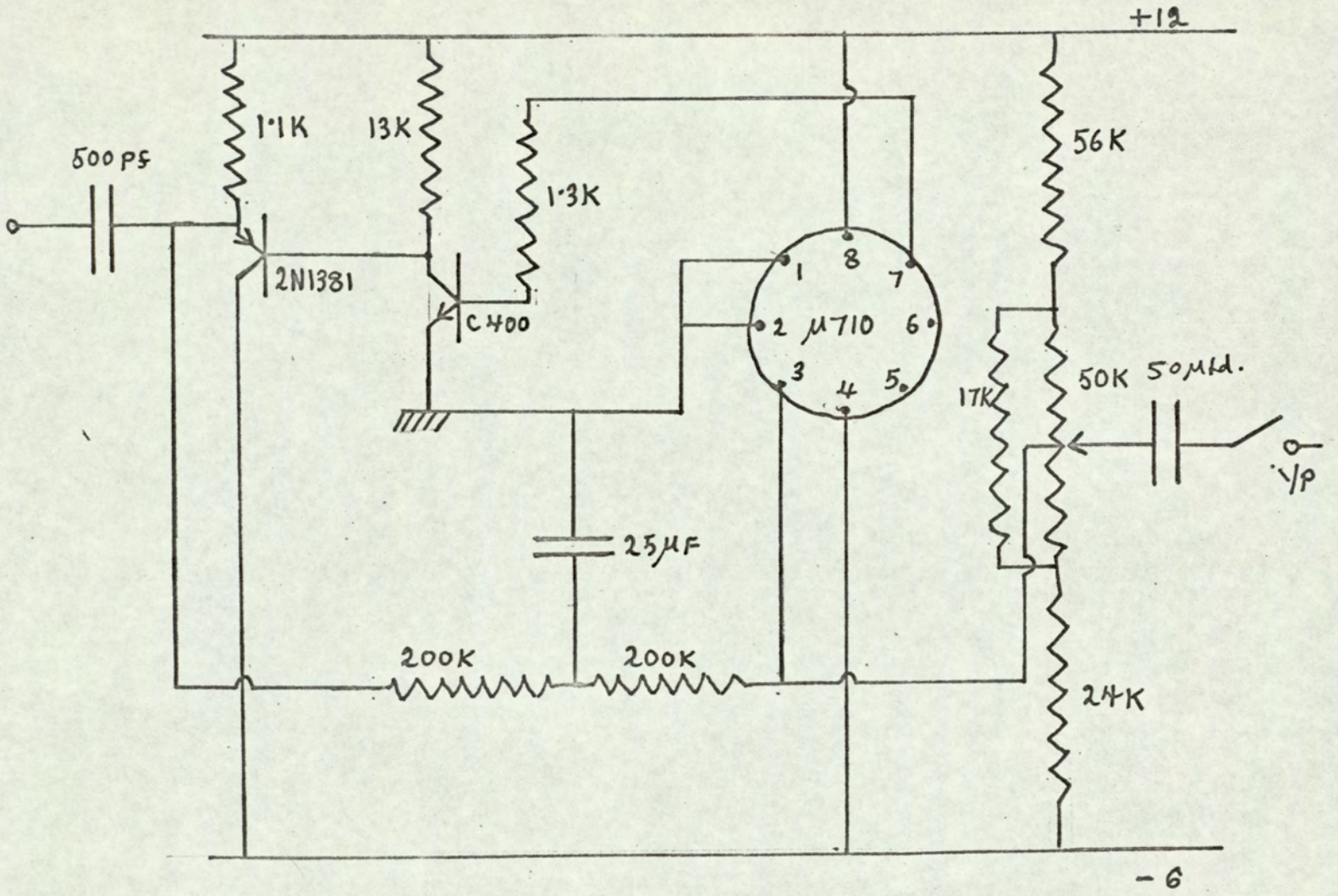

Fig.49 - Circuit diagram of Comparator; Channels A and B are identical.

amplified by a high input impedance amplifier, using an integrated circuit linear amplifier (μ 702C) and suitable transistor stages. The circuit is shown in Fig. 50. The waveform produced is fed into the comparator for zero crossing detection, producing a square wave which is used to stop the counter which was started by the voltage waveform. The time displayed gives a measure of the phase difference between the applied e.m.f. and the driving flux. Oscillograms of the relevant waveforms are shown in Figs. 51, 52, 53 and 54.

4.6 Considerations of the accuracy of the system

The system was tested for possible phase errors, ensuring that in the region of 50 c/s no phase errors were introduced. The errors in the measurement of the period time of the mains frequency depend on the counter and the frequency stability of the supply. The errors due to the insertion of the resistance in series with the shunt coil, and the time constant of the flux detector are negligible.

The main cause of error is the drift at the input of the comparator, this does not affect the voltage period measurement. Tests were conducted to determine this drift and from this and the amplitude of the waveform fed into the comparator and its frequency the maximum possible errors were estimated. These were,

$\pm$ 0.2% for phase between voltage and current

and $\pm$ 0.1% for phase between voltage and flux.

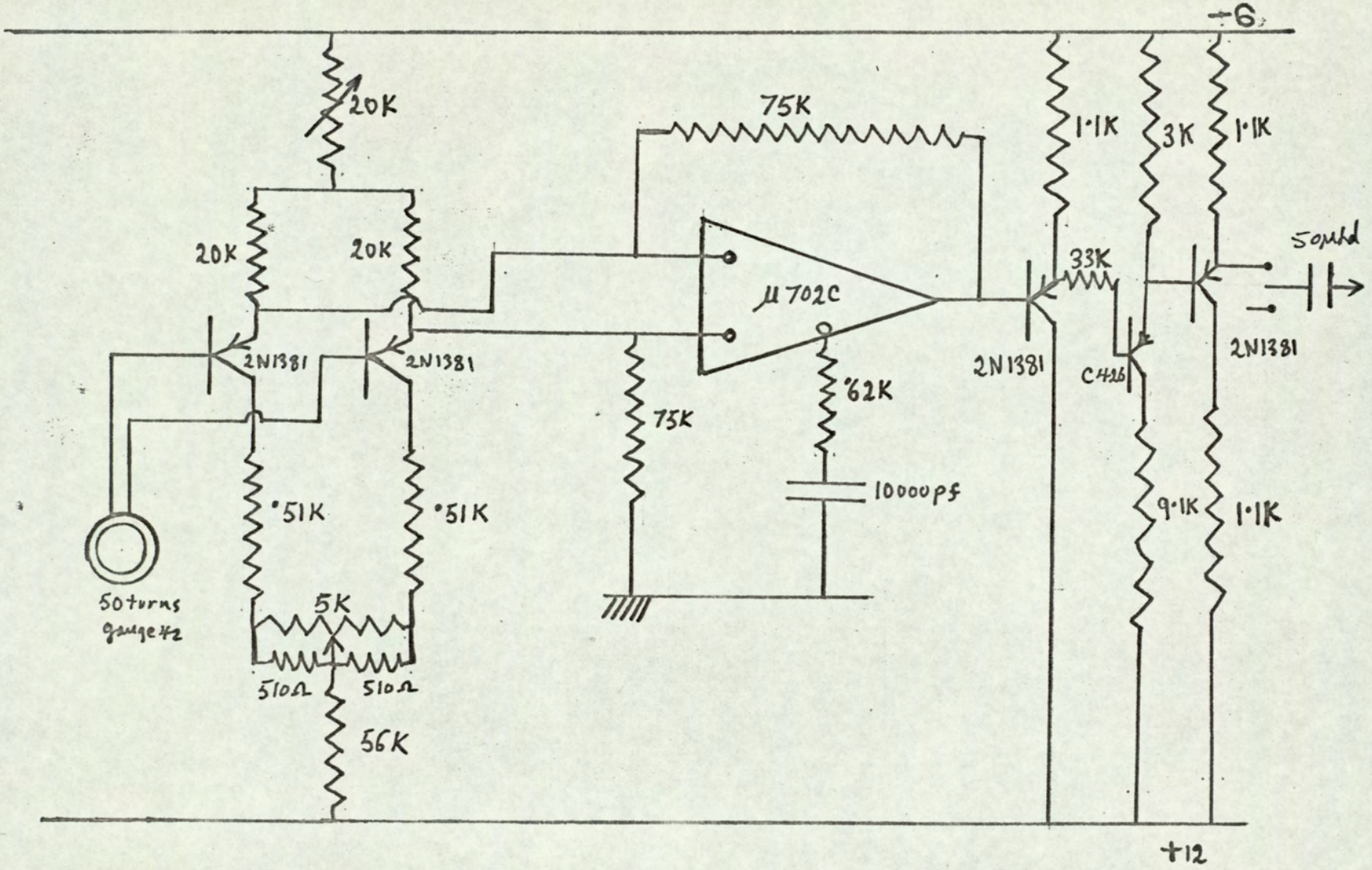

Fig.50 - Circuit diagram of flux amplifier.

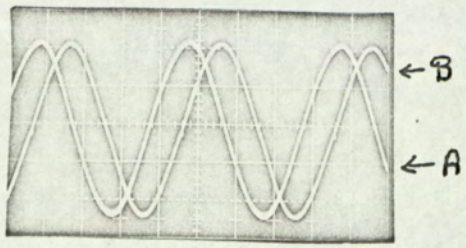

Fig. 51
Trace showing the voltage waveform (A) and the current waveform (B).

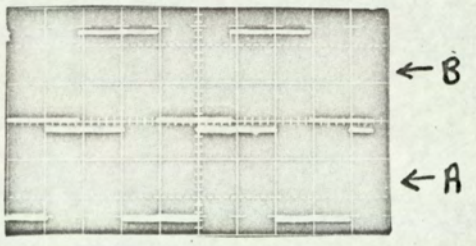

Fig. 52
Trace showing the comparators outputs which are being triggered by , 1)The voltage waveform (A).
2)The current waveform (B).

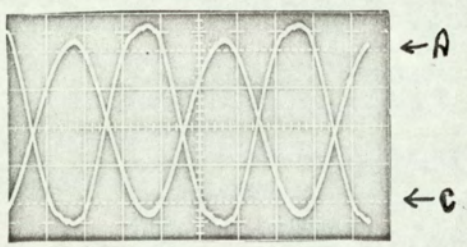

Fig. 53
Trace showing the voltage waveform (A) and the flux waveform (C).

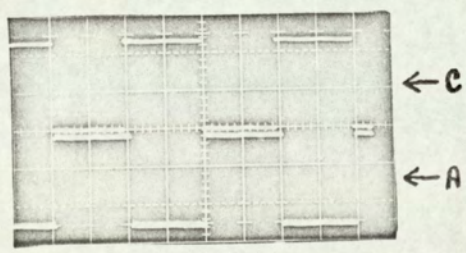

Fig. 54
Trace showing the comparators output which are being triggered by, 1)The voltage waveform (A).
2)The flux waveform (C).

These errors could easily be reduced by increasing the amplitude of the input waveforms and reducing the drift at the input of the comparator.

4.7 Test Procedure.

The period time for the mains frequency was ascertained prior to each test, as it suffers from frequent variations. This gave a time which is proportional to 360 degrees, using this the time displayed for a current or flux phase difference can be converted to degrees.

4.8 Test Results.

The effect of the inductive adjustment setting was studied first. Figs. 55 and 56, show this for flux and current phase angles, the series coil and disc being removed from the meter. The band was of the order of 3 degrees, and the flux lagged the current by about 3 degrees. The effect of the disc's separation from the sunt coil on the phase of the flux is shown in fig. 57. Tests for the meter with the disc and series coil show an increased lag for both the flux and current, and the angle between the current and phase has increased to about 18 degrees. The phase angle between the resultant flux under the central limb and the applied e.m.f., when the series flux was present is shown in fig. 60.

Now, the main object of this study was to find out the spread of the current phase angle for calibrated meters. The current

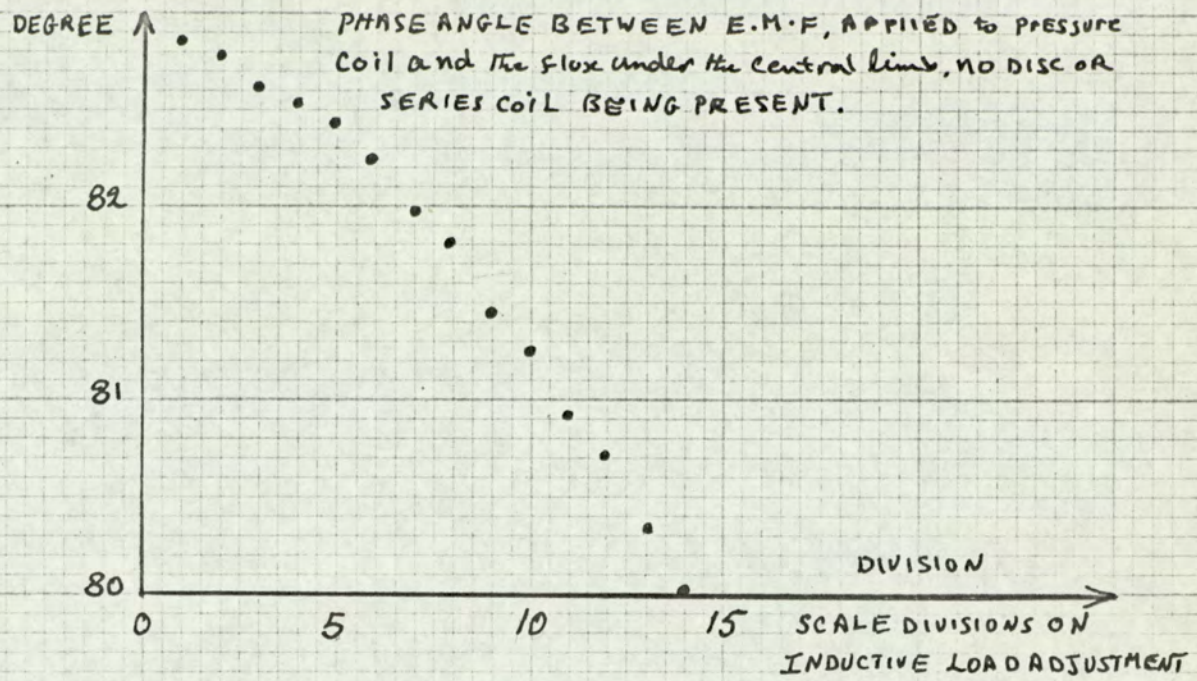

Fig. 55 - Graph showing the effect of the inductive adjustment setting on the phase relationship between the e.m.f. applied to the pressure coil and the flux under the central limb, no disc or series coil being present.

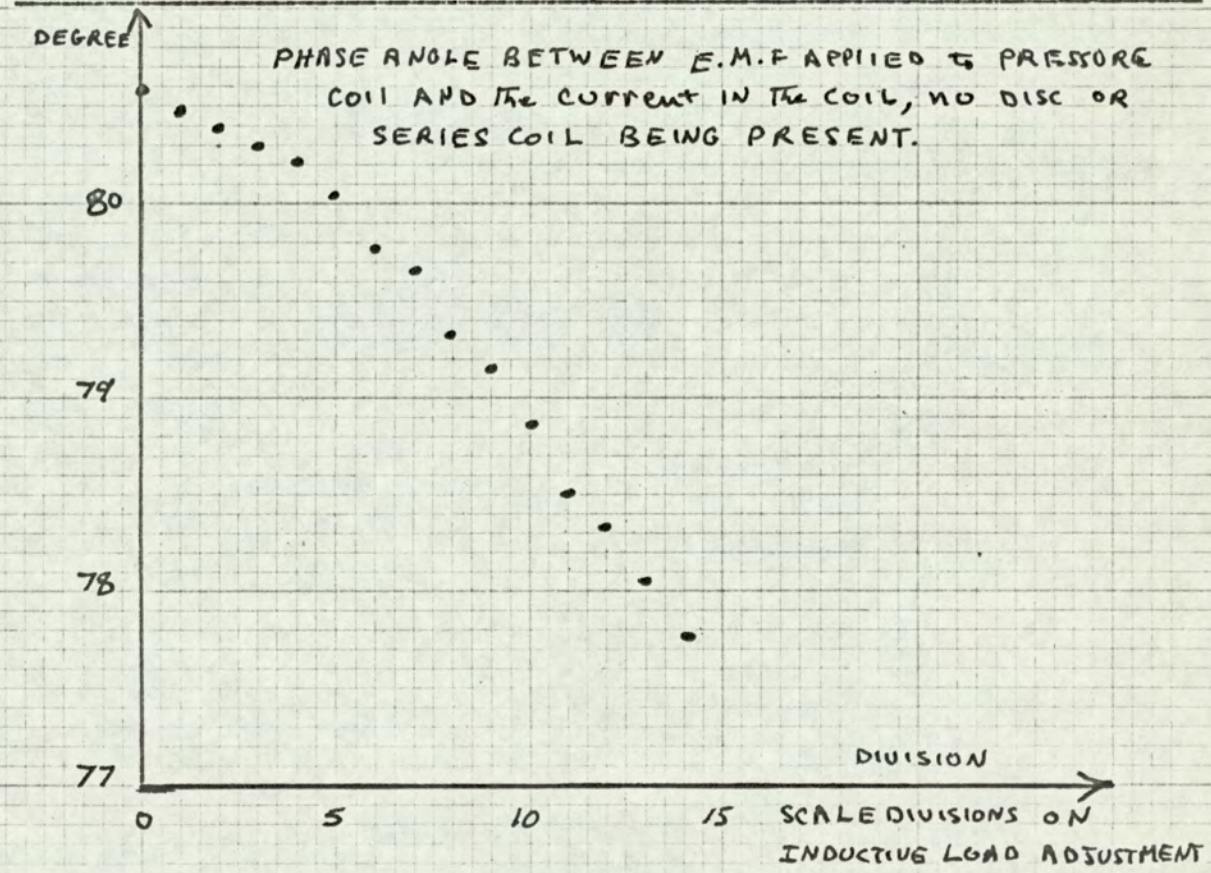

Fig.56 - Graph showing the effect of the inductive adjustment setting on the phase relationship between the e.m.f. applied to the pressure coil and the current in the coil, no disc or series coil being present.

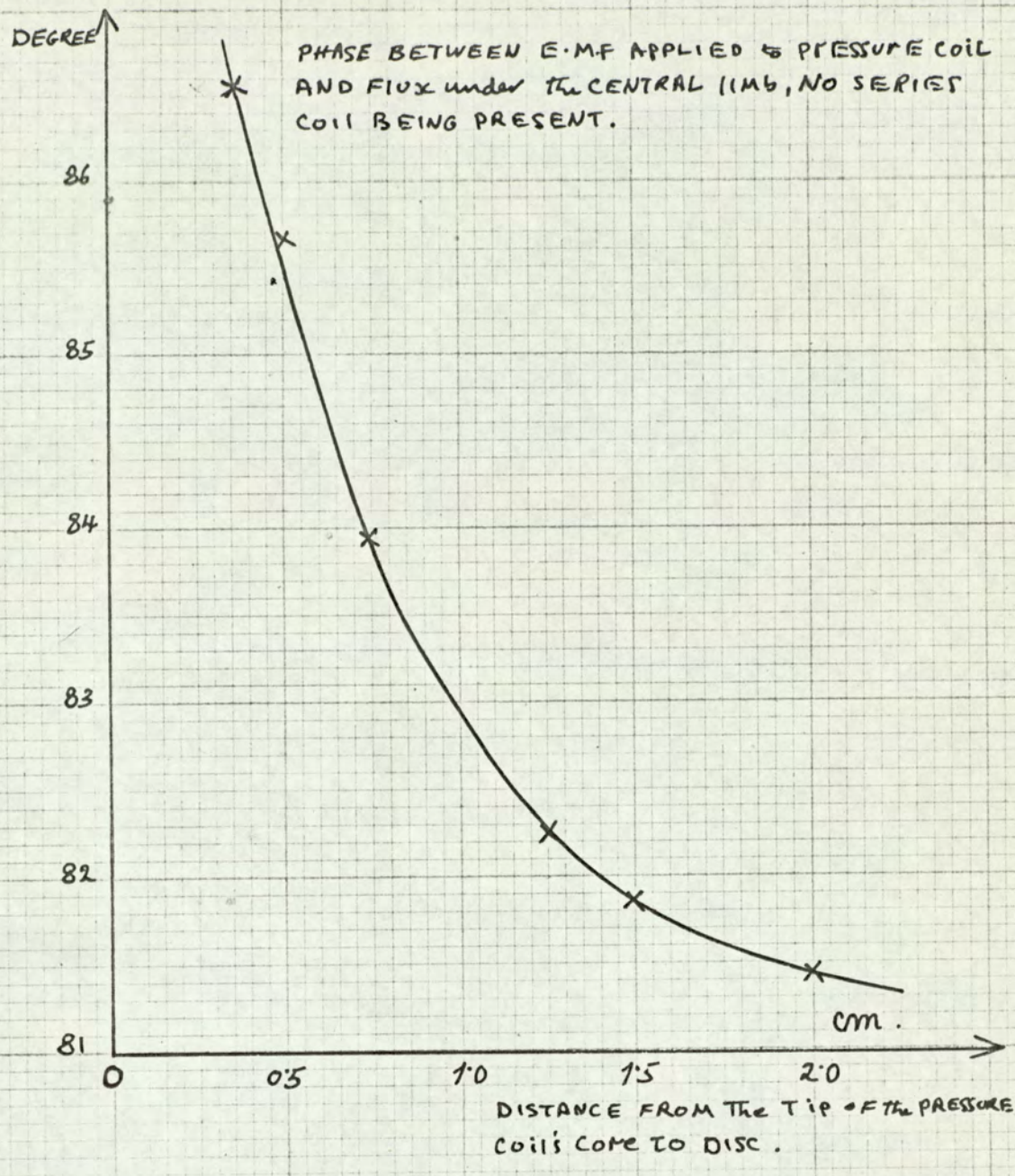

Fig.57 - Graph showing the effect of the disc's distance from the tip of the pressure coil, on the phase relationship between the e.m.f. applied to the pressure coil and the flux under the central limb, no series coil being present.

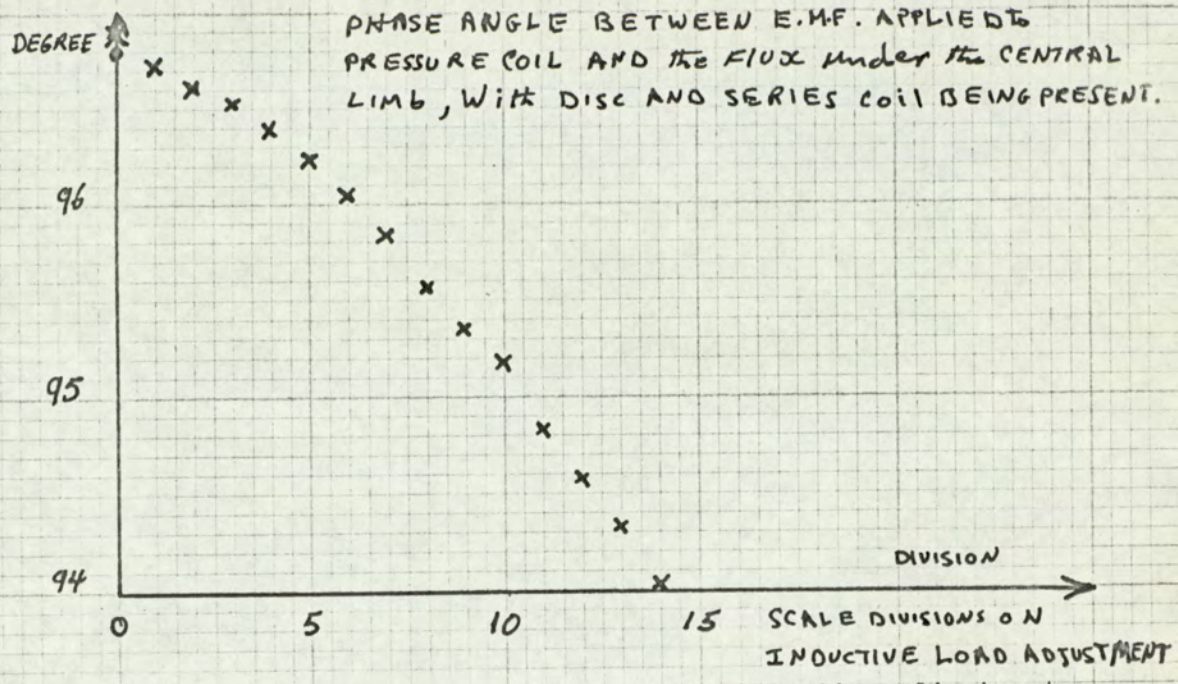

Fig. 58 - Graph showing the effect of the inductive adjustment setting on the phase relationship between the e.m.f. applied to the pressure coil and the flux under the central limb, the disc and series coil being present.

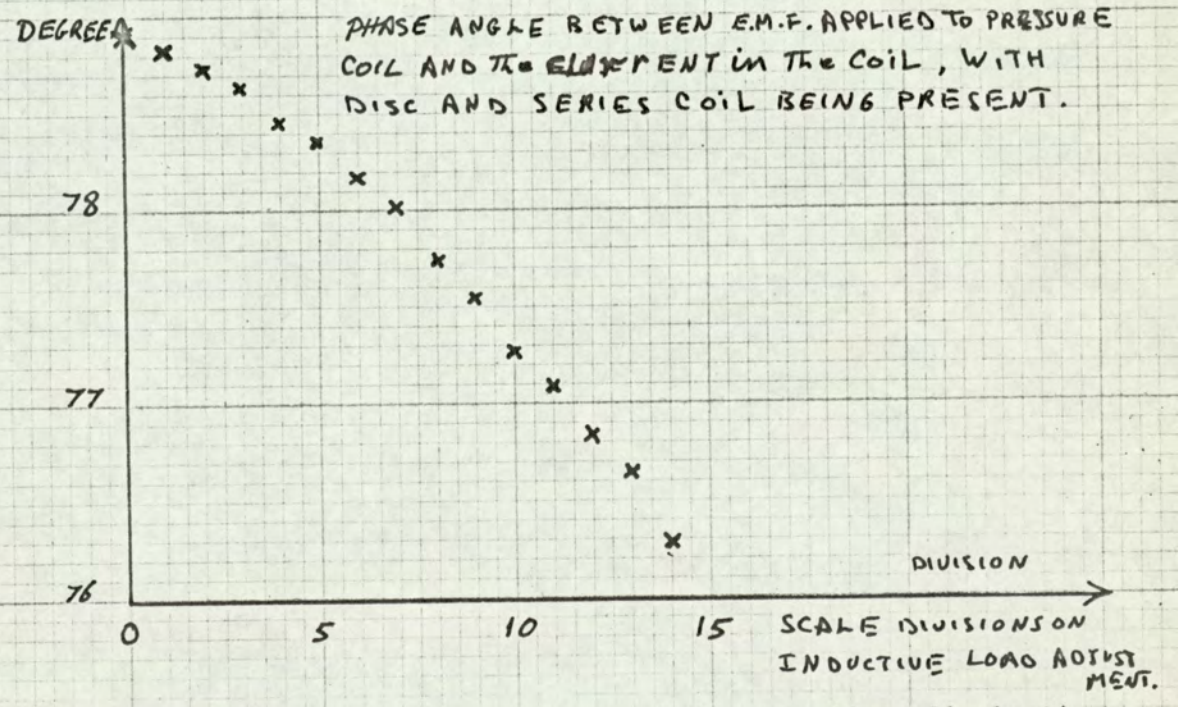

Fig. 59 - Graph showing the effect of the inductive adjustment setting on the phase relationship between the e.m.f. applied to the pressure coil and the current in the coil, the disc and series coil being present.

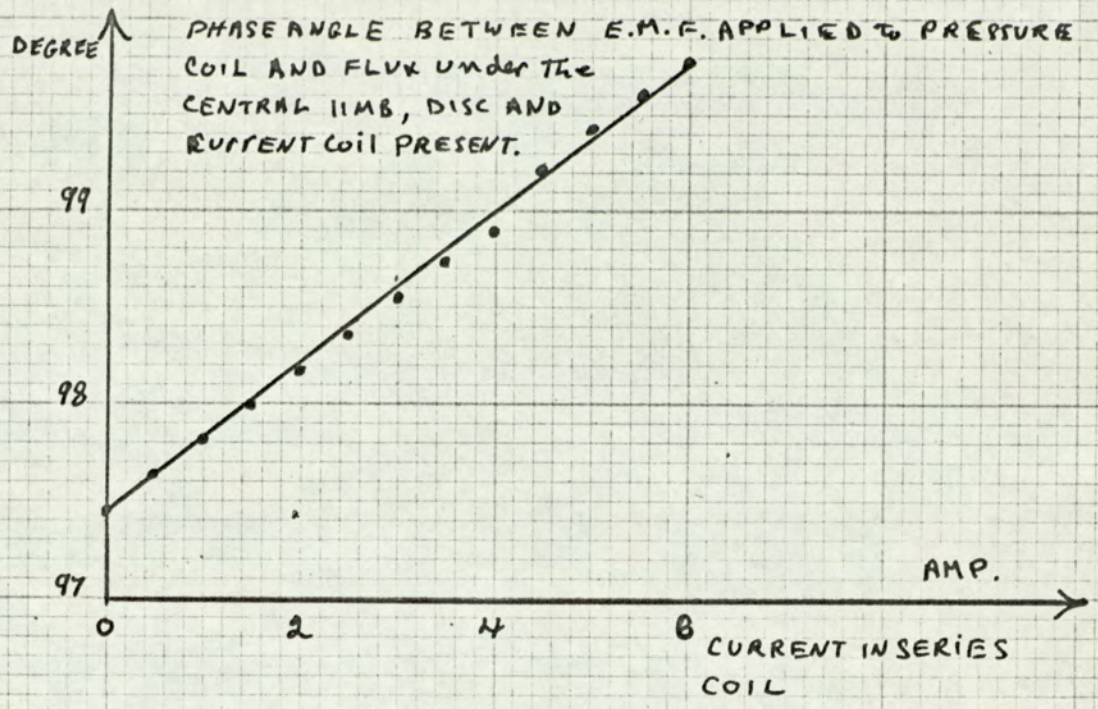

Fig. 60 - Graph showing the variation of the phase relationship between the applied e.m.f. to the pressure coil and the flux under the central limb, with the current in the series coil, the disc being present

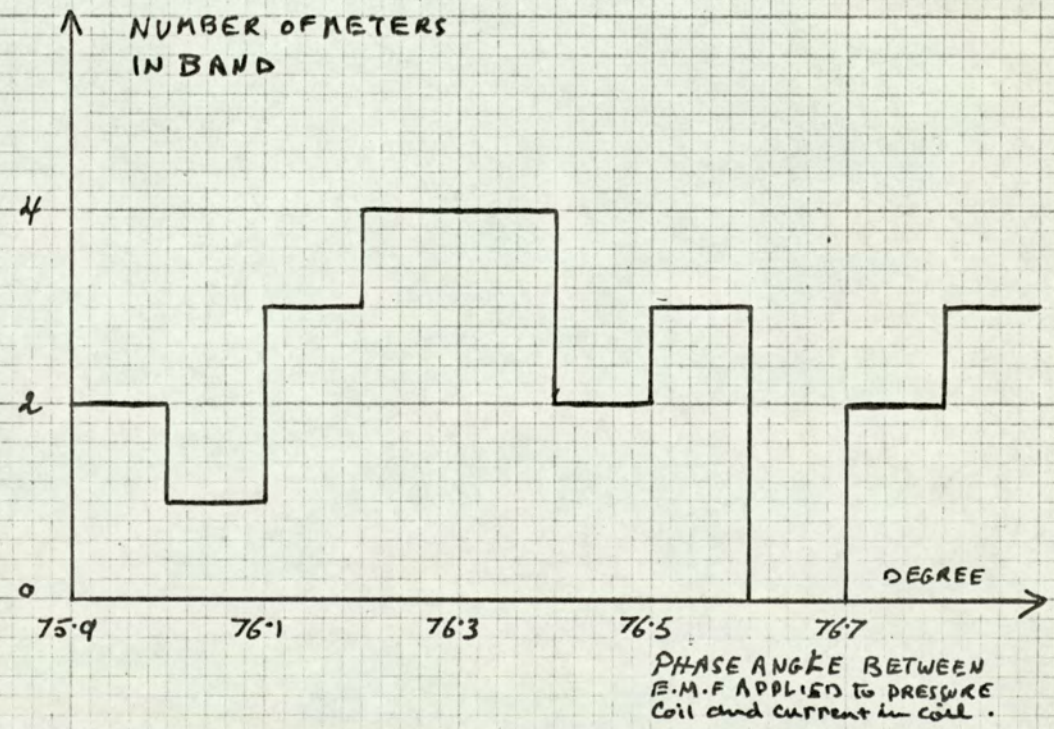

Fig. 61 - Graph showing the spread, for 25 calibrated meters, in the phase angle between the e.m.f. applied to the pressure coil and the current in the coil.

phase angle is a more reliable quantity than the flux, as the latter will need accurate positioning of the search coil and hence a long time for setting up. The spread for 25 calibrated meters is shown in fig.61. It is clear that most of the meters lie in a band of approximately $\pm$ 0.25% width.

4.9 A new technique for phase setting.

The result of fig.61 suggests a different approach to the phase adjustment of induction meters. If the mean value of the spread can be found by testing a large number of calibrated meters, this figure of current phase can be used, and meters can be set whilst on the production line to that value. Further investigations are required to assess the validity and accuracy of this method.

4.10 A modified system for production line tests.

The system can be modified to suit the production line. The requirements being the elimination of any need of calculation, simplicity of operation, and speed.

Fig.46, shows a block diagram of the modified system. A stable frequency supply is used to eliminate mains variations. The voltage current amplifiers, and comparators are retained. A variable pulse rate oscillator feeds a digital counter through suitable gates.

The operation of the system consists of;

i) The voltage waveform is used to control the gate, the pulse rate is varied by the operator till the digital display indicates a pre-determined figure. The system is then calibrated.

ii) The rising edge of the voltage waveform is used to open the gate and the rising edge of the current waveform to stop it. This produces a certain digital display, the operator then adjusts the meter till a display corresponding to the correct phase angle is shown.

The series coil is not energised during the test.

FRICTIONAL TORQUES IN THE SINGLE PHASE INDUCTION METER

5.1 Introduction[59]

The frictional torques present in the meter can be divided into the following components:

a) Air friction;

b) Pivot friction;

c) Register mechanism friction.

The first is prominent, at very high speeds of the disc, whilst the rest dominate at the lower speeds of the disc, in the region below 1/10 of full load. One of the major considerations in good meter design, is to minimise their effects; On the other hand, one of the objects of calibration is to compensate for any such torques present in the meter.

5.2 Air friction.

This torque is proportional to the square of the speed of the rotor, and is mainly determined by the shape of the rotor, and the speed range of the meter. As, flat, smoothe surfaced discs, and low speeds are used in induction meters, this effect is negligible.

5.3 Pivot friction[60,61,62]

The lower bearing of the meter is the major contributor to this friction. As this force increases with wear, it is one of the dominant factors determining the time interval between meter servicing.

Interest in jewels and bearings started centuries ago with the builders of clocks and watches, nevertheless, great advances have been effected in this century. Modern materials, designs and lubricants, linked with a better understanding of the action of frictional forces, has led to, products having a longer life time, and a great reduction of wear.

Parasitic forces[63] which act on the meter, and reach a maximum at no load, add to the wear of the jewel. An extensive study of these forces and their effects has been conducted by Schotter and Tagg[64]. Since the early days of meters, there have been attempts to suspend the meter magnetically, these have been partially successful and meters with partial magnetic suspension can be found in the market.

From the calibration point of view, the bearing friction provides a constant braking torque, which can be compensated.

5.4 Friction in the Register Mechanism[65]

The influence of the register mechanism on the accuracy of the meter is two fold:

i) It must integrate the rotor movement, giving a register of K.Wh. This necessitates a correct gear ratio in agreement with the meter's constant. High speed testing is used to assess the ratio and counters with the wrong ratio are rejected.

ii) It influences the speed of the rotor by providing a stictional torque that has to be overcome before any motion could ensue, and a constant dynamic frictional torque modulated by random variations. The long dial test is the usual way of testing the counters in order to assess the effect of these torques.

Three common types of meter counters are shown in Fig.62. These are:

a) Dial Counters: These have a good amount of backlash in the gears and may suffer from bad teeth, or teeth engaging too deeply; such effects occur suddenly and last an uncertain length of time.

b) Jump Counters: These will produce in addition a varying frictional torque which depends on the relative position of the jump weight; this can be overcome by a choice of the right gear ratio.

c) Roller Counters: These usually have more friction and more moving parts, and whilst motion is transmitted from one digit wheel through the pinion to another, more pressure is exerted on the pinion bearing and hence more frictional torque is presented to the drive.

The gearing arrangements of each of these counters is shown in figs. 63, 64 and 65. All three types use a bakelite wheel with a worm gear on its axis. The losses in the worm-

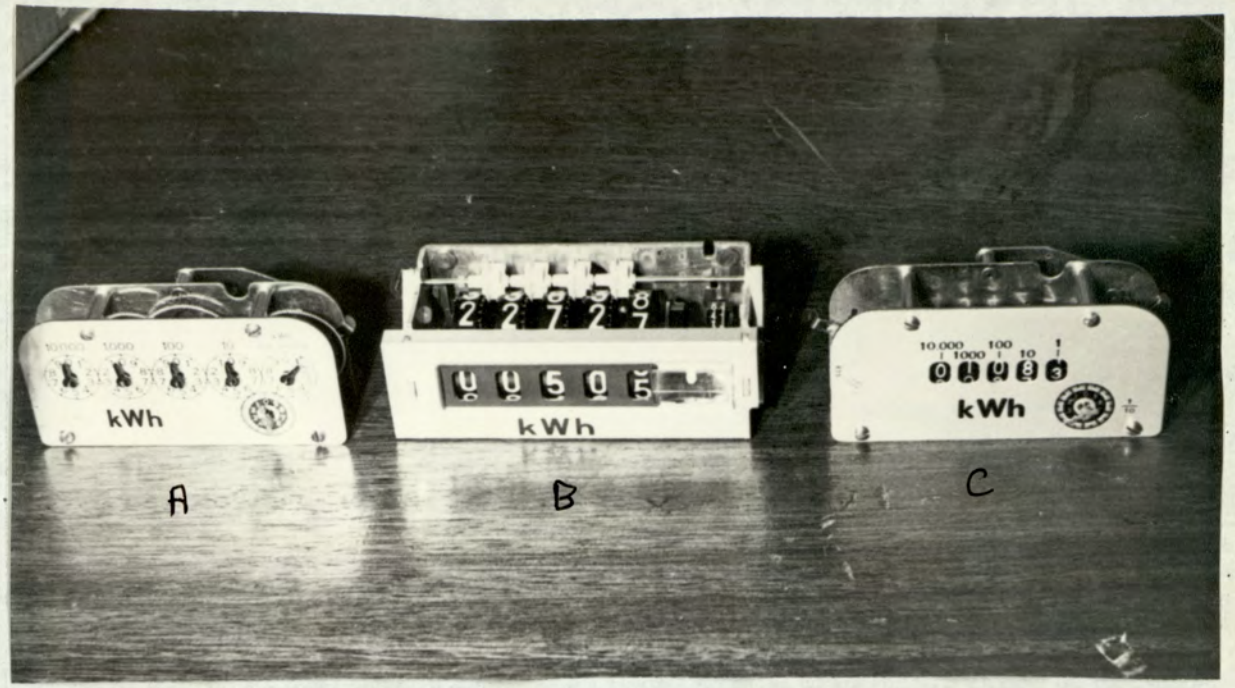

Fig.62 Plate showing types of Registers tested.
A) Dial Counter. B) Jump Counter. C) Roller Counter.

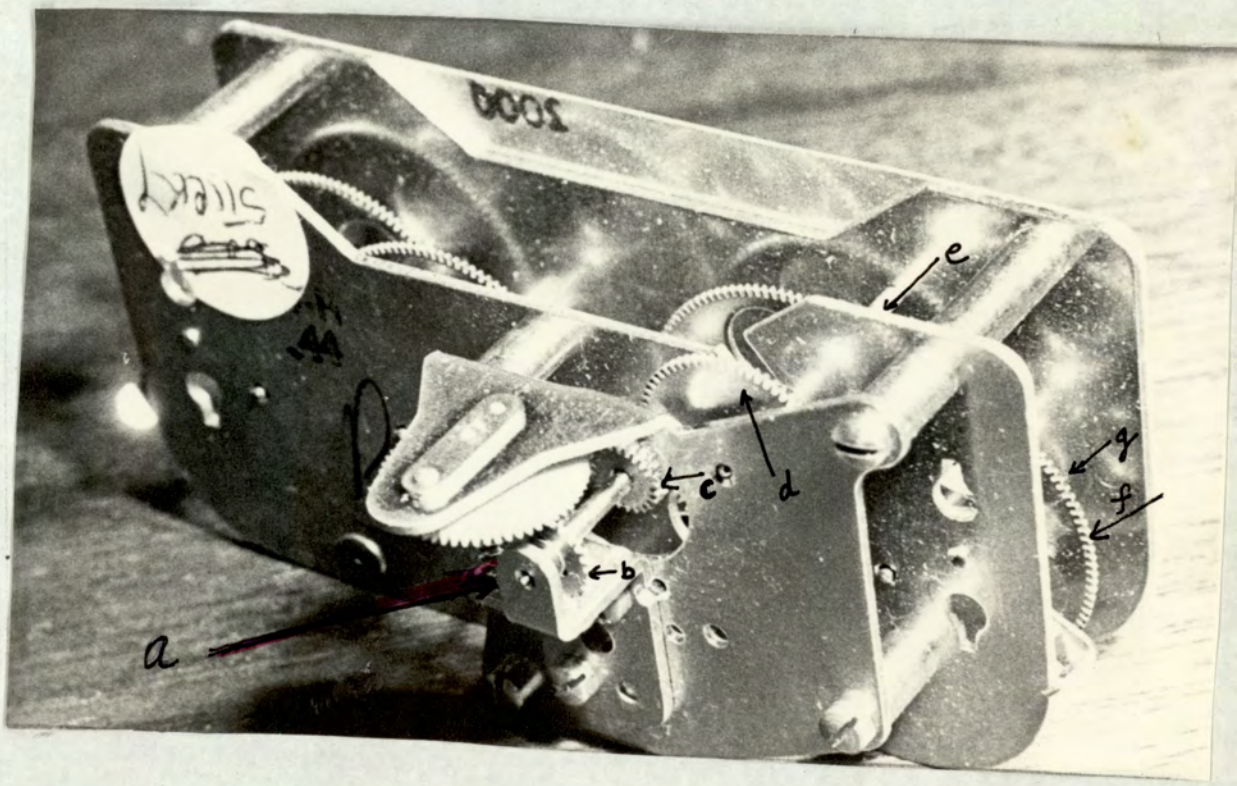

Fig.63. Plate showing gear arrangement of Dial Counter.

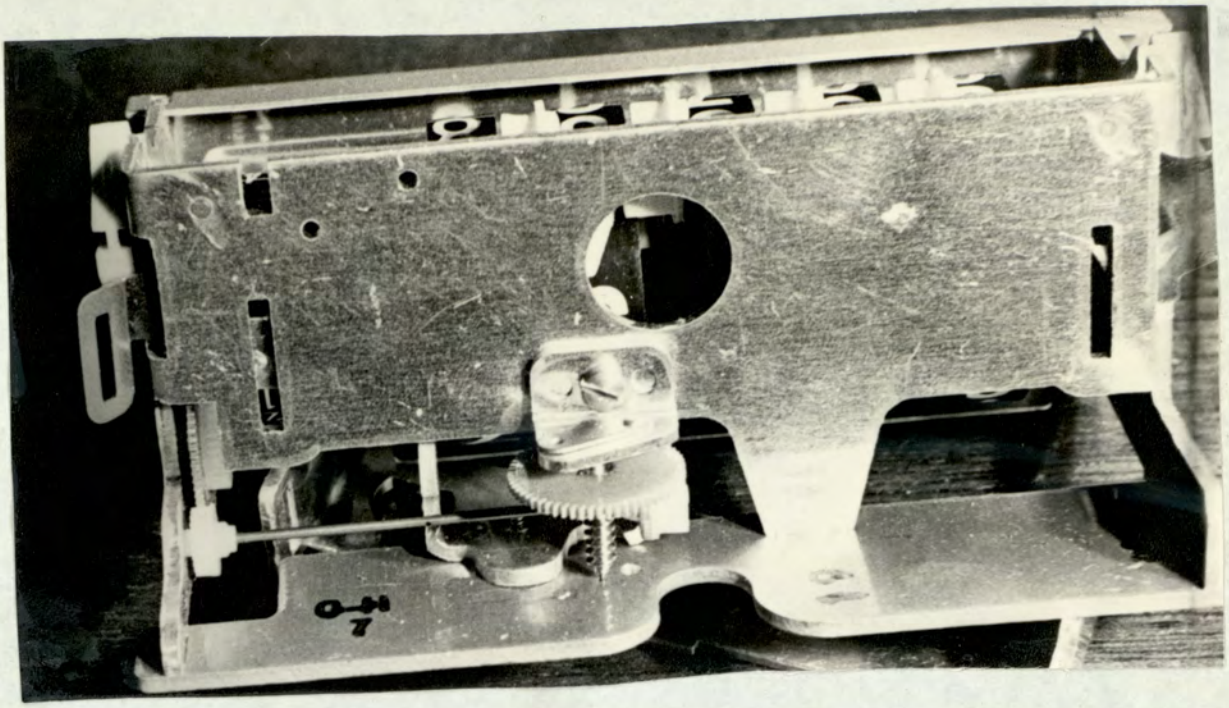

Fig. 64. Plate showing gear arrangement of Jump Counter.

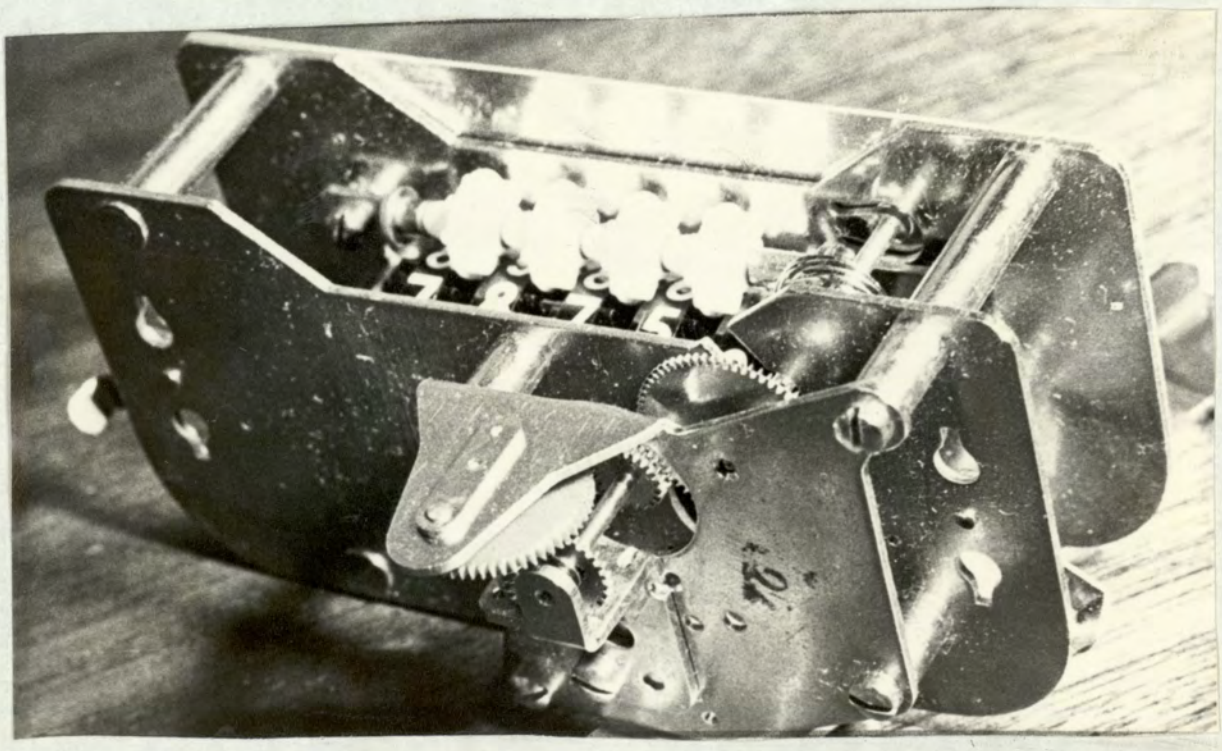

Fig. 65. Plate showing gear arrangement of Roller Counter.

gear are relatively high, because of the relative sliding of the teeth in the direction parallel to their tips, these losses depend on the, tooth load, the sliding speed and the coefficient of friction between the surfaces. There is also losses in the bearings that support the gears, these losses, in the absence of any lubricant will be proportional to the speed.

The frictional torque, which is the moment of frictional resistance of a spindle or a wheel is given by

$$P = m \times d \times \text{coefficient of friction} \quad \ldots\ldots \qquad (25)$$

where, m is the weight

and d is the diameter.

The frictional torque of a train of axles, each having a frictional torque of P Newton-meters; reflected to the first axle is given by;

$$P\left(1 + \frac{1}{g\,e} + \frac{1}{g^2 e^2} + \frac{1}{g^3 e^3} + \cdots\right) \ldots\ldots \qquad (26)$$

where, g is the gear ratio,

and e is the differential efficiency defined as,

$$\frac{\text{the increment of resisting moment on driven axle}}{\text{corresponding increment of torque on driving axle.}}$$

It is clear from this expression that the higher order axles contribute very little resistance to the driving element. However, it does not convey at which axle the contribution is rendered negligible.

The effect of a 'bad' counter on the speed of the rotor is shown in Fig.66, where the difference in the speed, between a meter when fitted with various 'bad' counters and when it is fitted with a normal 'good' counter, is plotted against load. The graphs show that for some counters, a one-revolution test will clearly point out their defects, these are mostly 'sticky' counters. There are, however, other random variations which present a higher value of frictional torque for an undetermined period of time. These are unlikely to be detected by a one-revolution test.

Friction was simulated in a 'good' dial counter by blocking some teeth of different gears, and observing its influence on the speed of the disc. The results are shown in graphs 67, a, b, c, d, e, f and g. This effect is similar to those produced by, bad teeth, or bent axles. The speed of the disc falls due to the increased frictional torque, the duration of this fall depends on the extent of the damage and on the position of the gear. As the distance of the gear, away from the worm gear, increases, its influence decreases, and in gears 'f' and 'g' a great amount of blocking material had to be used before any change of speed was decerned.

Consider a meter with a linear characteristic as in equation (17). If an increase in friction occurs in a gear, the gear having a period T at a given load; and the friction, which is

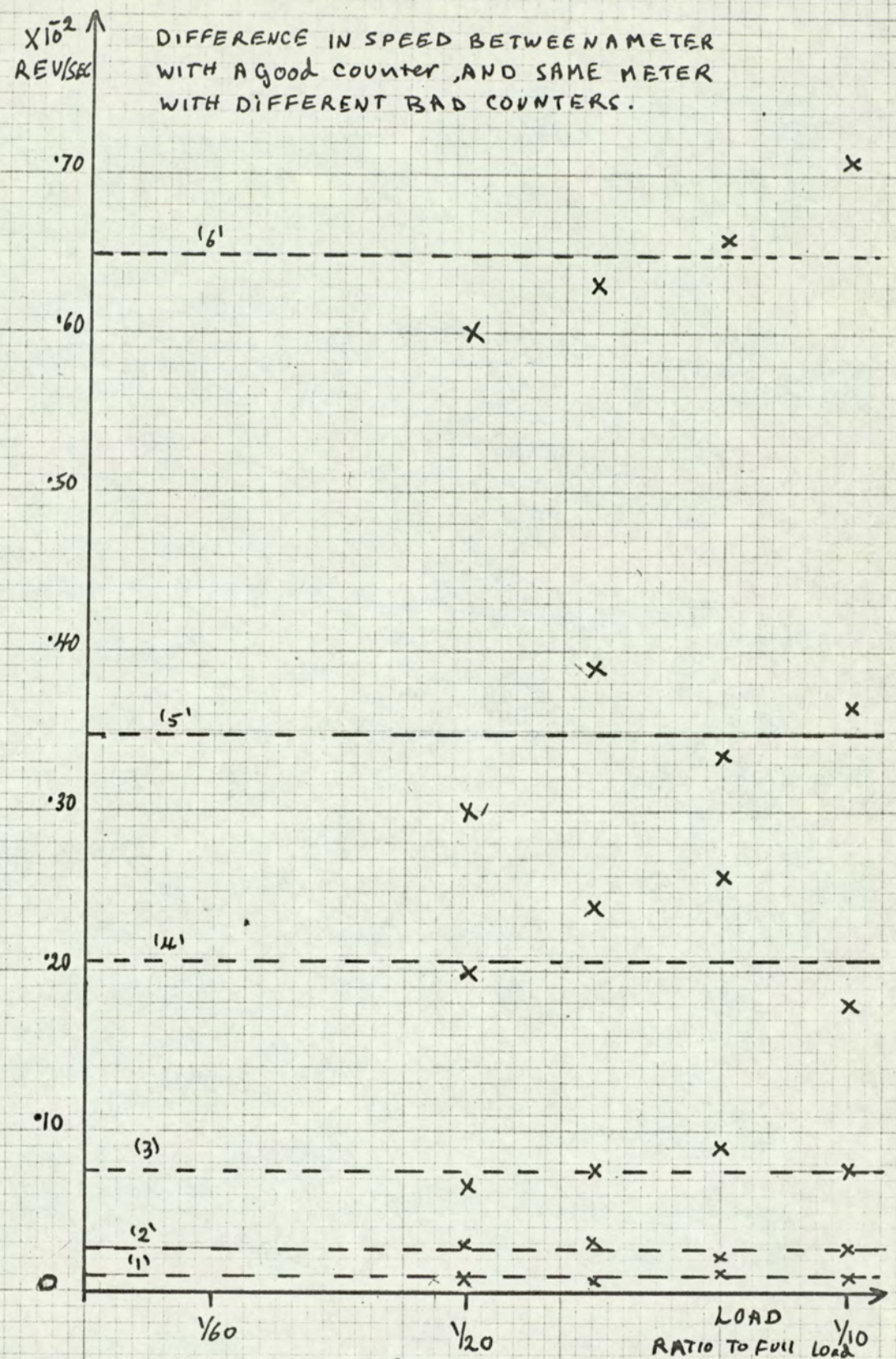

Fig. 66. Graph showing the difference in speed between a meter fitted with rejected counters, and when fitted with a normal counter.

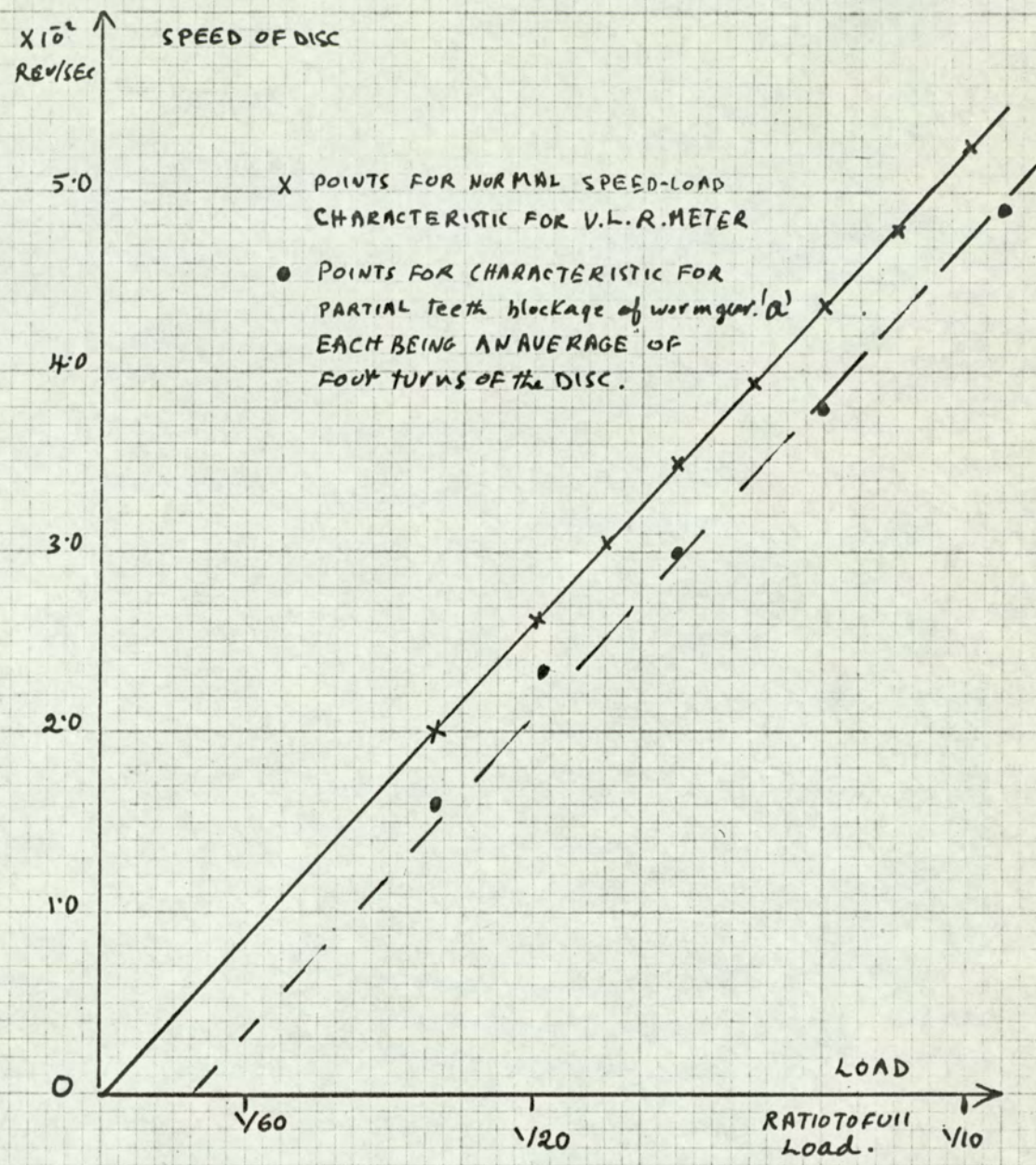

Fig.67(a): Graph showing the effect of simulated friction in the worm gear on the speed-load characteristics of the meter

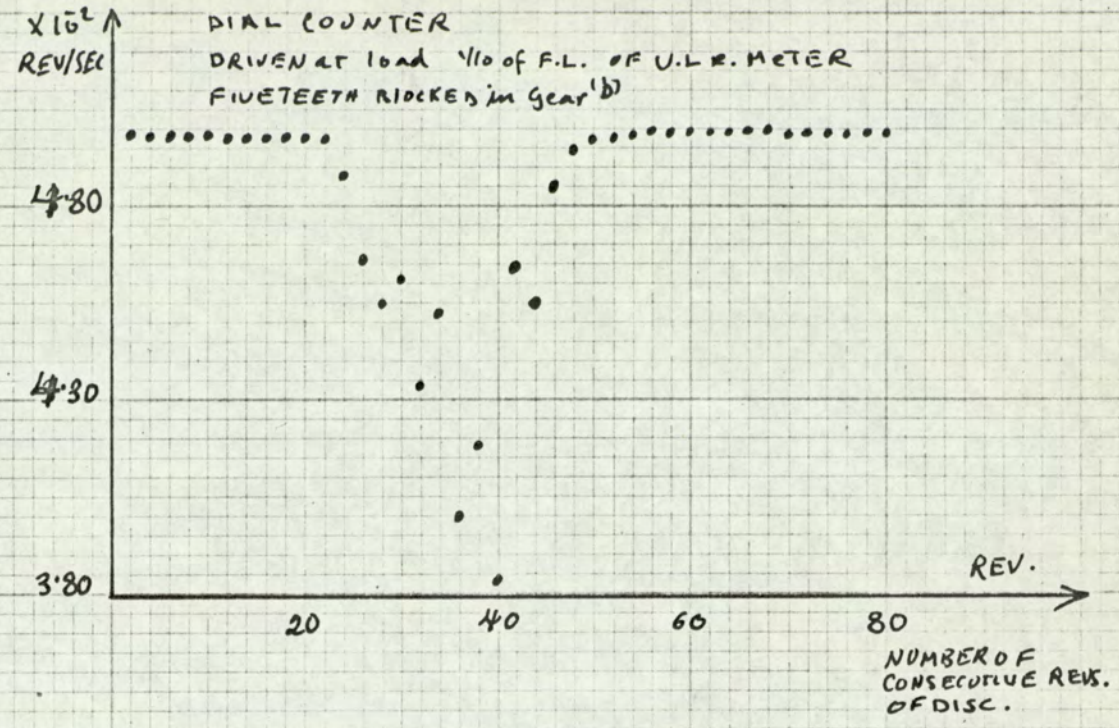

Fig.67(b) Graph showing the effect of simulated friction in gear 'b' of a dial counter, on the speed of the disc, under constant load

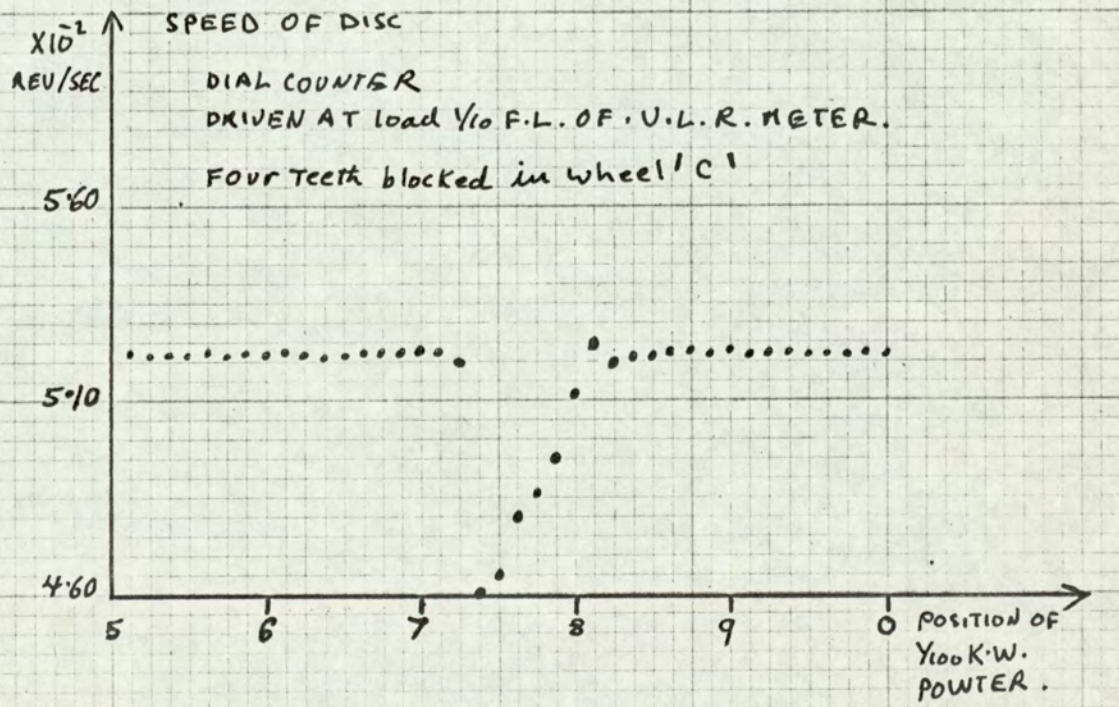

Fig.67(c) Graph showing the effect of simulated friction in gear 'c' of a dial counter, on the speed of the disc, under constant load

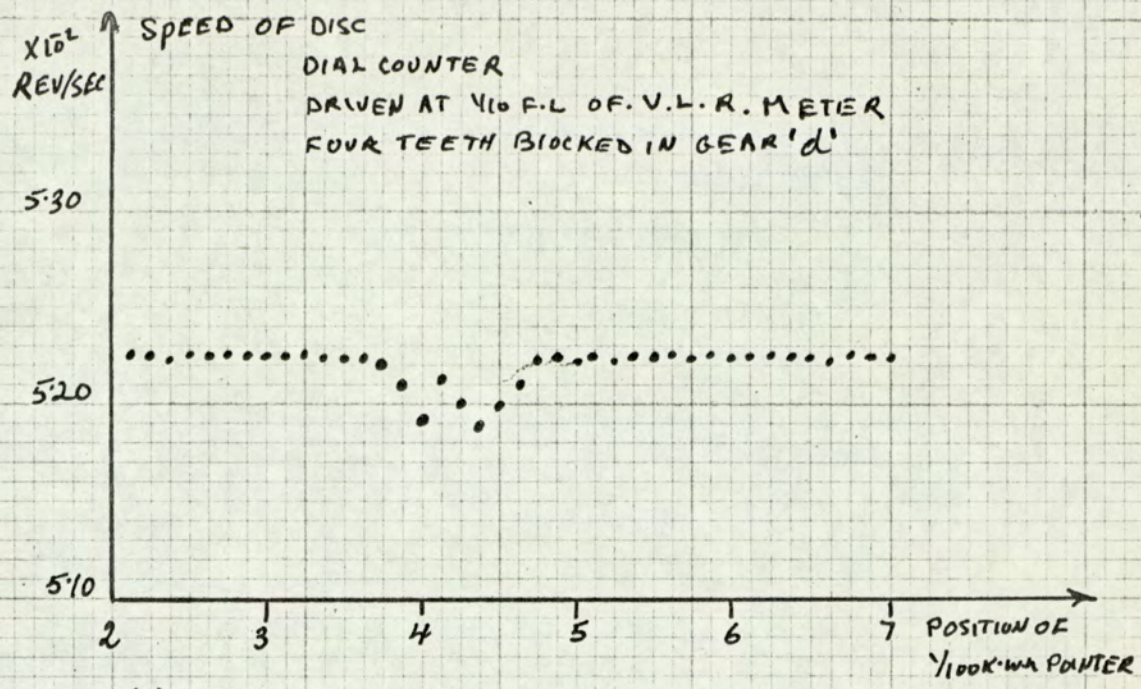

Fig. 67(d) Graph showing the effect of simulated friction in gear 'd' of a dial counter, on the speed of the disc, under constant load.

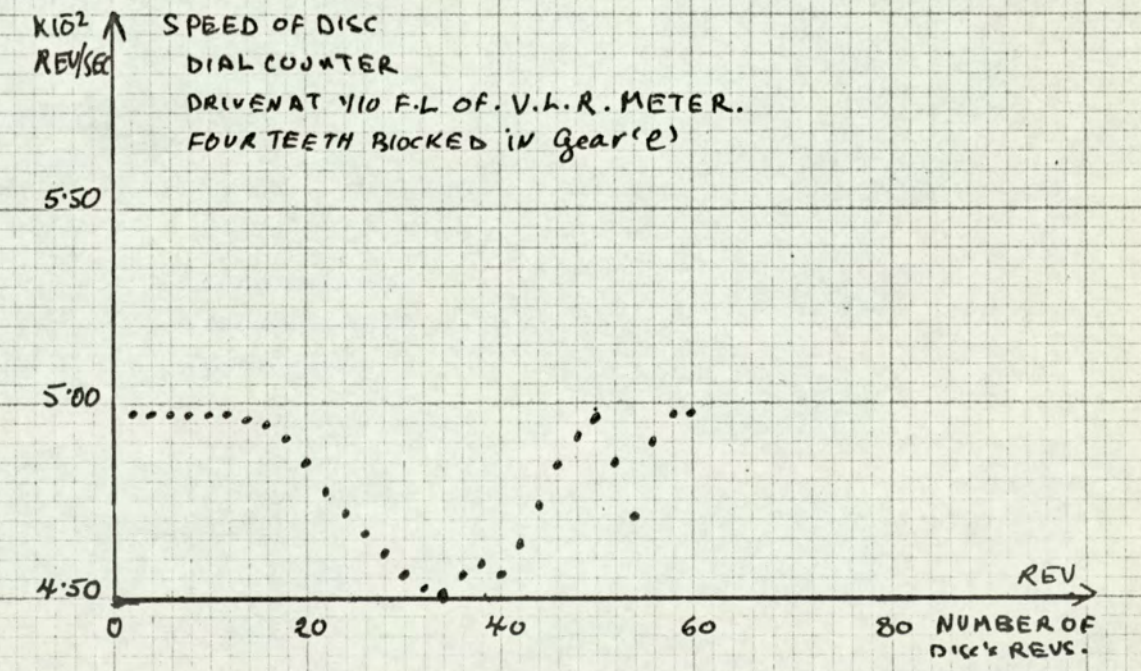

Fig.67(e) Graph showing the effect of simulated friction in gear 'e' of a dial counter, on the speed of the disc, under constant load.

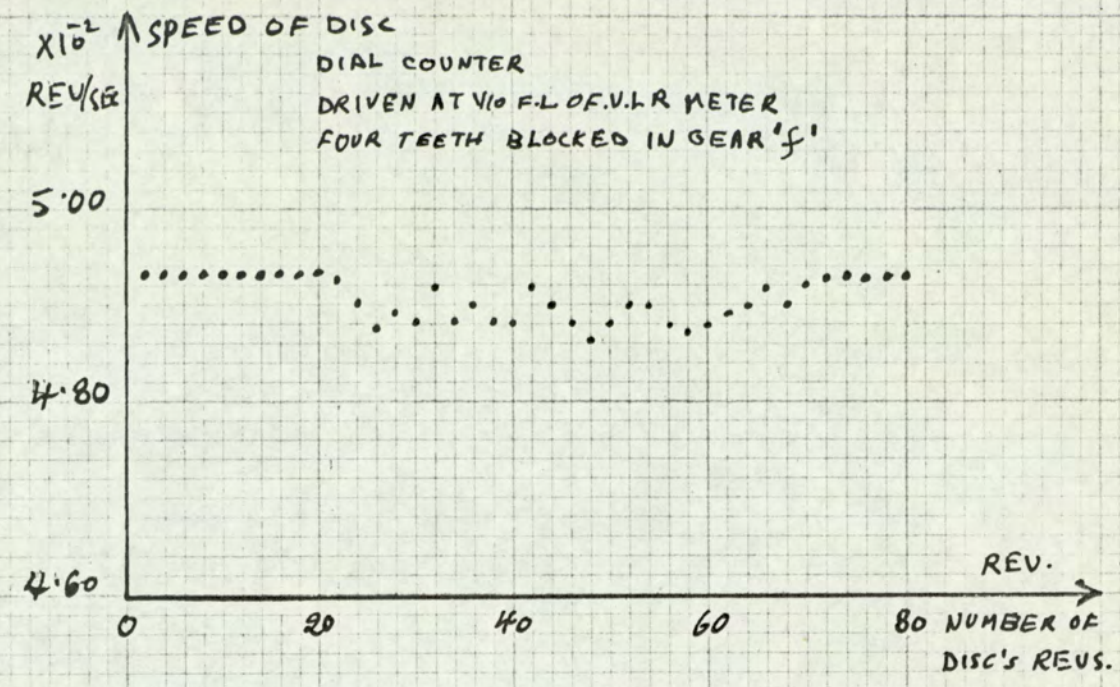

Fig.67(f) Graph showing the effect of simulated friction in gear 'f' of a dial counter, on the speed of the disc, under constant load.

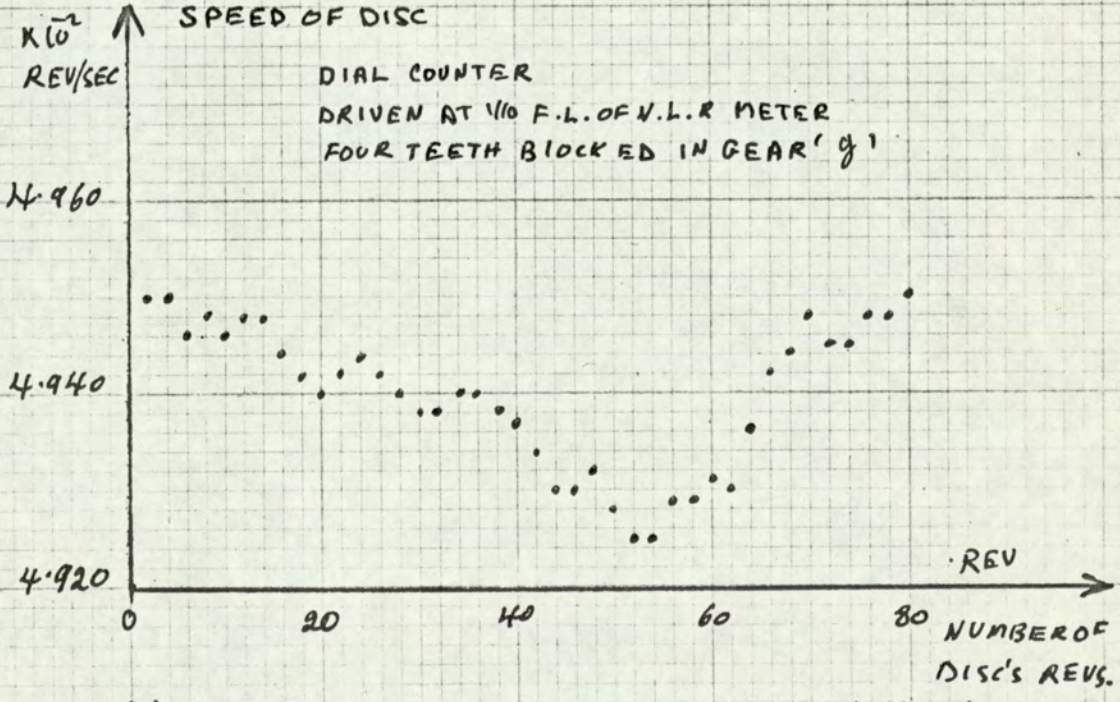

Fig.67(g) Graph showing the effect of simulated friction in gear 'g' of a dial counter, on the speed of the disc, under constant load.

assumed to attain a constant value, to last for a time T_1 at the same load; The equation of the meter during the time T_1 will be ;

$$S_1 = a W + b_1 \quad \ldots\ldots \quad (27)$$

where b_1 allows for the increase in the friction during the time T_1.

This event repeats itself once every 'T', so the average speed of the meter will be

$$= \frac{\int_0^{T-T_1} S \cdot dt + \int_{T-T_1}^{T} S_1 \cdot dt}{T} \quad \ldots\ldots \quad (28)$$

From which, after integration and reduction;

$$\text{The average speed} = S - (b - b_1) \frac{T_1}{T} \quad \ldots\ldots \quad (29)$$

If $(b - b_1) \frac{T_1}{T}$ is small, whilst $(b - b_1)$ is beyond the acceptable limits of a 'good' counter, a long dial test will show the counter to be acceptable, whilst a one-revolution test, during which the friction has its high value, will reject the counter. Now, under operational conditions, the overall accuracy of registration will not suffer if such a counter is used. Thus, any method for testing the friction in counters must take into account the following important elements;

1) The amount of stiction present in the counter.

2) The amount of dynamic frictional torque present.

3) The ratio of the duration of an increment in the value of the dynamic friction, to the periodicity of the wheel concerned.

4) The order of the gear in question.

5.5 The determination of the gear order, up to which, the counters should be tested.

The system used is shown in fig.68. The bakelite wheel of the counter under test is driven by an air supply through a suitable nozzle. A hole in the wheel provides a light impulse, every revolution, this is detected by a photoelectric detector similar to that described in (3.2). By shutting off the air supply and starting the U.V. recorder, a deceleration curve for the motion can be found from the record. This curve can be plotted as an acceleration curve under a force equivalent to the frictional force; as more axles are added to the counter their effect can be detected from the shape of the curve. Figs. 69 a, b and c * show this for the three types of counters, and indicates that after the third axle the increase in the dynamic frictional torque due to added axles, as seen at the driving end, is very small. This, establishes the limit to which it is necessary to test the counters. Figs. 70 a, b and c, show the spread in the value of the dynamic frictional torque for four counters from each type, taken at random from the production line.

* This part of the work was done in collaboration with Mr.A.K.Bhowmick.

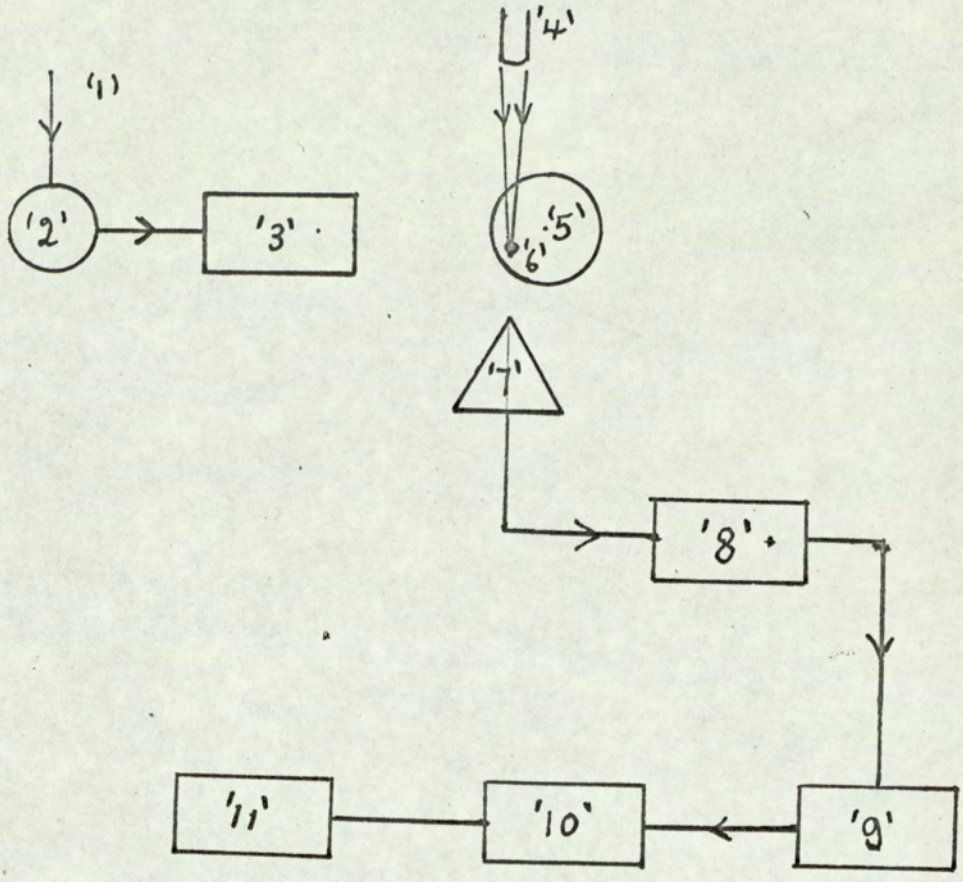

Fig.68 : Block diagram showing the system used to record the retordation of the counters.

1. Air supply
2. Reduction valve.
3. Nozzle.
4. Light source.
5. Bakelite wheel of counter.
6. Hole in the wheel.
7. Photo-elector.
8. Amplifier.
9. Schmitt trigger.
10. Attenuater and matching.
11. U.V. Recorder.

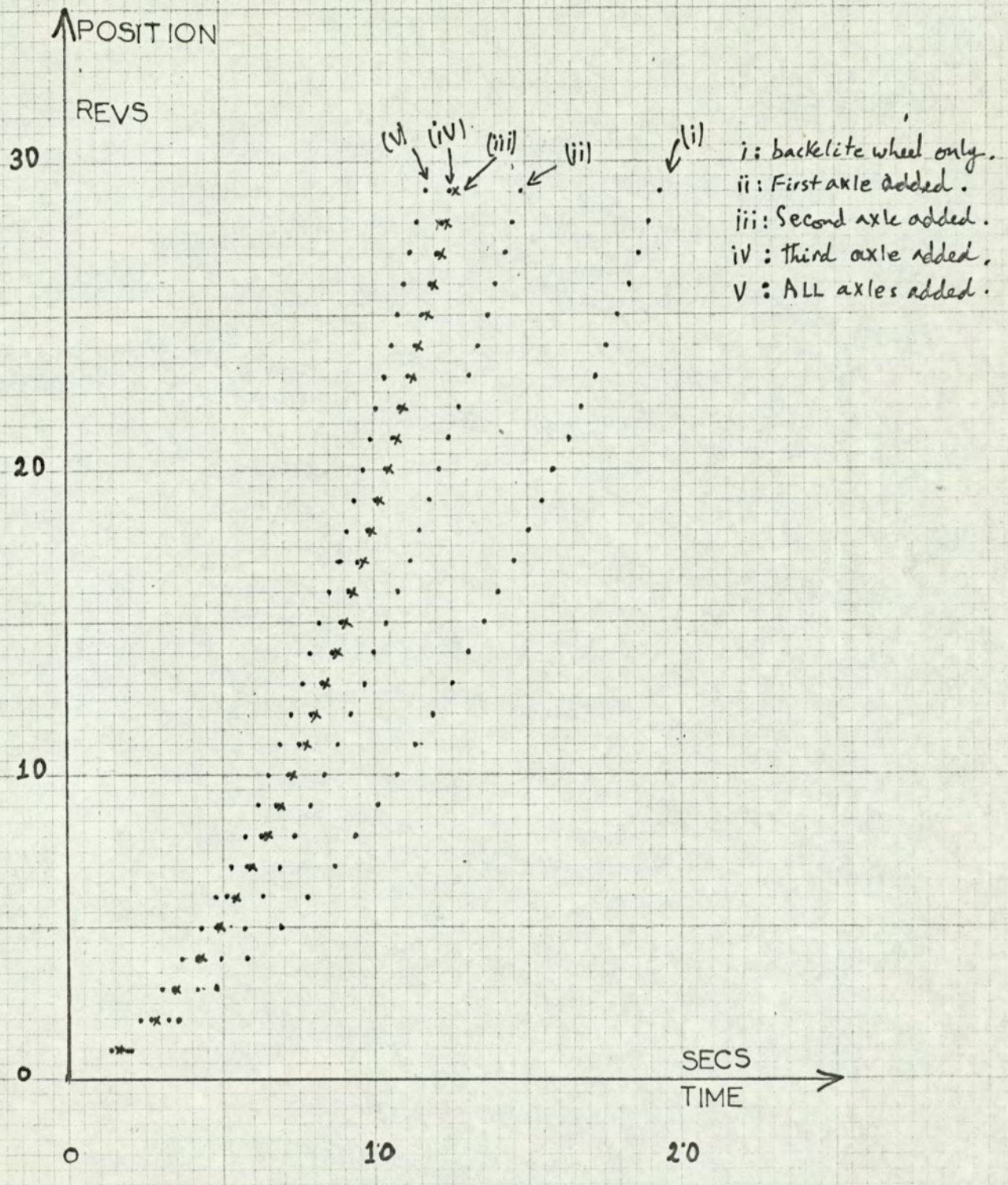

Fig. 69(a) Graph showing the effect of added gears to the amount of dynamic friction present in the gear train, for a dial counter

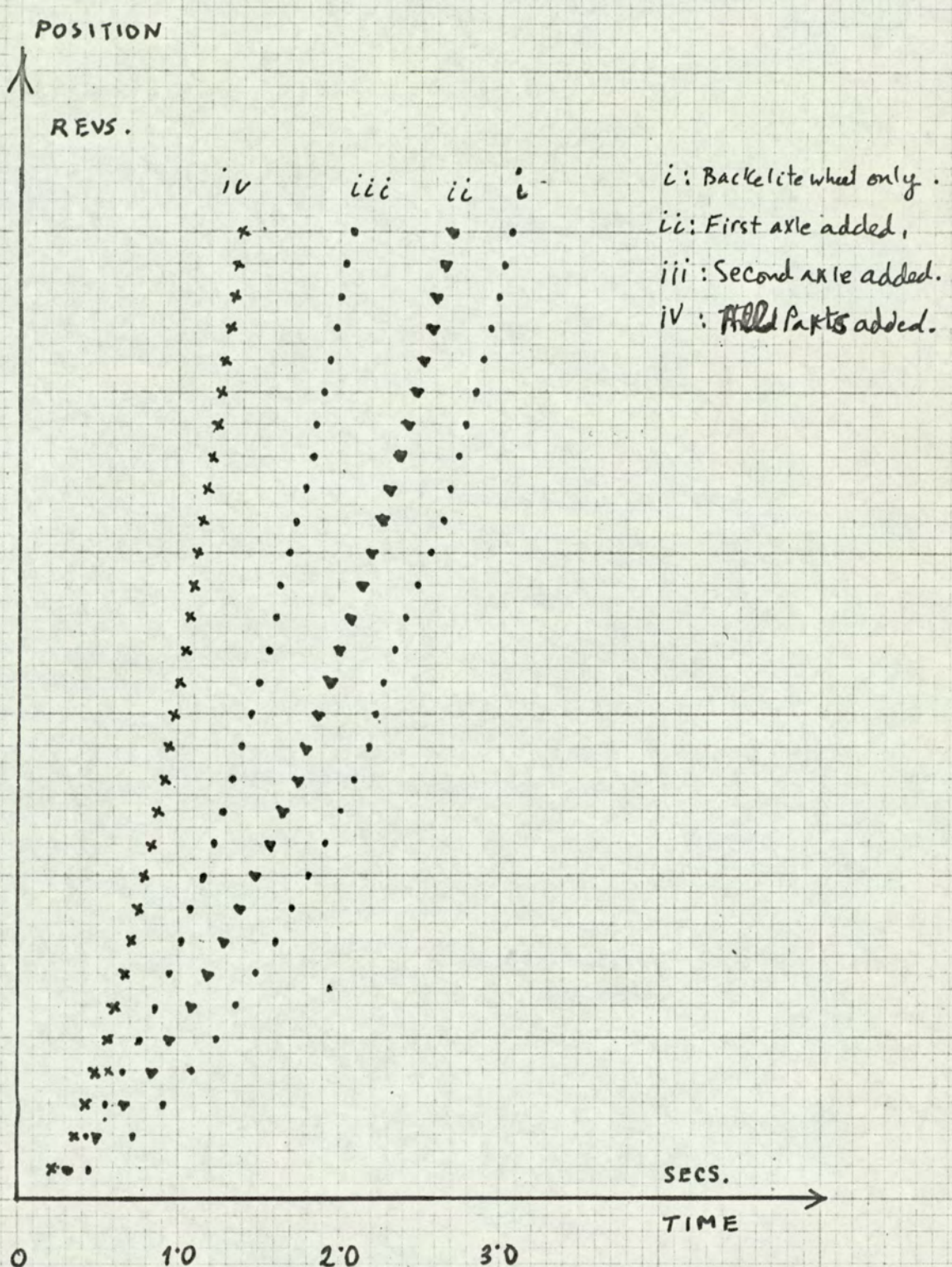

Fig.69(b) Graph showing the effect of added gears to the amount of dynamic friction present in the gear train, for a jump counter.

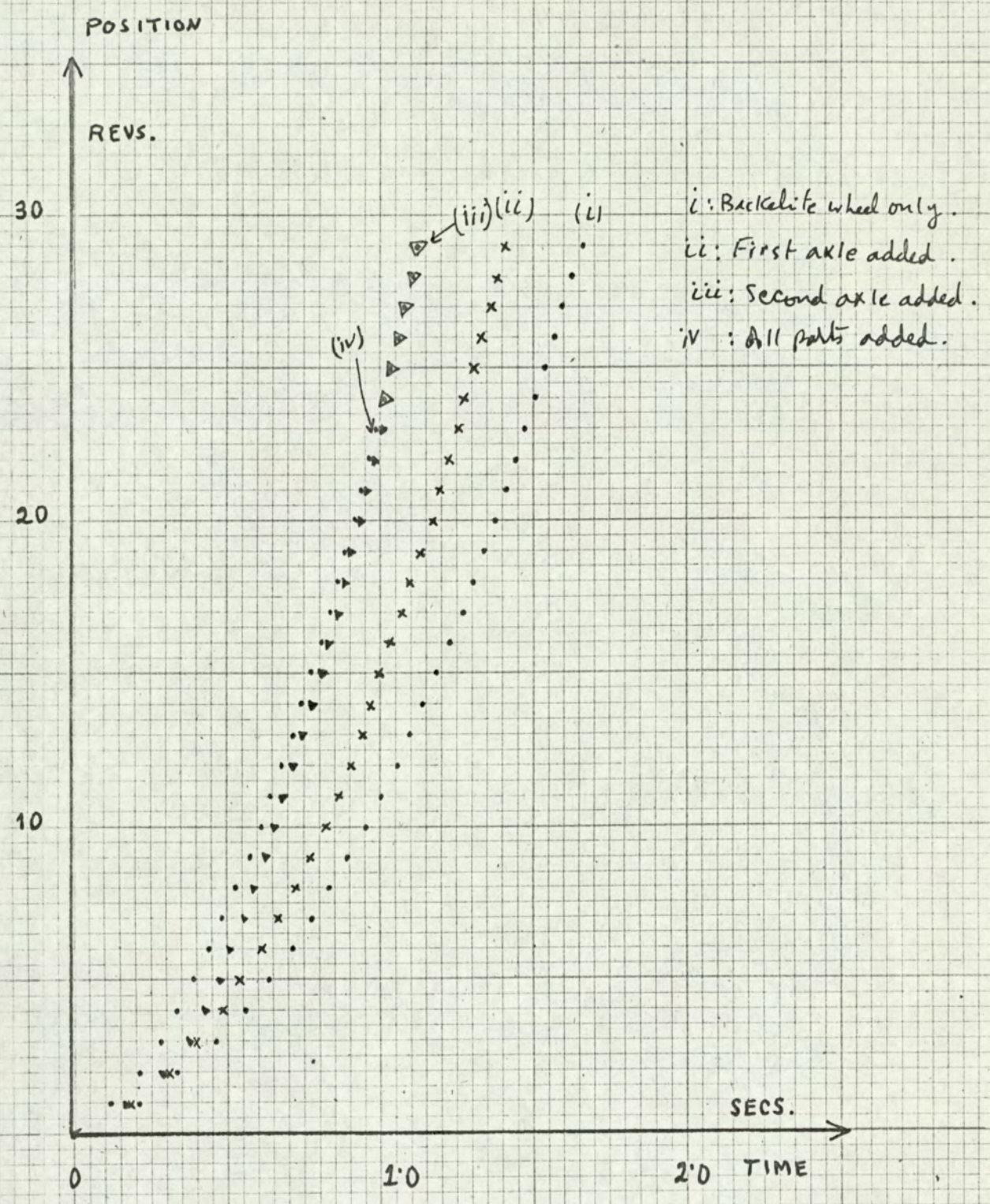

Fig.69(c) Graph showing the effect of added gears to the amount of dynamic friction present in the gear train, for a Roller counter.

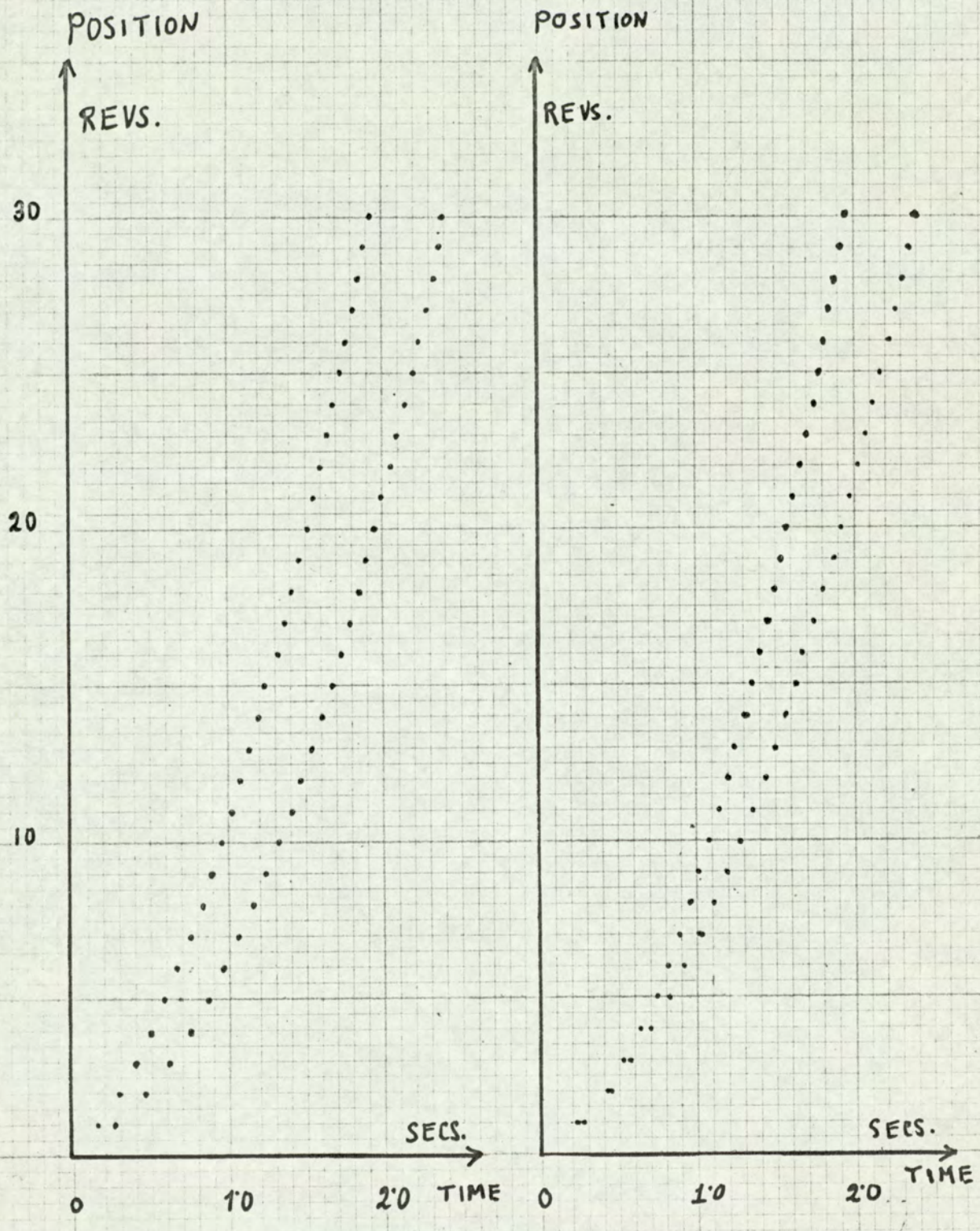

Fig.70(a) Graph showing the spread of dynamic friction for four dial counters.

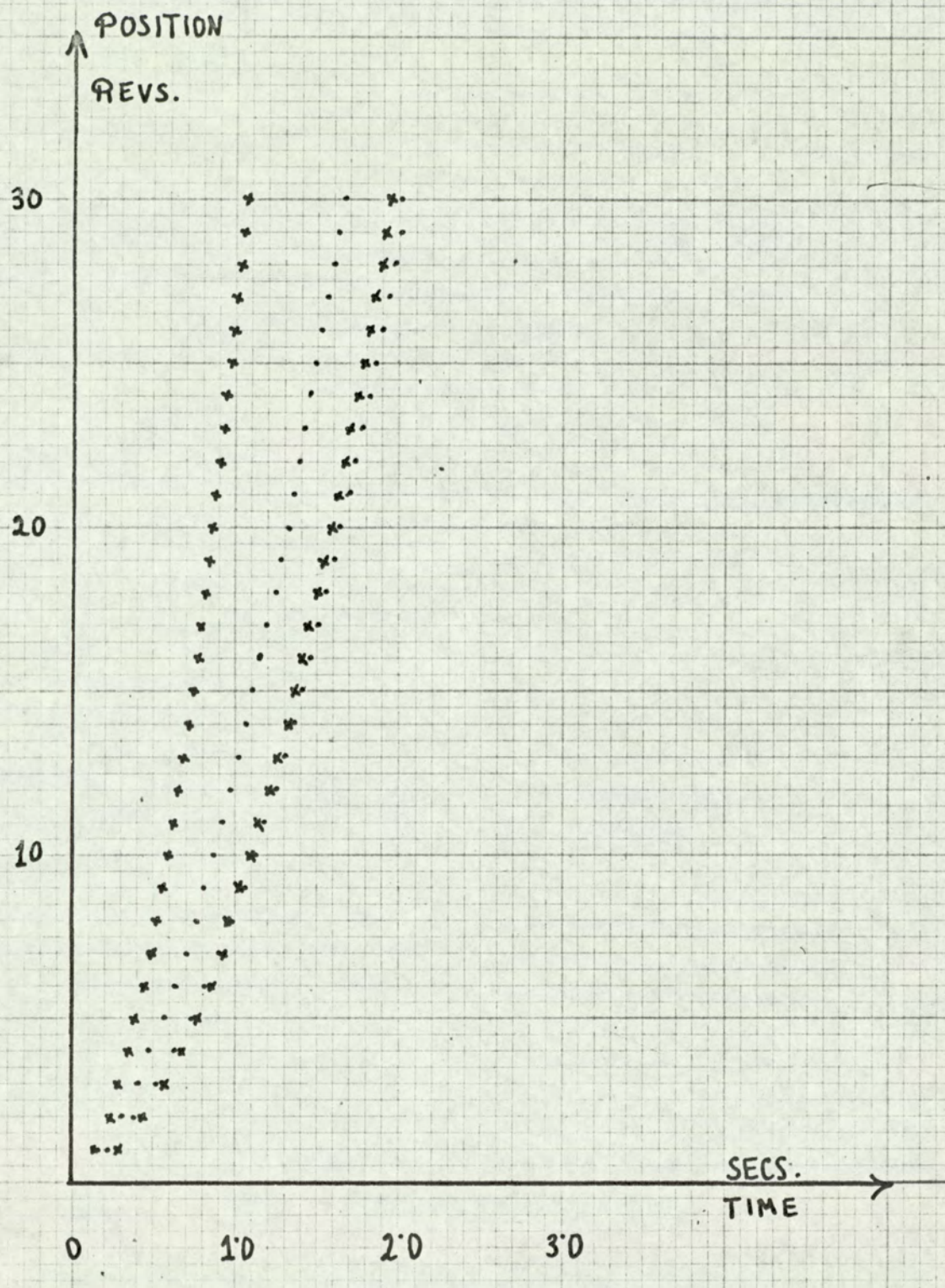

Fig.70(b) Graph showing the spread of dynamic friction for four Jump Counters

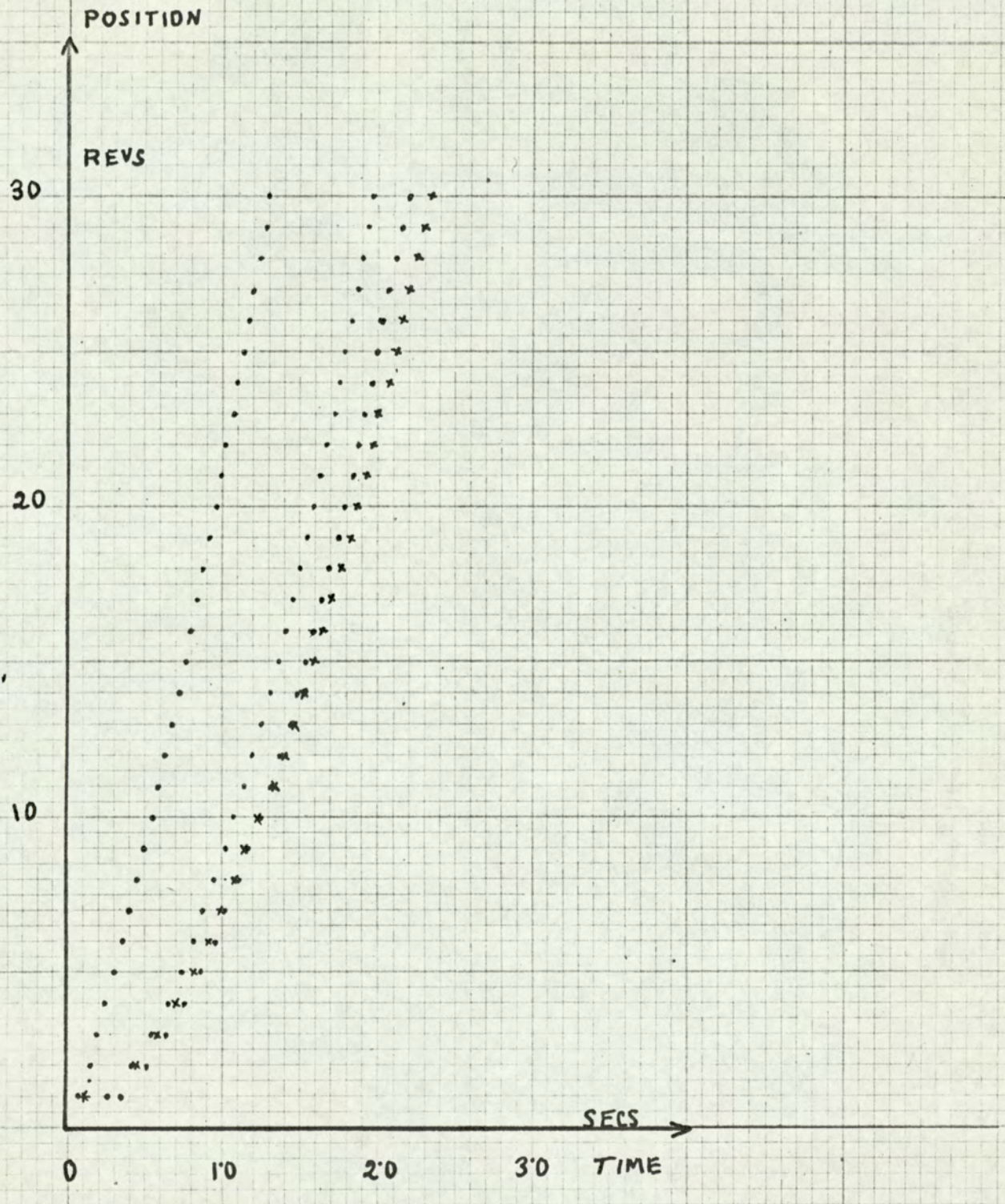

Fig.70(c) Graph showing the spread of dynamic friction for four Roller Counters

5.6 The description of an instrument for testing Electric Meter Registers. (66) *

An instrument which takes into account the factors discussed in 5.4 (1,2,3,and 4), is described. Fig.71 shows a block diagram of the instrument. A regulated air supply controlled by a three way solenoid valve is used to drive, through suitable nozzles, a number of meter registers. One of these registers is a counter which has a minimal amount of friction and is used as a standard for comparison. When the air supply is applied, each revolution of the standard is detected by a photo-electric system, which produces a pulse per revolution, these are fed to a count down electronic counter which is set to a certain count, and when the count is over it actuates a relay which in turn controls the solenoid valve and stops the air supply. The registration of the counters under test are compared with the standard and are accepted if they lie in a certain specified band.

The air pressure is adjusted to a value, such that the wheel will not be driven if the counter has a value of stiction greater than a prescribed value. The speed of the drive is also chosen, such that, the bearing of the bakelite wheel will not be damaged if driven at that speed. Tests have shown that the instrument is capable of detecting the quality of a counter in a time of the order of three minutes.

* The system based on an idea of D.Karo, Dr.es Sc., Dr.Eng., Ph.D., B.Sc., Dipl.Eng., C.Eng., F.I.E.E. was undertaken by Mr.A.K.Bhowmick as part of his M.Sc. project in Precision Measurement and Instrumentation.

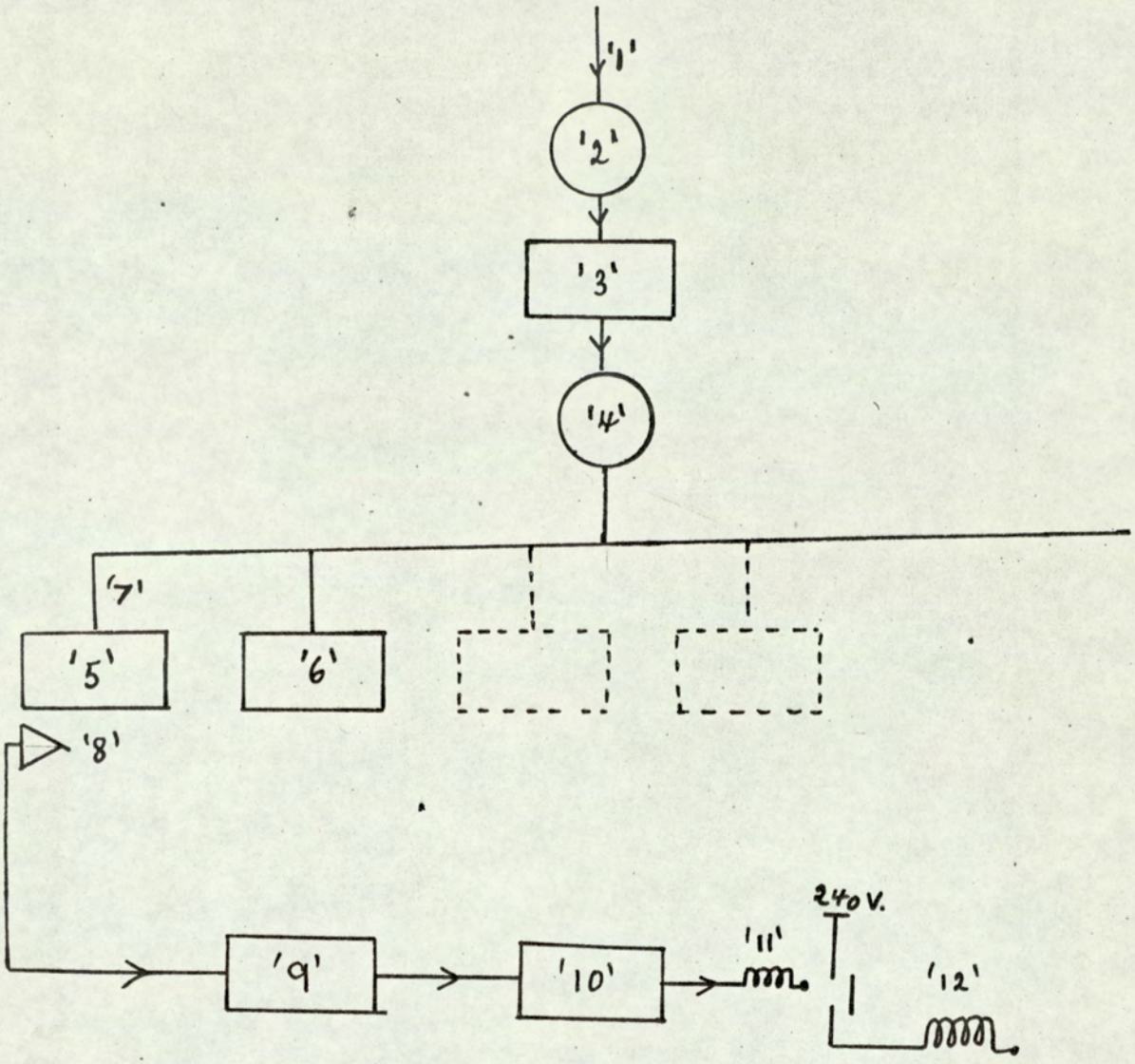

Fig.71. Block diagram showing an instrument for testing Electric Meter Registers.

1. Air Supply.
2. Valve.
3. Air Regulator.
4. Solenoid valve.
5. Standard counter.
6. Counter under test.
7. Nozzle.
8. Photo-detector.
9. Counter.
10. Switch.
11. Relay.
12. Solenoid.

THE DESIGN OF AN INSTRUMENTATION SYSTEM FOR THE CALIBRATION OF SINGLE PHASE INDUCTION TYPE ENERGY METERS

6.1 Introduction (67)

In any calibration technique, the accuracy is assessed relative to the primary standards, this accuracy is reduced whenever intermediate steps separate the standards and the calibration process. In meter calibration two main sub-standards are used;

i) A dynamometer wattmeter, which can be calibrated against D.C. standards to an accuracy of about $\pm$ 0.1%.

ii) A rotating sub-standard, this being calibrated against a wattmeter and stop watch, has a lesser accuracy, of about $\pm$ 0.245%.

It is clear then that the 'time-power' method of calibration, is inherently more accurate than the comparison method, its main disadvantage being the need of very stable supplies, having a stability of few parts in ten thousand. The comparison method suffers, in addition to reduced accuracy, from some difficulties associated with that particular method, rendering it a less accurate and a more expensive method of calibration. The main difficulties being;

a) The cost of accurately dividing the disc of the rotating sub-standard, and the difficulty and cost of detecting the pulses.

b) The need of frequent calibration of the rotating sub-standard.

c) A misleading display of error can be obtained at low loads, due to the non uniform speed of the disc.

d) The necessity of a standard for each meter type, or the need of expensive current transformers.

The main advantage of the comparison method being that supplies with regulation of the order of 0.1% are acceptable.

6.2 A proposed design of the system

The 'time-power' method of calibration was chosen as basis for the system. The main aims of the design were;

1) Conformity with B.S. regulations.

2) Reduction of personal and systematic errors.

3) Economic factors;

   a) Reduction of the time required for calibration per meter;

   b) Aiming for simple reliable design, using a minimal of components;

   c) Ability to use the system to calibrate a range of meters having different load capacities.

A block diagram of the electronic part of the proposed system is shown in Fig.72. A crystal oscillator provides a suitable time standard. The frequency of the standard being determined from the knowledge of the meter constant. The type of the meter to be tested

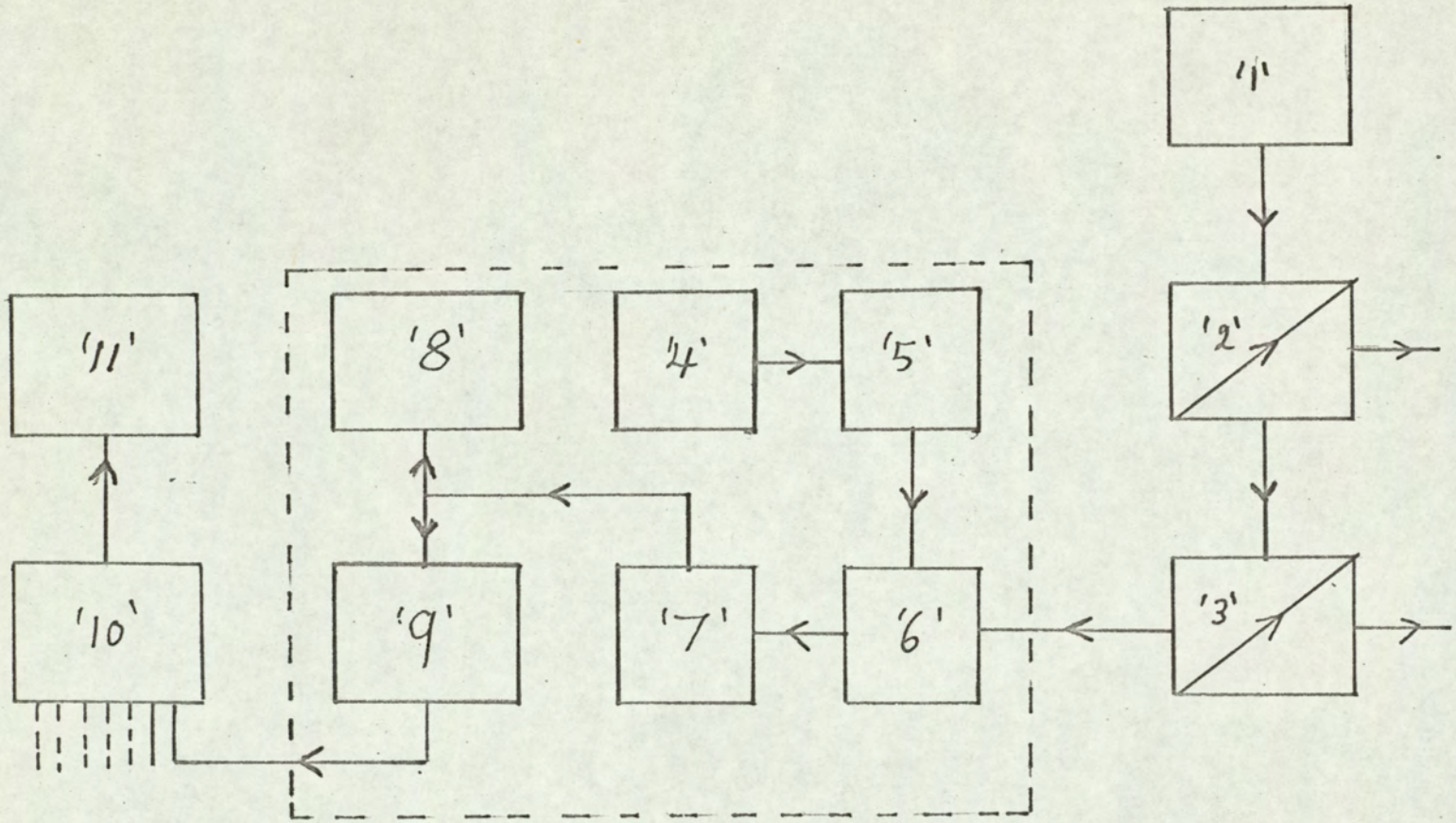

Fig.72. Block diagram showing the time standard, detector, store and display units of the proposed system.

1. Standard Oscillator
2. Meter type selector
3. Meter load selector
4. Photo-detector and shaper.
5. Sequence logic
6 & 7. Logic and counter.
8. Meter fast or slow display
9. Percentage error store.
10. Meter selector and decoder.
11. Digital display.

decides, by suitable selection, the fundamental frequency of the standard, and selects at the same time the appropriate load range. The clock frequency is further divided by suitable selection of the load selector, so as to provide 10,000 pulses for every complete revolution of the disc at the prescribed load. The load selector selects also the correct load to be applied to the meter. A photo detector, detects one revolution of the disc producing shaped pulses which are used to drive the sequence logic; This controls the sequence of the arriving pulses and can be made to provide a facility whereby the meter load is scanned automatically and the errors at each load stored, this is useful for testing meters, whilst in calibration, the meter would be adjusted continuously giving no need for an automatic scan. A counter which counts 10,000, used with associated logic and gates provides the means to produce a percentage error of the meter at a given load, and a visual display of whether the meter is slow or fast. The percentage error is stored in a store, which can be connected to a printer, or, by suitable selection, to a decoder and then a digital display. The system is intended for calibrating a number of meters simultaneously, the operator selecting the meter whose percentage error he wishes to display, this saves the need of separate digital displays for each meter.

The arrangement of the load sources and circuits must vary with the size of the establishment and the method of calibration.(68,69,70)

The 'time-power' method imposes very stringent requirements on load stability, this can be implemented by using feedback electronic stabilisers. Gynne [71] and Patchett[72] describe such stabilisers, where a stability of the order of one part of Ten Thousand or better was achieved. There are nowadays systems, available in the market, with the load capacities up to 2.5 KVA, regulation accuracy of $\pm$ 0.01% and a response time varying from 0.1 seconds in conventional regulators to 50 μ.s in electronic regulators.

Fig.73 shows a block diagram of the proposed system for a regulated voltage, current and power factor supply. It comprises of a voltage stabiliser, the output voltage of which is detected and an error signal, amplified electronically, adds or subtracts to the supply voltage keeping it constant. This stable voltage drives a suitable transformer which has a voltage winding, this being used to energise the voltage coils of the meters under test and the sub-standard wattmeter; it provides also a reference voltage signal; The transformer has also a multiple low voltage high current side, the meter type selector selects the appropriate tapping for the meter range. A current derived from the transformer feeds the watt-meter series coil and the series coils of the energy meters under test, the current passes also through a temperature independent resistor, the correct value of the resistor being chosen by the load selector, this provides a voltage proportional to the current, this

Fig.73. Block diagram of the proposed system for voltage, current and phase regulation.

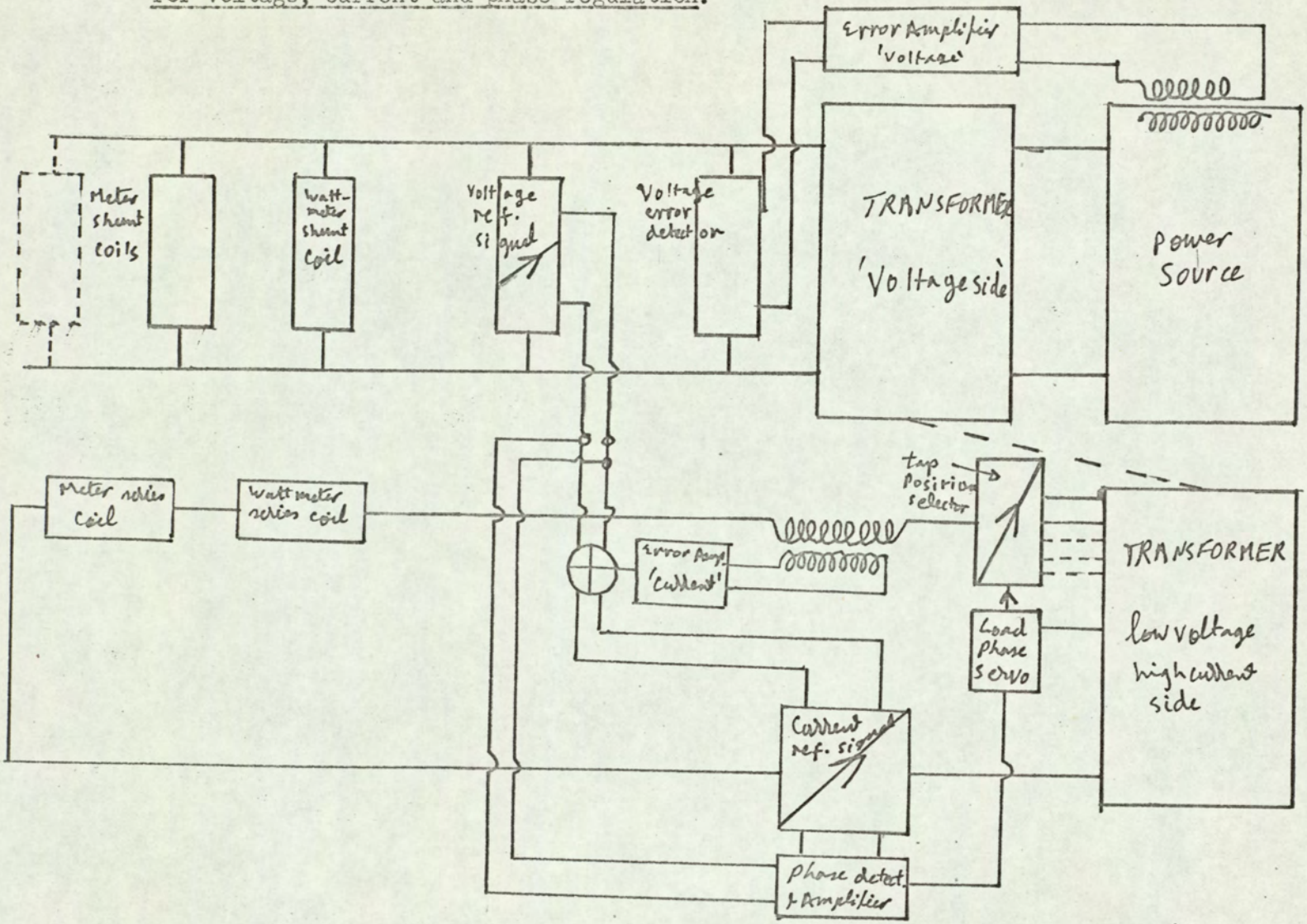

is compared with the reference voltage and an error signal derived, which, after being amplified by an electronic amplifier, adds or subtracts to the low voltage supplying the current, keeping the value of the currents constant. The voltage and current reference waveforms are also used to provide a signal proportional to the phase difference between them. This is used to drive a suitable servo which shifts the phase of the current to produce 0.5 p.f. lag. behind the voltage when such a load is selected. Hence, by the use of such a system, stable voltage, current and power factor are obtained.

The 'time-power' method needs also an accurate indication of power. The indication must be near the operator so that he notices any deviation of the value of power from the nominal value. The usual instrument used is the dynamometer wattmeter. Alternative and accurate ways of measuring power exist;

i) An electrometer can be used to measure power, this has less transfer errors and a null position technique can be used. Choudhury and Bhattacharyya [73] describe such a technique where, the a.c torque is counter balanced by a d.c. torque; this can be made automatic and a digital display can be used to give a reading proportional to the power.

ii) Schotter and Hawkes A.C./D.C. comparator [74] can be modified and used.

iii) A three voltmeter or a three ammeter method, using thermo-couples as elements, and a digital display would also be an alternative.

6.3 Consideration of the optimum number of meters to be tested simultaneously.

In calibration, there is a choice between calibrating;

a) One meter at a time;

b) A number of meters simultaneously.

The two main factors in such a choice are, the time of calibration per meter, and the cost of calibration per meter.

i) The cost of calibration per meter

For, n meters to be tested simultaneously, the equipment needed, based on a system similar to the one proposed, would basically be;

1) Supplies and regulators of suitable capacity.

2) Load selectors and switches.

3) A crystal clock and dividers.

4) A digital display, decoder and selector.

5) N, detectors, amplifiers, counters, logic and stores.

If item (5) is assigned a cost weight 'm_1' and items (1, 2, 3 and 4) a cost weight of '$c_1\ m_1$'. The total cost of the system calibrating n meters at a time,

$$= n\ m_1 + c_1\ m_1, \quad \ldots\ldots \quad (30)$$

the cost per meter would be,

$$= m_1 \left(1 + \frac{c_1}{n} \right) \quad \ldots\ldots \quad (31)$$

c_1 is estimated to be of the order '10'. A graph showing the cost per meter, scaled to units of m_1, plotted against

the number of meters, is shown in fig.74.

ii) The time of calibration per meter,

If we consider a normal calibration process using equipment similar to that described before, the time of calibration can be broken down to its constituent components.

Let, t_1, be the time taken for placing a meter in position and removing it.

t_2, be the time taken for a full load test of one revolution.

t_3, be the time taken for a single adjustment.

t_4, be the time taken for the selection and display of meter error.

1, be the average number of times an adjustment is set

An estimate of the total time, T_t, taken for adjusting and calibrating n meters can be made.

$$T_t = nt_1 + 1 \cdot 3\, n(t_3 + t_4) + 126\, t_2 \quad \ldots\ldots \qquad (32)$$

this assumes tests at full load, 0.5 power factor full load and at 1/60 of full load.

The time of calibration per meter will be given by;

$$= t_1 + 31\,(t_3 + t_4) + \frac{126\,1}{n}\, t_2 \quad \ldots\ldots \qquad (33)$$

Substituting in the equation, estimates of the unknown based on experience in calibration and observations, A graph of, time of calibration per meter, in units of 25 seconds,

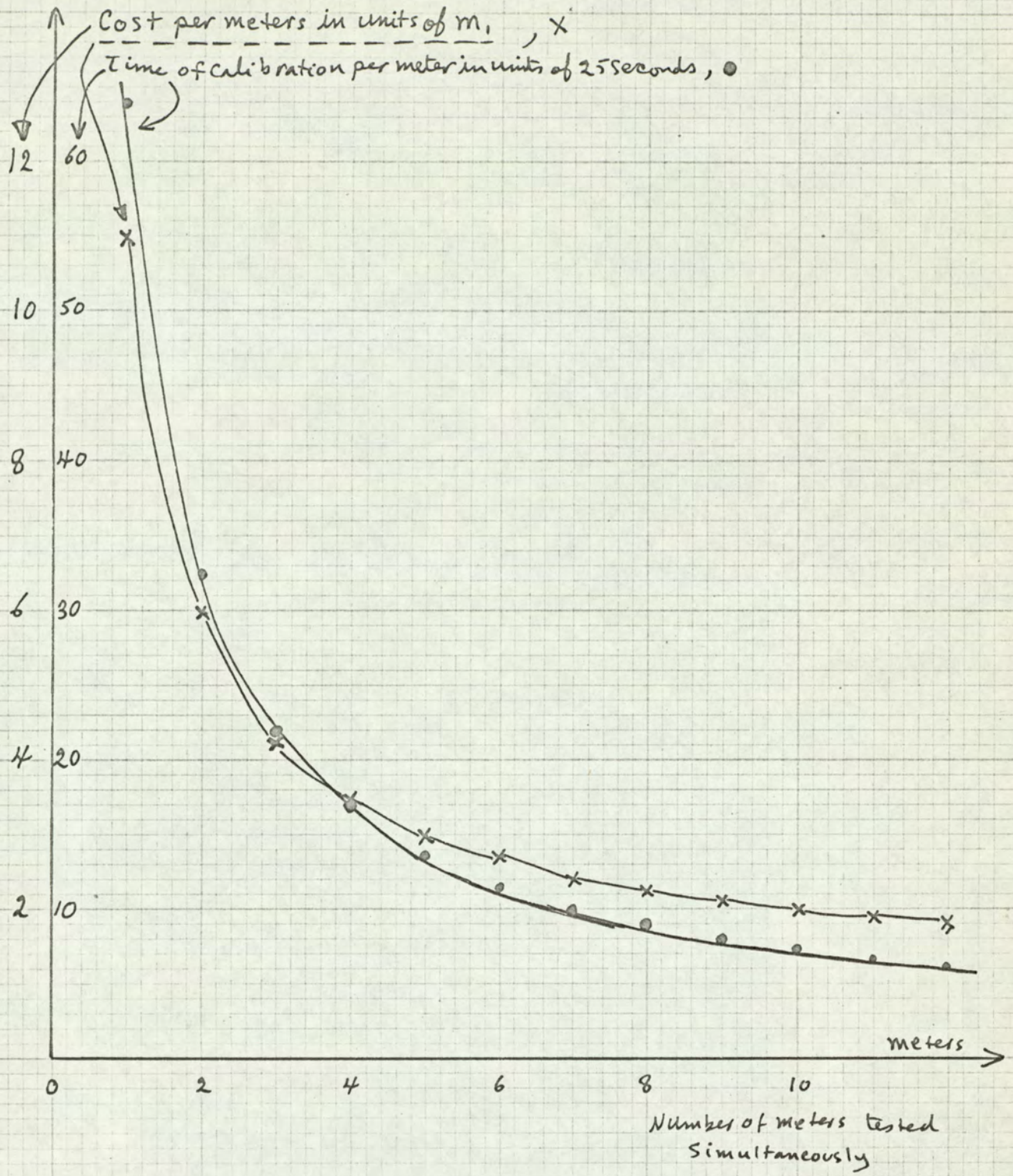

Fig.74 Graphs showing plots of,

i) Cost per meter in units of m_1.

ii) Time of calibration per meter in units of 25 seconds. against number of meters tested simultaneously.

against the number of meters calibrated simultaneously, can be plotted. This is shown also in Fig.74.

The graphs of Fig.74, indicate that the optimum number of meters calibrated simultaneously would be in the region of 8 - 12 meters, as the curves tend to flatten out after that. A group of 10 meters with constants of 1200 rev/K.Wh. 5A. Full load, would require about 3 minutes per meter for calibration.

6.4 The Design and Construction of a Prototype System

A prototype system with facilities for calibrating one meter only was designed and constructed. It consisted of two main parts;

a) An Electronic Section:

This resembles the proposed system and it was constructed using mainly the Mullard OMY range of integrated circuits, (OMY 126, J.K.flip flops and OMY 122 double gates). The main constituents of the section were:

1) The Photodetector, amplifier and Shaper: The passage of the black spot on the disc is detected by a photodetector; the circuit is shown in Fig.75. The light source used was simply a 2 volt bulb, which shines a beam of light on the edge of the disc, without the need of focusing. A phototransistor, used as a diode, detects the passage of the black spot, the pulse derived is amplified and used

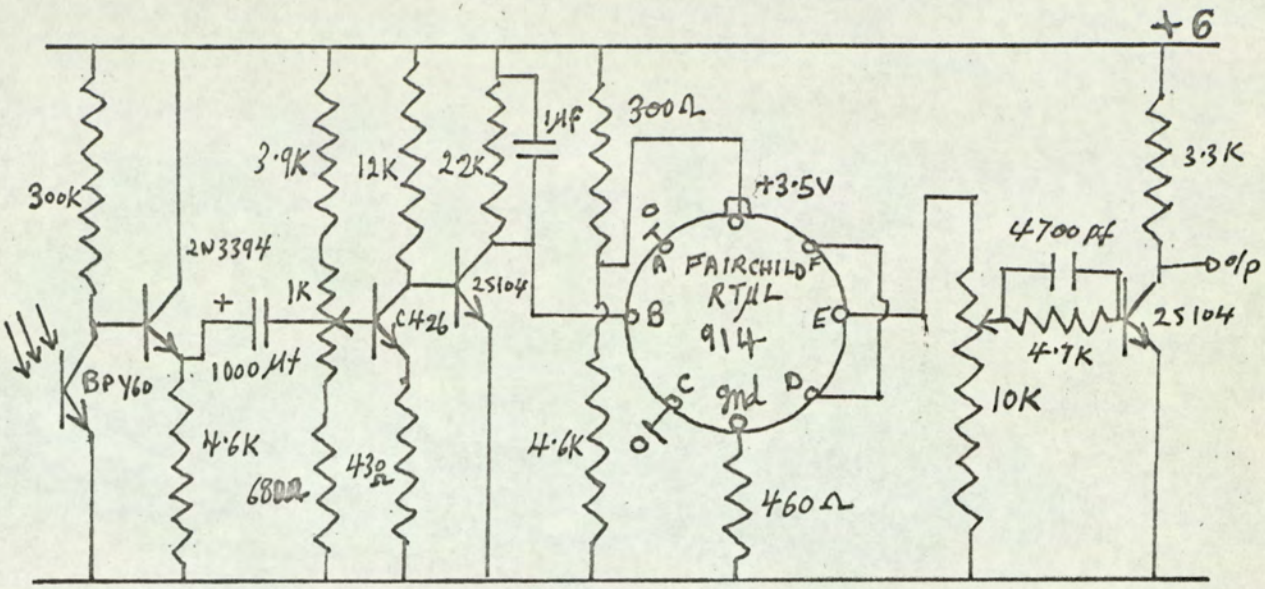

Fig.75 Circuit of the photodetector, amplifier, schmitt trigger and shaping network.

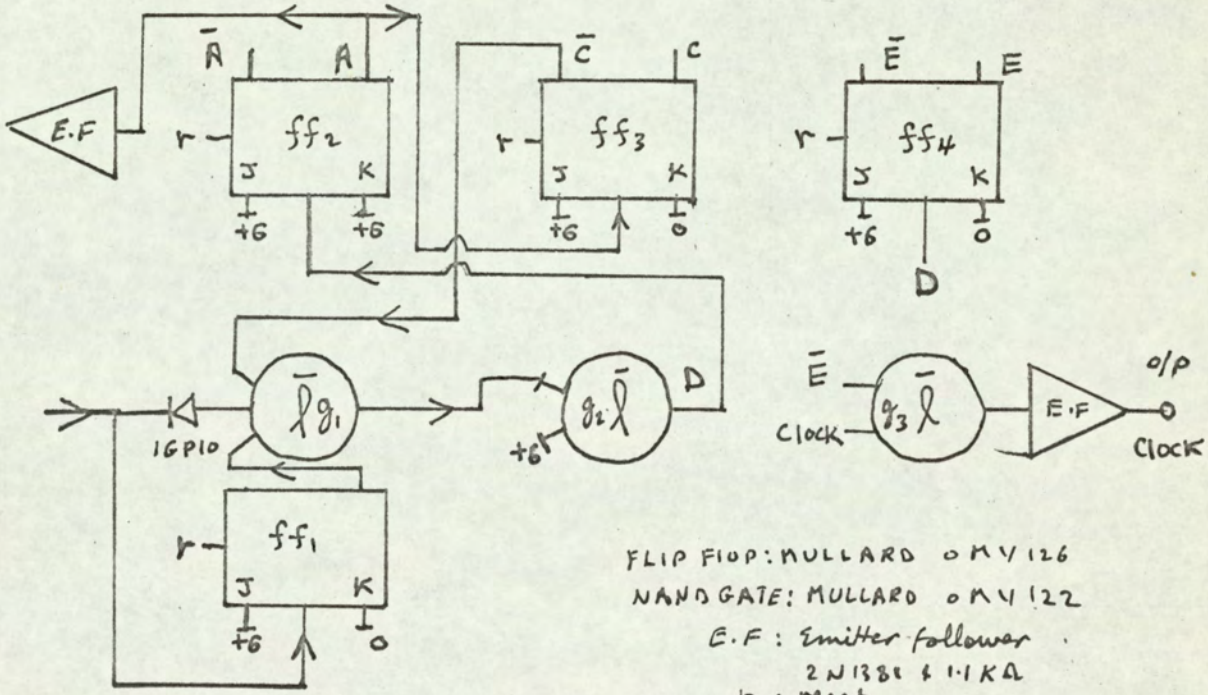

Fig.76. Functional diagram showing the sequence logic control.

to trigger a schmitt trigger, which was made from a double gate (Fairchild RT μL 914) and suitable resistors. The detector was designed so that it ignores any pulses due to irregularities on the edge of the disc, and to respond only to the black spot. There is also an amount of noise due to the 50 c/s pick-up, and to background light (fluorescent), the effect of these noises have been eliminated by the choice of a proper width of the schmitt trigger. The output of the schmitt had to be suitably shaped so as it could drive the Mullard OMY range of integrated circuits.

2) The sequence logic Control: A functional diagram of the arrangement is shown in Fig.76. The first pulse arriving from the detector, is not transmitted; but it triggers the latch flip flop ff_1, this opens gate g_1 allowing the second pulse to pass through and to trigger ff_2 producing thus a 'start' command, this also triggers ff_4 which is a latch flip flop controlling, through gate g_3, the transmission of the clock pulses. The third pulse is passed through triggering ff_2 and producing the 'stop' command, this triggers ff_3 which closes gate g_1, stopping thus any subsequent pulses from being passed through until the system is re-set.

3) The time standard and dividers: A Marconi crystal oscillator (F 3170-05, 16 K c/s medium stability) was used as a time standard it had an accuracy of the order ± 0.01%. A shaping circuit had to be used to make the waveform suitable for driving the OMY range. The frequency was divided to produce an 8 Kc/s clock pulse, which is in conformity with the speed of the meters to be calibrated. The circuit is shown in Fig.77. The frequency was divided further, and by the use of the 'Meter type selector' two fundamental frequencies of, 8 K c/s for the 10A, 40A, 80A Meters and an 4 K c/s for the 5A meters, could be selected. This fundamental frequency is taken through the 'meter load selector', as the standard clock. The selector produces clock waveforms of the following frequencies, appropriate to each meter load.

Meter load	Clock frequency for 5 amp Meters.	Clock frequency for 10, 40, 80 amp meters.
Full load	4 K c/s	8 K c/s
0.5 lag. Full load	2 K c/s	4 K c/s
1/10 of Full load	400 c/s	800 c/s
1/20 of Full load	200 c/s	200 c/s
1/60 of Full load	66.6 c/s	133.3 c/s

These are produced by suitable dividers. Fig.78 shows a functional diagram of the arrangement.

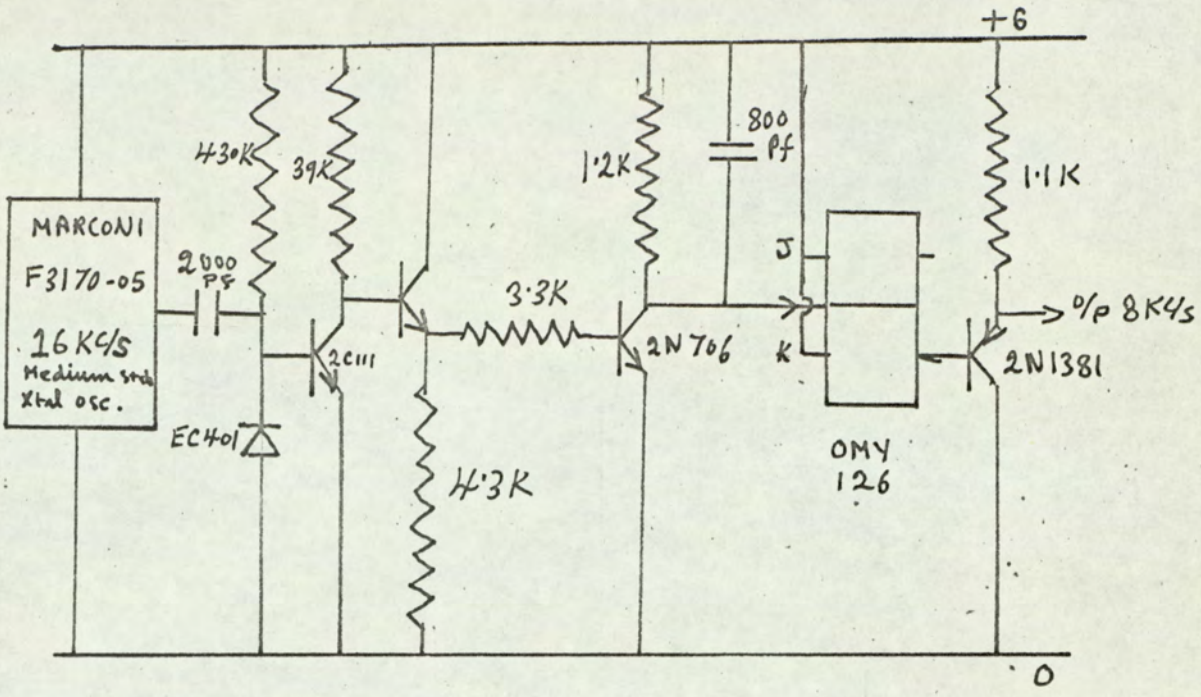

Fig.77 Circuit showing the crystal oscillator and its associated shaping and dividing networks.

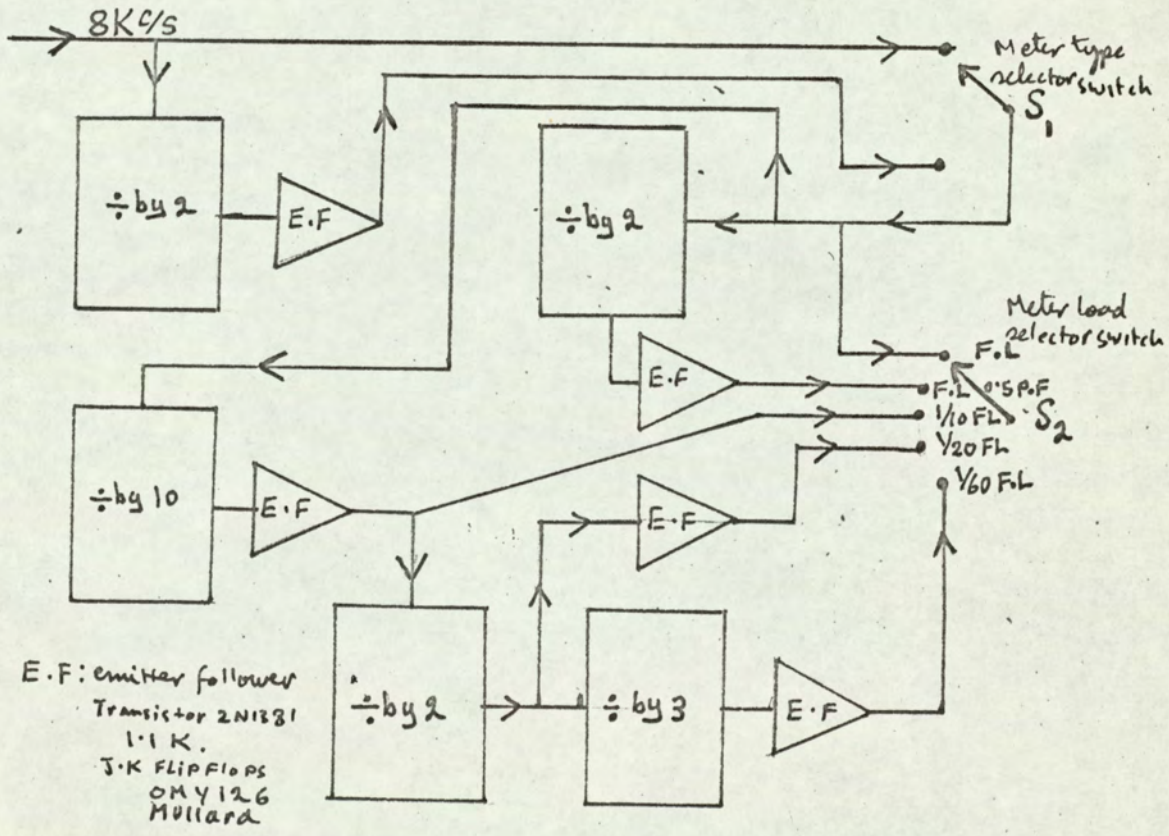

Fig.78. Functional diagram showing the frequency division of the clock waveform by the 'Meter type selectors switch' and the 'Meter load selector switch'

4) The counter, associated logic, display and store:

The functional diagram of this part is shown in Fig.79. A synchronus 'one-change' code, chain of four decade counters shown in Figs.80 and 81, is used to count 10000, this corresponds to one complete revolution of a meter perfectly calibrated at any of the prescribed loads. The initiation of the count is controlled by gate (1). This gate allows the clock pulses to enter the counter only on the 'start' command and stop them at the end of the count. Gate (2), which lets the clock pulses pass on the 'stop' command and stops them at the end of the count, determines if the meter is fast, if so, it triggers first a latch flip flop which drives a light labelled 'meter fast', and it allows secondly the clock pulses corresponding to the percentage error, to be driven to the store through an OR gate. Gate (3), which lets the clock pulses pass on 'end of count' command, and closes it at the 'stop' command, determines if the meter is slow, if so, it triggers first a latch flip flop which drives a light labelled 'meter slow', and it allows secondly the clock pulses corresponding to the percentage error to be driven to the store through an OR gate. The store which consisted of a chain of three (Fairchild cμ L 9958) decade counters, was not used, as one meter is

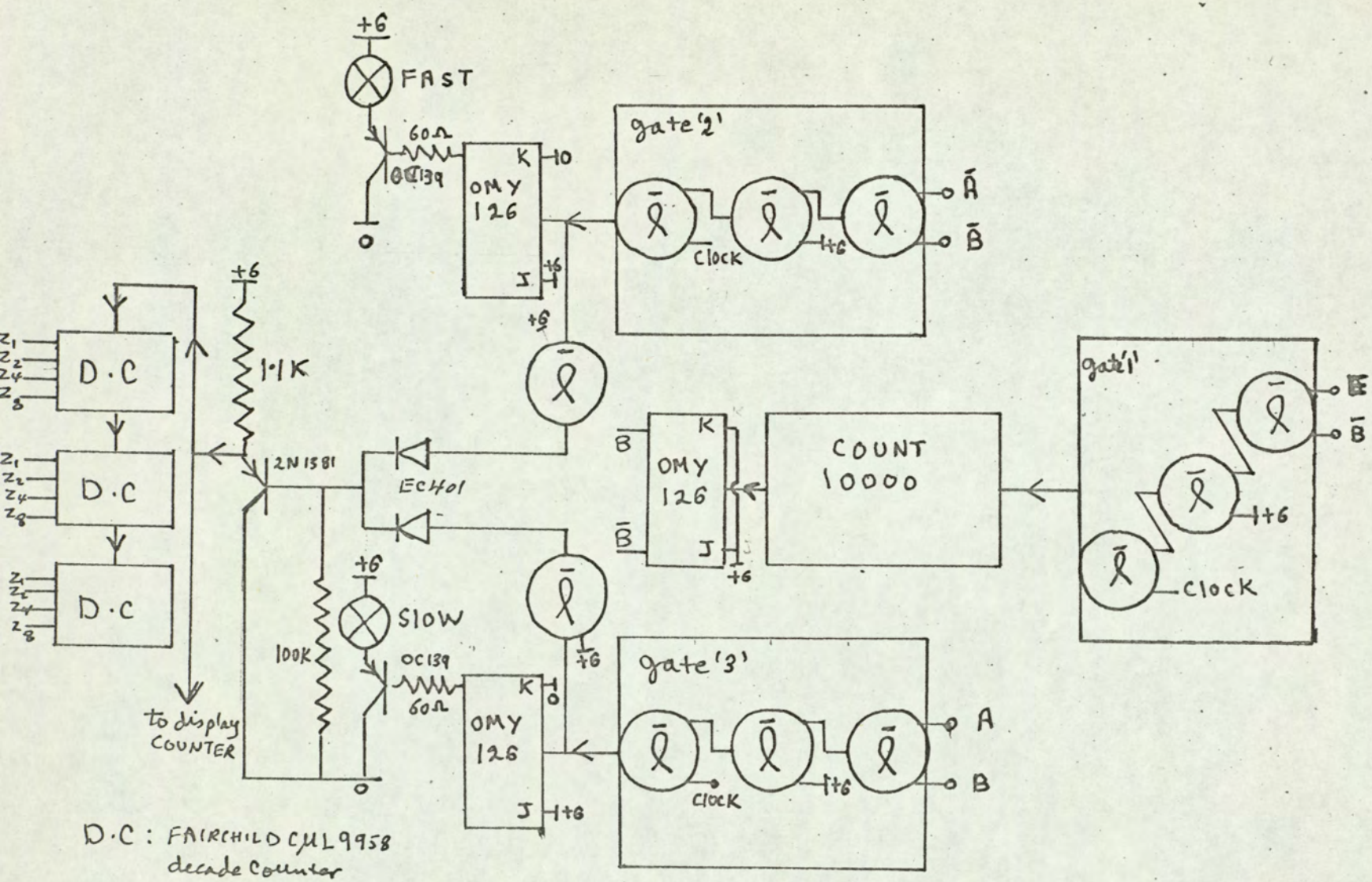

Fig.79 Functional diagram showing the counter and its associated logic, the meter fast or slow visual indicators and the stores.

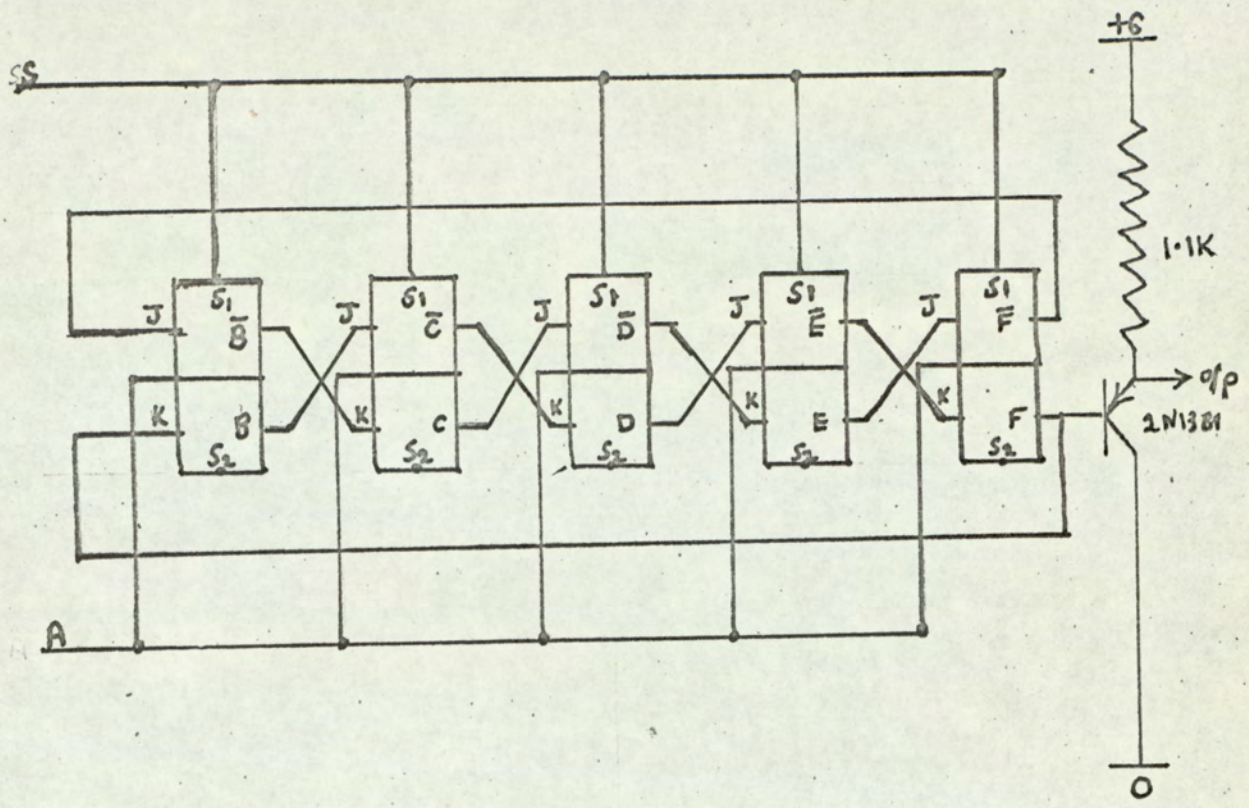

Fig.80: Diagram showing the arrangement of a synchronous "one-change" code decade up counter.

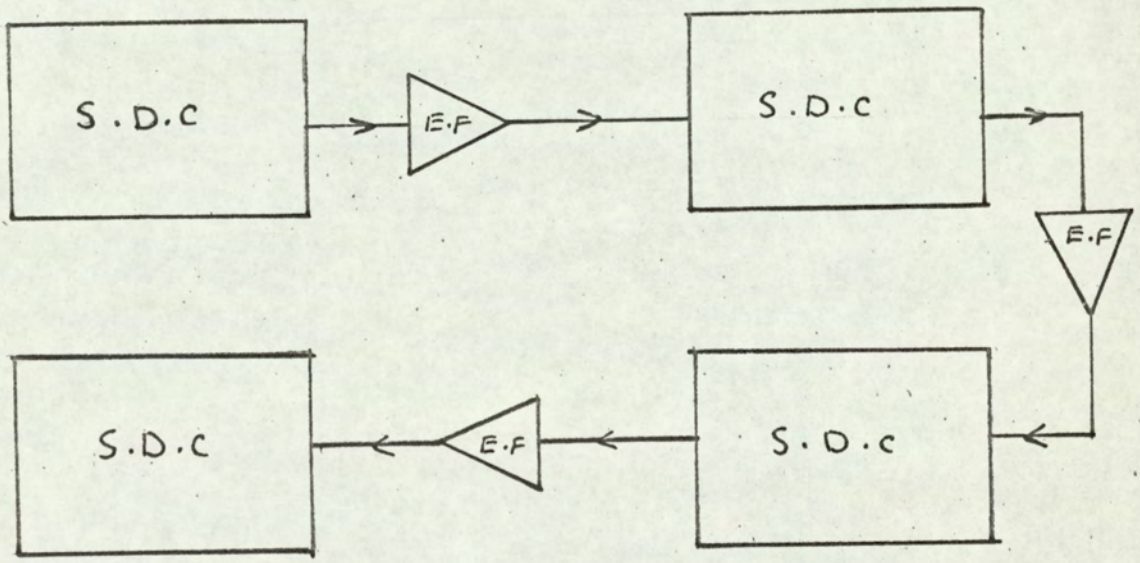

Fig.81: Diagram showing the "10000" count, up counter.

connected only, the percentage error pulses were driven into a DAWE SA 111 display counter, which displayed the percentage error to a resolution of one in ten thousand.

b) The supplies and load selection section

The supplies used for the prototype were not as specified in the proposed system, as they were intended mainly for demonstration purposes. The main parts were;

1) The supply and load arrangement: This is shown in Fig.82. The mains voltage fed through a power switch and a variac is regulated by a commercial servo regulator, which gives an output of 220 volts. This feeds a 1 KVA transformer with two sets of windings, a voltage side at 220 volts, which feeds a monitoring voltmeter, the voltage coils of the sub-standard wattmeters, and the voltage coil of the meter under test; and a low voltage high current side (8 amps max.) which was used to provide the current supply and is controlled by resistors, it feeds the current coil of the meter under test. The system is protected by appropriate fuses. The 0.5 p.f. lag is provided by a suitable combination of L and R.

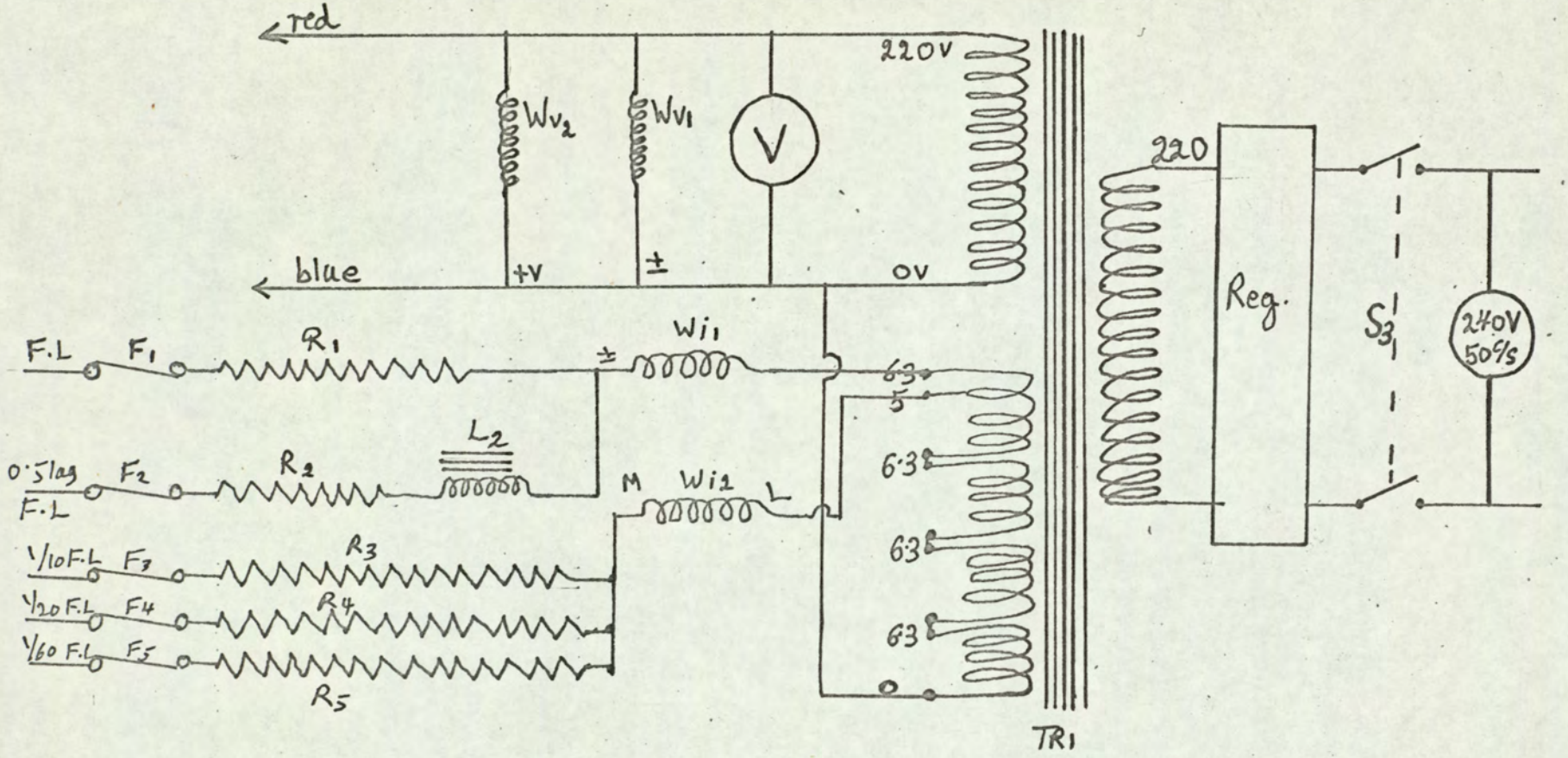

Fig.82: Diagram showing the supply and load arrangement for the prototype system

S_3 : Power switch

Reg: Variac and servo voltage regulator.

TR1: Transformer 1 KVA

V : Monitoring Voltmeter.

R_1, R_2, R_3, R_4, R_5 : Variable resistors.

L_2 : Inductor.

F_1 : 10A Fuse.

F_2 : 5 A.

F_3 : 750 MA

F_4 : 750 MA

F_5 : 500 MA

Wv_1 : Voltage coil of sangemo weston wattmeter.

Wv_2 : Voltage coil of Elliot wattmeter.

Wi_1 : Current coil of sangemo weston wattmeter.

Wi_2 : Current coil of Elliot wattmeter.

2) Internal supplies and load selection: This is shown in Fig.83, and provides the appropriate D.C. supplies, and has a number of A.C. relays which connect the appropriate current to the series coil of the meter under test, this is selected by the 'Meter load selector'.

Plates showing the prototype system are shown in Fig.84.

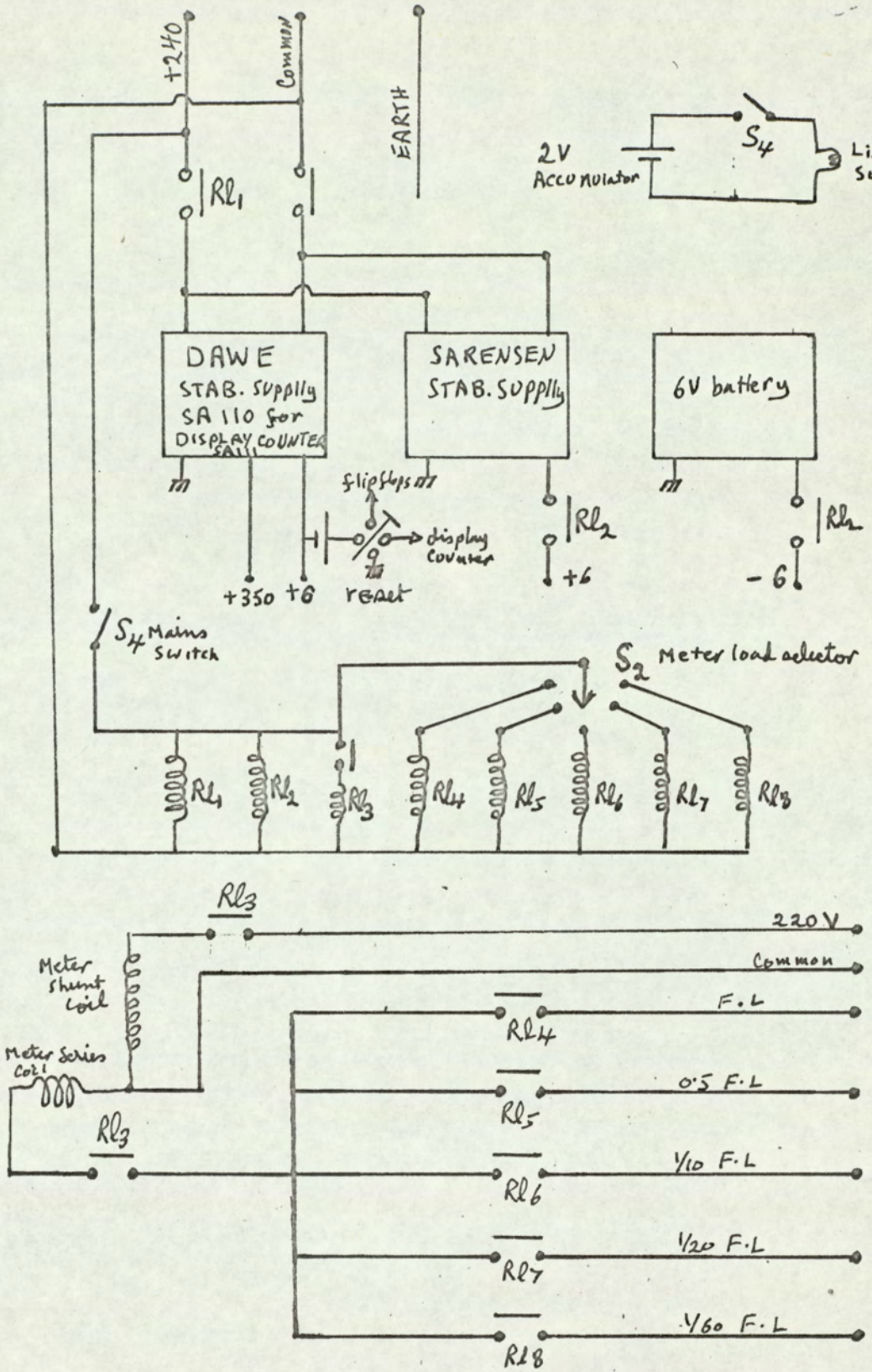

Fig.83. Diagram showing the internal supply and the load selection arrangement for the prototype system.

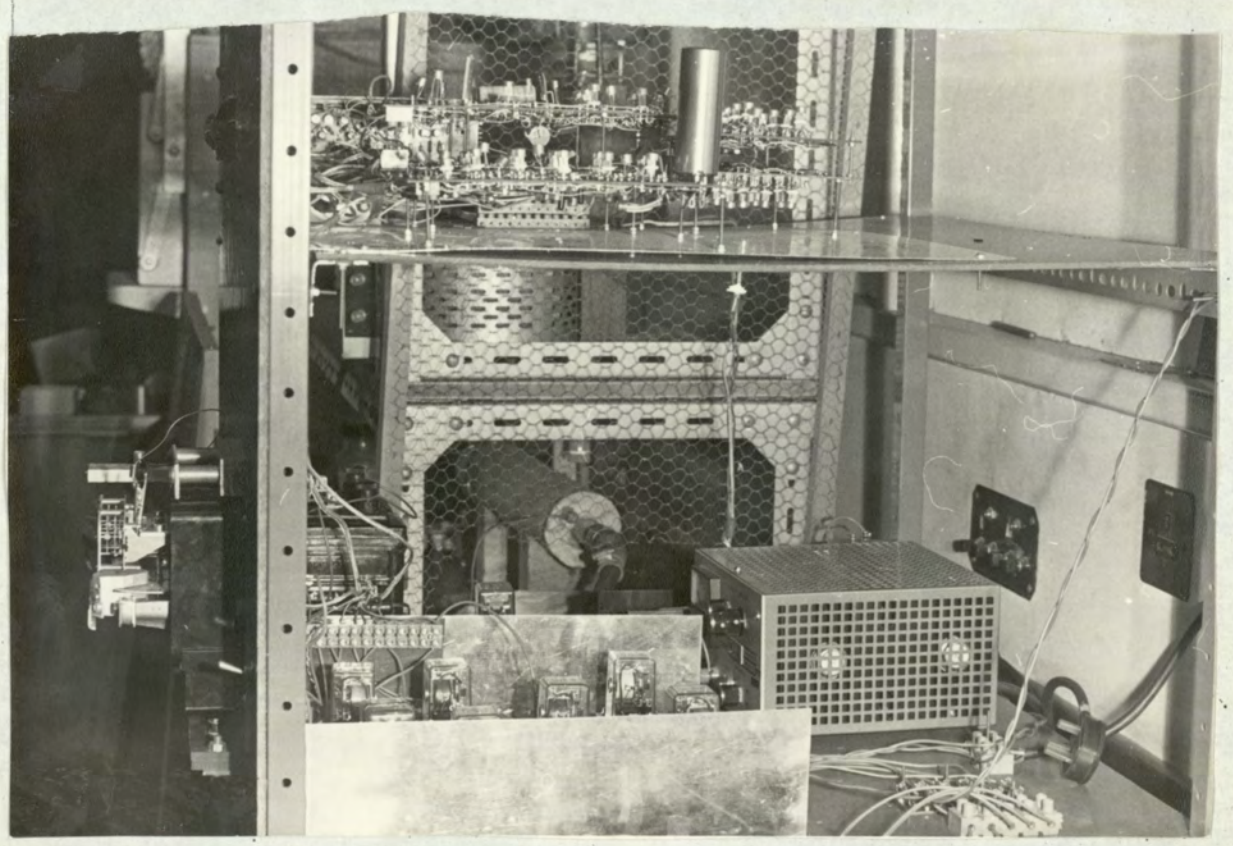

Fig.84 : Plates showing the prototype system.

7. CONCLUSIONS

The study, of the behaviour of the induction meter, conducted has led to two techniques for the calibration of the meters;

i) A low load technique, where, the percentage error of the meter at low loads (1/60 of full load) can be predicted from two observations at the higher loads (1/10 and 1/20 of full load). This leads to a reduction of the time needed for low load calibration.

ii) A phase adjustment technique, where, by using a precision phase meter to indicate the phase angle between the applied e.m.f. and the current in the shunt coil, the phase angle can be set directly to an optimum value found from a statistical study of the phase angles of calibrated meters. The technique does not require the series coil to be energised, this leads to savings in time and equipment.

The initial results were encouraging, and suggests that a further study be made on a large amount of meters, which should be calibrated using these techniques and then their errors assessed by the conventional methods.

The experiments conducted, to ascertain the cause of the cyclic variations in the speed of the disc, has led to the conclusion that this is caused mainly by mechanical and geometrical factors, and that

the creep holes play a minor part only in producing such an effect. These experiments have led also to a better understanding of the magnitude of these variations and their effect on various calibration techniques.

The instrumentation system designed was based on the most accurate method of calibrating meters; it should provide a fast and accurate means of calibration. The long period dial test has been substituted by a test on the counters themselves, speeding thus the calibration process. The study of the optimum number of meters to be calibrated simultaneously indicates a provisional figure of 8 - 12 meters.

It is hoped that the adoption of such an instrumentation system and calibration techniques would lead to a reduction in the cost of meter calibration and to an improved accuracy resulting in a lower rate of meter rejection.

APPENDIX I

A Brief review of the theories of action of the single phase induction meter

Two theories have been developed for the operation of the induction meter;[75]

i) The travelling field theory: This assumes the existence, within a well determined region of the rotor, of magnetic fields characterised by sinusoidal time variations, and by a sinusoidal distribution of their flux densities along the path described by a point on the revolving rotor. This travelling field in moving across the air gap, produces a torque in the disc.

ii) The transformer theory: This assumes the existence at well defined points in the rotor, of sinusoidally, time-variable fluxes which depend, respectively, on the voltage across the meter, and on the load current. Each of these fluxes induces currents in the rotor. These currents depend on the transformer e.m.f. as well as on the rotational e.m.f. which is proportional to the speed of rotation of the rotor, interaction between the corresponding fluxes and currents in the rotor give rise to a torque proportional to the power, a torque proportional to the speed of rotation and the square of the voltage, and one proportional to the speed of rotation and the square of the

load current. This theory was developed by Rogowski[76], in his original paper he used Maxwells equations to produce expressions describing the current distribution, the driving torque and the power dissipation in the disc. His equations are used in design [77] and referred to extensively in explaining the action of the meter.[78]

Controversy has raged, for many years, about the best theory of analysing the meter. Schotter[64] attempted to refute the rotating field theory. Barlow,[79] however, using the concept of absorbing the momentum of a travelling field as means of producing a mechanical force proportional to the power dissipated, develops a simple theory which appears to be satisfactory over a wide range of frequencies.

The induction meter undergoes a change of behaviour due to changes in voltage, frequency and temperature. Moore and Slater[80] investigated the effects of frequency variations, whilst the effects of temperature variations have been investigated by Kinnard and Faus [81] and Canfield [82].

GENERAL INFORMATION

APPARATUS:

A) Types of Electricity Meters Tested.

i) V.L.R. (very low range). type K.

1500 Rev/K.W.H.

240 V/5 A full load.

ii) L.R. (low range) type K.

1200 Rev/K.W.H.

240 V/10 A. full load.

B) Instruments used in Measurements:

1. Portable Reflecting Wattmeter No.R 578 Model 5999 Elliot (iron less dynamometer).

Accuracy 0.6% f.s.d. (6.25 watt).

This was calibrated against a D.C. Potentiometer to within its reading error.

Range	Max Reading error
0.5A	$\pm$ 0.005 watt
1.0A	$\pm$ 2 X 0.005 watt.

2. Portable Reflecting wattmeter No. R 404 Model 5999 Elliot (iron less dynamometer).

Accuracy 0.6% f,s.d. (62.5 watt)

This was calibrated against a D.C. Potentiometer to within its reading error.

Range	Max. Reading Error.
0.5A	$\pm$ 0.05 watt.
1.0A	$\pm$ 2 X 0.05 watt.

3. Sangemo Weston A.C/D.C. lab. standard wattmeter.

No.A077270 Model S91. (electrodynamometer).

Accuracy 0.1% f.s.d. (1.5 k.w.)

Range	Max. Reading error
1.5 K.W.	$\pm$ 0.5 watt.

4. Sangemo Weston A.C/D.C. Voltmeter.

No.A077266 Model S92. (electrodynamometer).

Accuracy 0.1% f.s.d. (300 V)

Range	Max. Reading error
300 V	$\pm$ 0.1V.

5. Marconi Counter/Frequency Meter type TF.1417 No.25135/068

Accuracy time interval $\pm$ 0.1 μs $\pm$ stability

Stability Short term : 2 parts in 10^7

Long term : 3 parts in 10^7

6. Ultra Violet Recorder S.E. Labs. Type SE 2000.

Freq. response of galvo. up to 400 c/s.

Paper speed accuracy $\pm$ 2%

7. Advance Voltstat type CVS.

Output voltage stabalised to within $\pm$ 1% of the adjusted value for a variation of $\pm$ 15% of input voltage.

8. Claude-Lyons automatic voltage stabaliser type T.S.IR. Mk.III

Output voltage stabalised to $\pm$ 0.5% of adjusted value.

REFERENCES

1. Recent Developments In Electricity Meters with Particular Reference to those for Special Purpose.
J.L. Carr. J.I.E.E., Vol. LXV11; P.859.

2. Integrating Electricity Meters.
E. Fawset. J.I.E.E., 1931, Vol.69, P.545.

3. The History and Development of the Integrating Electricity Meter.
A.E. Moore, J.I.E.E., Vol.LXXV11, P.851.

4. Grid Metering.
J. Henderson, J.I.E.E., Vol.LXXV, P.185.

5. Electrical Measuring Instruments.
J.I.E.E. 1937; Vol.80, P.190-206.

6. Standarization of Integrating Electricity Meters.
C.W. Bridgen, J.I.E.E., 1943, Vol.90; P.397-410.

7. Evaluation of Single Phase Metering Practice Based on Meter Performance and Load Characteristics.
J.M. Van der leck. Trans. A.I.E.E., 1958, Vol.77, Pt.1, P. 727 - 738.

8. House Service Meters.
Electrical Review,(G.B.) September 15th, 1961, Vol.169, No.11, P.415 - 419.

9. Elektrizitätszähler.
K. Engelbach, A.T.M., August 1961, V340-F_3, No.307. P. 189 - 190.

10. Meter Problems and Consumers Load Characteristics.
L.B.S. Golds, P.Schiller; Proc. I.E.E., 1953, Vol.101 Pt.II, P. 619 - 631.

11. New Sampling Technique Cuts Meter Testing Cost.
W.C. Harrison, Elec.World, July 15th, 1957, P.72 - 74.

12. The Electricity Supply (Meters) Act, 1936 - It's Legal and Technical Implications.
A. Evans, J.I.E.E., August 1941, Vol. 88, Pt.II, P.253 - 275.

13. British Standard 37 Pts.1 and 2. 1952.
Electricity Meters British Standards Institution.

14. Electricity Meters and Meter Testing.
G.W. Stubbings, 1939.
Chapman and Hall Ltd.

15. Electricity Supply Meters.
A.E.B. Perrigo,
Chapman and Hall.

16. Electricity Meters and Instrument Transformers.
S. James.
Chapman and Hall.

17. Meter Engineering.
J.L. Ferns.
Pitman.

18. Allgemeine Zählerprüfverfahren Für Induktionszähler.
K. Engelbach.
A.T.M., Jan.1957, Z 7 33-8, P.21 - 24.

19. Correction factors of Deflection Wattmeters.
D.Karo. J.O.S. Inst. Dec.1964, Vol.41, P.740 - 746.

20. Improvements in Meter Testing Equipment.
W.A. Nash, Trans. of the S.A. Institute of Engineers.
March 1956; Vol.47, Pt.III, P.77 - 96.

21. Neuzeitliche Zähler Prüfgeräte
K. Engelbach. A.T.M. August 1957, Z 733 - 739.

22. Dal Cronometro Alla Trascrizione Automatica Degli Errori
Di Un Contatore Ad Indusione.
E. Maggio. RC(63) Rium Assoc. Elettrotec. Ital. (Ischia 1962)
Fsc.II, Paper 22.

23. An Automatic Counting and Timing Mechanism for Testing Electricity Meters.
A. Felton. J. of S. Inst. Dec.1933, Vol.X, No.12, P.370 - 373

24. Un Moderno Banco Per La Taratora Ela Verifica Di Contatori Monofasi.
G. Pagliari - E. Varé - G. Venni.
R.C.(63) Rium Assoc. Elettrotec. Ital.(Ischia 1962) Fsc.II. Paper 37.

25. Photo-electric Test Table Facilitates Meter Checking.
T. Oakley. Elec. World, Dec.26th, 1942, Vol.118, P.21 - 22.

26. Watt-Hour Meters Compared by "Magic-Eye" Wink.
H.S. Bull, Elec. World, Nov.27th, 1943. Vol.120

27. A New Device for Calibrating Watt-Hour Meters.
H.F. Robison and W.H. Wickham Trans. A.I.E.E., 1950,
Vol.69, Pt.II, P. 732 - 734.

28. Automation Speeds Meter - Testing.
A.W. Rauth. Elec.World, June 13th, 1955, Vol.143,
P. 86 - 88.

29. Precision Testing of Watt hour Meters.
Elec. Times, 6th Jan. 1955, P.19 - 20.

30. Electronics Speed K. Whr. Meter Testing.
C.A. Antonelli, Elec. World, Sept 1st, 1958,
Vol. 150, P.51 - 52.

31. One - Revolution Watt-Hour Meter Testing.
N.R. Rogers. Elec. Light and Power. Aug. 1958,
Vol. 36, Pt.16, P.45 - 48.

32. Meter Testing In The Sixties.
A.J. Baggott. Elect. Times. 25th Feb.1965. P. 277 - 281.

33. Elektrizitätszählerprüfverfahren Mit Vergleichszählern Hoher Genauizkeit.
R. Fiedl. Z. Instrumentenkunde April 1963, Vol.71, No.4,
P. 102 - 107.

34. Methods and Apparatus Employed in the Testing of Single - Phase A - C Watt hour Meters.
F.C. Holtz. T.A.I.E.E. Jan.1952. Vol.71, P.61 - 69.

35. Elec. Light and Power. Dec.15th, 1954, Vol.32, Pt.14,
P. 102 - 104, 106.

36. Meter Calibration and Testing.
H.J. Lovegrove and G.E. Parkin.
Elec. Review, 22nd Sept. 1961, P.460 - 464.

37. Blathy O.T.
"Improved process of and apparatus for testing Electricity Meters" B.P. No.5319, 1915.
"Improvements in or relating to the setting of the Electricity Meters" B.P. No.173519, 1921.

38. Stroboscopic Method of testing watthour Meters.
H.P. Sparkes.
Trans. A.I.E.E. 1927, p.405 - 408.

39. Stroboscopy and the testing of Rotary Meters.
G.E. Moore
The Electrician, Aug.3, 1928. p. 117 - 118.

40. La Stroboscopic,
P. Maurer.
Revue Generale De l'Electricité
1933, Vol.34, p.79 - 80.

41. The Stroboscopic timing of rotating meter discs.
E. Bradshaw.
Journal of the Royal Tech. College, Glasgow, 1939.
Vol.4, pt.III, p.542 - 550.

42. Stroboscopic Calibration at low loads.
The Elec. Times, Jan.4, 1940.
Vol.97, p.3 - 4.

43. Meter Tables combine strobo and photo-electric.
L.D. Price.
Elec. World 1942, Vol.118, p.56.

44. Improvements in Modern Meter testing technique,
E.E. Lynch and M.A. Princi.
Trans. A.I.E.E., 1942, Vol.61, p. 218 - 223.

45. Recent Developments in Comparative Methods of Testing A.C. Electricity Meters.
S.F. Musson and R.E. Mell.
Proc. I.E.E. 1950, Vol.97, pt.II, No. 56.

46. Modern Meter Testing.
H.S. Petch.
Elec. Review, 22 April 1955. p. 653 - 656.

47. The Characteristics of Induction watthour Meters.
S. Jimbo.
Researches of the electro technical Laboratory, Tokyo, Japan.
No. 235 and 320.

48. Load curves of single phase Induction type watt-hour Meter.
P.V.N. Ramanathan.
Journal of INTN. ENGRS. (INDIA) Aug. 1963.
Vol.43, p. 306 - 322.

49. The Mean error of an Electricity Meter.
G.W. Stubbings.
J.I.E.E. 1921, Vol.59.
p. 335 - 338.

50. A Study of the induction watt-hour meter, with special reference to the cause of errors on very low loads.
T. Havekin, J.I.E.E., 1935
Vol.77, p.355 - 367.

51. The accuracy of watt-hour meters on intermittent loads.
M.A. Faucett, C.A. Keener, M.S. Helm.
Trans. A.I.E.E., 1940, Vol.59, p.460 - 464.

52. Der Winkelfehler bei Induktionzählern.
H. Schering und R. Schmidt.
Archiv fur Elektroteknic, 1924, Vol.14, p. 511 - 526.

53. Induction type single phase energy meter 90^{o} Compensation.
P.V.N. Ramanthan. Journal of the Instn. Engrs.
Elec.Eng.Div. April 1964, Vol.64, pt.EL4. P.317 - 330.

54. Direct Reading of Phase Angles on an Oscilloscrope.
C.R. Wischmeyer and P.E. Pfeiffer.
Review of Scientific Instruments, Jan, 1954.
Vol.25 No.1, p.41 - 42.

55. A direct method of phase measurement on the cathoderay tube.
D. Karo
British Journal of Applied Physics.
Jan.1955, Vol.6, p.10 - 12.

56. 6 Ways to Measure Phase Angle.
R. Staffin.
Control Engineering, October 1965, p.78 - 83.

57. Transistor Audio-Freq. Phase meter.
F. Butler,
Wireless World. Sept. 1964, p.453 - 459.

58. Phase Measurement.
Electronic Equipment News.
March 1966, p.82 - 87.

59. Electrical Measuring Instruments.
Drysdale and Jolley.
Benn, 1924. p.66.

60. The Rotor Bearings of Elec. Meters.
W.Lawson. J.I.E.E., 1929,
Vol.LXVll. p.1147.

61. Problems relating to use of pivots and jewels.
V.Scott. J.I.E.E. 1931. Vol.69.

62. Watt-hour Meter Bearings.
I.F. Kinnard and J.H. Goss.
Trans. A.I.E.E. Jan.1937, p.129 - 137.

63. The anomalous behaviour of the moving systems.of
single-phase A.C. Watt hour Meters at no load.
F.C. Holtz. Trans. A.I.E.E., Feb.1940
Vol.59, p.116 - 121.

64. Induction-type integrating meters.
G.F. Shotter and G.F. Tagg,
Pitman 1960.

65. The variable resistance to motion offered by The
Registering trains of Electric Supply Meters.
S.Evershed, J.I.E.E., Vol.53. 1915. p.498 - 511.

66. The Design of an Instrument for Testing Electric
Meter Registers.
A.K. Bhowmick, October 1967.
M.Sc. Project in Precision Measurement and Instrumentation.

67. A Precision Rotating Standard for the Measurement of
Kilowatt-hours.
J.H. Goss and A. Hansen.
Trans. A.I.E.E. 1940 Vol.59. p. 412 - 416

68. Organization of a Meter Test Department of a large supply undertaking, with special reference to the Electricity Supply (Meters) Act.1936.
C.W. Hughes. J.I.E.E.
1938 Vol.82, p.410 - 428.

69. Test-station Design and Organization for the smaller undertakings under the electricity supply (Meters) Act.1936.
E. Jacks, J.I.E.E., 1940, Vol.87, p.687 - 689.

70. Design of a wattless test circuit for Meters and Relays.
S.C. Ghose. App. Physics Quarterly (India)
Part I - June 1961 p.21 - 27.
Part II - Dec. 1961 p.103 - 114.
Part III - March 1961 p.2 - 6.

71. A differential Electronic Stabilizer for alternating voltages and some applications.
A. Glynne. Proc. I.E.E. 1943.
Vol.90, part II, p.101 - 115.

72. A new precision A.C. Voltage stabiliser.
G.N. Patchett, Proc. I.E.E. 1950.
Vol.97, pt.II. p.529 - 542.

73. Use of an electrostatic wattmeter as a.c./d.c. Comparator.
J.K. Choudhury and S.N. Bhattacharyya.
Proc. I.E.E., Vol.114 No.8, August 1967.

74. A precision A.C./D.C. Comparator for Power and Voltage Measurements.
G.F. Shotter and H.D. Hawkes, J.I.E.E., 1946.
Vol. 93 II, p.314 - 328.

75. Existing theories of operation of induction meters.
A. Podemski, Proc.I.E.E. 1965, Vol.112, No.8.

76. Über die Vorgange in der scheibe eines Wechselstrom Motorzählers. Teil I.
W. Rogowski.
Electrotechnic und Maschinenbau, 1911, Heft 45, p.915 - 921.

77. Development of a Modern Watt-hour Meter.
I.F. Kinnard and H.E. Trekell.
Trans, A.I.E.E., 1937, p.472 - 179.

78. The Torque of an Induction type meter
D. Connelly, B.E.A.M.A. Journal,
Dec.1950, p.377-380 and
Feb.1951, p. 36 - 40.

79. Travelling - field theory of Induction type Instruments and Motors.
H.E.M. Barlow, Proc. I.E.E. vol.112, No.6.
June 1965, p.1208 - 1214.

80. An investigation of the frequency variation in Induction watt-hour meters.
A.E.Moore and W.T. Slater,
J.I.E.E., Vol.68, 1930, p.1023 - 1033.

81. Temperature Errors in Induction Watt-hour Meters.
I.F. Kinnard and H.T. Faus,
Trans. A.I.E.E., vol.XLIV, 1925, p.275 - 287.

82. Theory of Action of the Induction watt-hour meter and analysis of its temperature errors.
D.T. Canfield. T.A.I.E.E. 1927,
Vol.XLVI, p.411 - 420.